The Physics and related R&D of the Mu2e Experiment at Fermilab

Doug Glenzinski

Fermilab

October-2016

Preface

Fermilab's Muon Campus will host a program that uses muons as probes for new physics

- Muon g-2 experiment (data 2017)
- Mu2e experiment (data 2020)
- Share common cryogenic facility, bunch formation, transfer lines, beam delivery ring, etc.
- Total cost of both experiments + common infrastructure ~$385M
- In total employ ~160 FTE at Fermilab
- Collaborations of ~200 members each
- Future possibilities for other muon-based experiments, e.g. muon EDM, other cLFV channels

Precision a_μ probes Λ_{NP}~few TeV

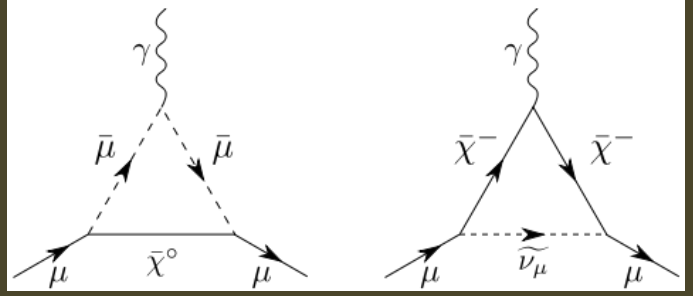

Precision $R_{\mu e}$ probes Λ_{NP}~ 10^4 TeV

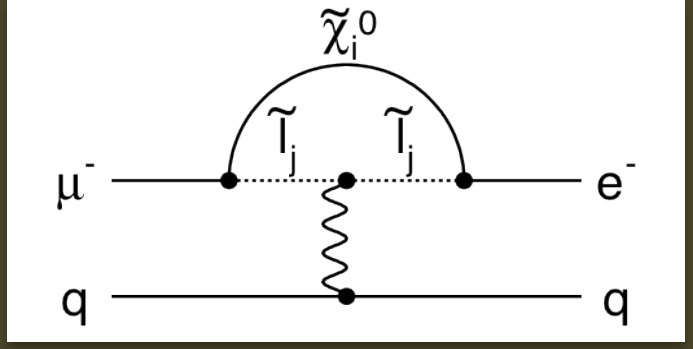

muons as probes of new physics…

Fermilab's Muon Campus

- New facility under construction
  - Two new experimental halls and the associated beamlines
  - Will produce world's highest intensity muon beams

g-2 Experimental Hall ("MC-1")

- Completed in 2014
- Data taking to begin in 2017

Mu2e Experimental Hall

East Face, September 2016

- Structurally complete. Outfitting well along.

Introduction

- What is Mu2e?
  - A search for Charged-Lepton Flavor Violation via

$$\mu^- N \rightarrow e^- N$$

  - Will use *current* Fermilab accelerator complex to reach a sensitivity 10 000 better than current world's best
  - Will have *discovery* sensitivity over broad swath of New Physics parameter space

Flavor Violation

- We've known for a long time that quarks mix → (Quark) Flavor Violation
  - Mixing strengths parameterized by CKM matrix
- In last 15 years we've come to know that neutrinos mix → Lepton Flavor Violation (LFV)
  - Mixing strengths parameterized by PMNS matrix
- Why not charged leptons?
  - Charged Lepton Flavor Violation (CLFV)

CLFV in the Standard Model

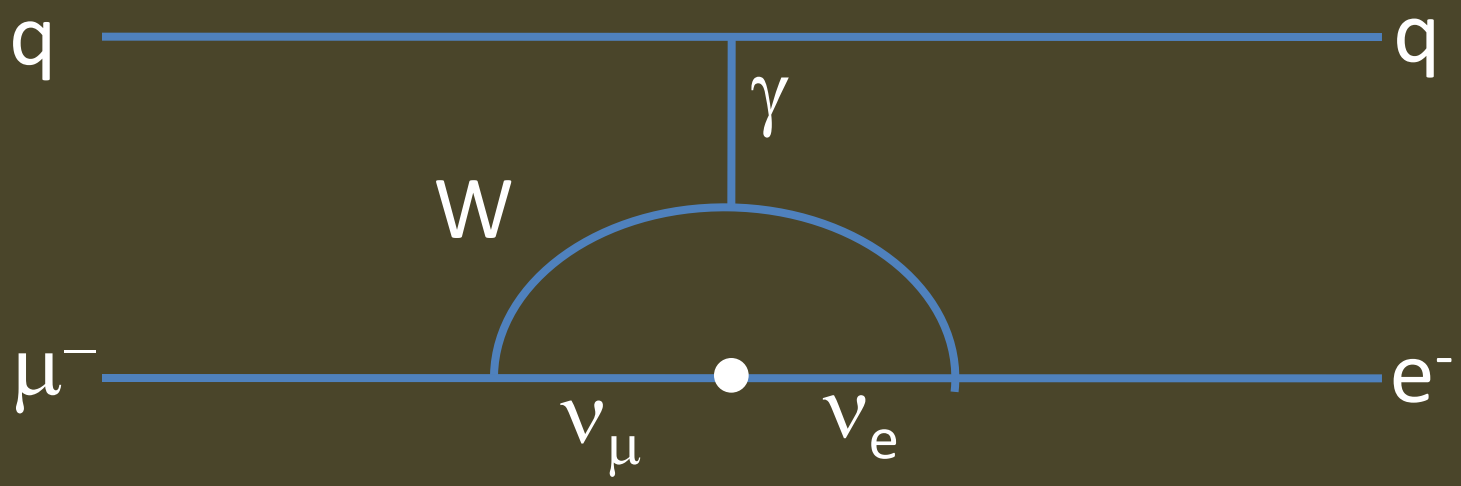

- Strictly speaking, forbidden in the SM
- Even in ν-SM, extremely suppressed
  (rate ~ $\Delta m_\nu^4 / M_w^4 < 10^{-50}$)
- However, most all NP models predict rates observable at next generation CLFV experiments

Some CLFV Processes

Process	Current Limit	Next Generation exp
$\tau \rightarrow \mu\eta$	BR < 6.5 E-8	
$\tau \rightarrow \mu\gamma$	BR < 6.8 E-8	10^{-9} - 10^{-10} (Belle II)
$\tau \rightarrow \mu\mu\mu$	BR < 3.2 E-8	
$\tau \rightarrow eee$	BR < 3.6 E-8	
$K_L \rightarrow e\mu$	BR < 4.7 E-12	
$K^+ \rightarrow \pi^+ e^- \mu^+$	BR < 1.3 E-11	
$B^0 \rightarrow e\mu$	BR < 7.8 E-8	
$B^+ \rightarrow K^+ e\mu$	BR < 9.1 E-8	
$\mu^+ \rightarrow e^+\gamma$	BR < 4.2 E-13	10^{-14} (MEG)
$\mu^+ \rightarrow e^+e^+e^-$	BR < 1.0 E-12	10^{-16} (PSI)
$\mu N \rightarrow eN$	$R_{\mu e}$ < 7.0 E-13	10^{-17} (Mu2e, COMET)

(current limits from the PDG)

- Most promising CLFV measurements use μ

CLFV Predictions

M.Blanke, A.J.Buras, B.Duling, S.Recksiegel, C.Tarantino

ratio	LHT	MSSM (dipole)	MSSM (Higgs)
$\frac{Br(\mu^- \to e^- e^+ e^-)}{Br(\mu \to e\gamma)}$	$0.02 \ldots 1$	$\sim 6 \cdot 10^{-3}$	$\sim 6 \cdot 10^{-3}$
$\frac{Br(\tau^- \to e^- e^+ e^-)}{Br(\tau \to e\gamma)}$	$0.04 \ldots 0.4$	$\sim 1 \cdot 10^{-2}$	$\sim 1 \cdot 10^{-2}$
$\frac{Br(\tau^- \to \mu^- \mu^+ \mu^-)}{Br(\tau \to \mu\gamma)}$	$0.04 \ldots 0.4$	$\sim 2 \cdot 10^{-3}$	$0.06 \ldots 0.1$
$\frac{Br(\tau^- \to e^- \mu^+ \mu^-)}{Br(\tau \to e\gamma)}$	$0.04 \ldots 0.3$	$\sim 2 \cdot 10^{-3}$	$0.02 \ldots 0.04$
$\frac{Br(\tau^- \to \mu^- e^+ e^-)}{Br(\tau \to \mu\gamma)}$	$0.04 \ldots 0.3$	$\sim 1 \cdot 10^{-2}$	$\sim 1 \cdot 10^{-2}$
$\frac{Br(\tau^- \to e^- e^+ e^-)}{Br(\tau^- \to e^- \mu^+ \mu^-)}$	$0.8 \ldots 2.0$	~ 5	$0.3 \ldots 0.5$
$\frac{Br(\tau^- \to \mu^- \mu^+ \mu^-)}{Br(\tau^- \to \mu^- e^+ e^-)}$	$0.7 \ldots 1.6$	~ 0.2	$5 \ldots 10$
$\frac{R(\mu\mathrm{Ti} \to e\mathrm{Ti})}{Br(\mu \to e\gamma)}$	$10^{-3} \ldots 10^{2}$	$\sim 5 \cdot 10^{-3}$	$0.08 \ldots 0.15$

Table 3: *Comparison of various ratios of branching ratios in the LHT model ($f = 1\,\mathrm{TeV}$) and in the MSSM without [92, 93] and with [96, 97] significant Higgs contributions.*

arXiv:0909.5454v2[hep-ph]

- Relative rates model dependent
- Measure several to pin-down theory details

CLFV Predictions

M.Blanke, A.J.Buras, B.Duling, S.Recksiegel, C.Tarantino

ratio	LHT	MSSM (dipole)	MSSM (Higgs)
$\frac{Br(\mu^- \to e^- e^+ e^-)}{Br(\mu \to e\gamma)}$	$0.02 \ldots 1$	$\sim 6 \cdot 10^{-3}$	$\sim 6 \cdot 10^{-3}$
$\frac{Br(\tau^- \to e^- e^+ e^-)}{Br(\tau \to e\gamma)}$	$0.04 \ldots 0.4$	$\sim 1 \cdot 10^{-2}$	$\sim 1 \cdot 10^{-2}$
$\frac{Br(\tau^- \to \mu^- \mu^+ \mu^-)}{Br(\tau \to \mu\gamma)}$	$0.04 \ldots 0.4$	$\sim 2 \cdot 10^{-3}$	$0.06 \ldots 0.1$
$\frac{Br(\tau^- \to e^- \mu^+ \mu^-)}{Br(\tau \to e\gamma)}$	$0.04 \ldots 0.3$	$\sim 2 \cdot 10^{-3}$	$0.02 \ldots 0.04$
$\frac{Br(\tau^- \to \mu^- e^+ e^-)}{Br(\tau \to \mu\gamma)}$	$0.04 \ldots 0.3$	$\sim 1 \cdot 10^{-2}$	$\sim 1 \cdot 10^{-2}$
$\frac{Br(\tau^- \to e^- e^+ e^-)}{Br(\tau^- \to e^- \mu^+ \mu^-)}$	$0.8 \ldots 2.0$	~ 5	$0.3 \ldots 0.5$
$\frac{Br(\tau^- \to \mu^- \mu^+ \mu^-)}{Br(\tau^- \to \mu^- e^+ e^-)}$	$0.7 \ldots 1.6$	~ 0.2	$5 \ldots 10$
$\frac{R(\mu\mathrm{Ti} \to e\mathrm{Ti})}{Br(\mu \to e\gamma)}$	$10^{-3} \ldots 10^{2}$	$\sim 5 \cdot 10^{-3}$	$0.08 \ldots 0.15$

Table 3: *Comparison of various ratios of branching ratios in the LHT model ($f = 1\,\mathrm{TeV}$) and in the MSSM without [92, 93] and with [96, 97] significant Higgs contributions.*

arXiv:0909.5454v2[hep-ph]

- Relative rates model dependent
- Measure several to pin-down theory details

New Physics Contributions to μN→eN

Loops

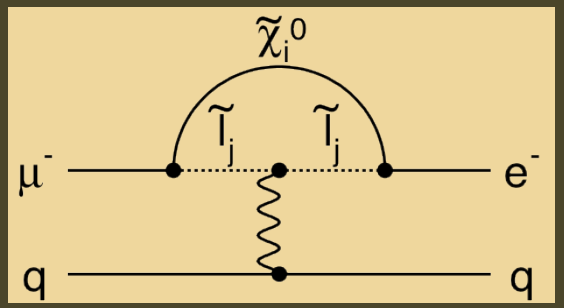

Supersymmetry

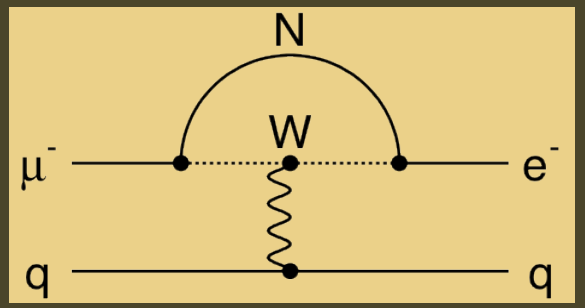

Heavy Neutrinos

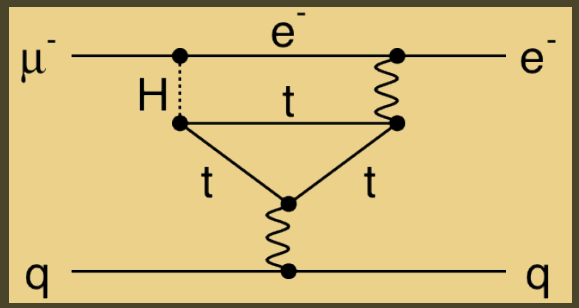

Two Higgs Doublets

Contact Terms

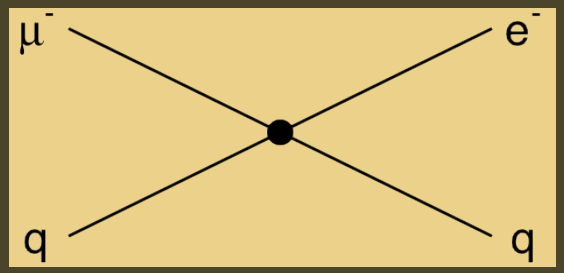

Compositeness

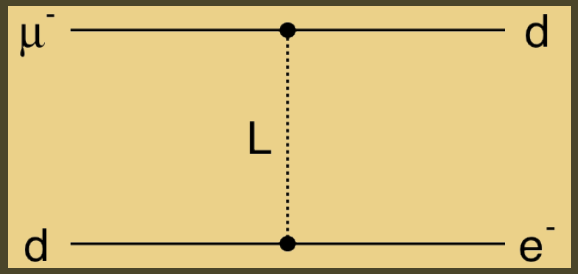

Leptoquarks

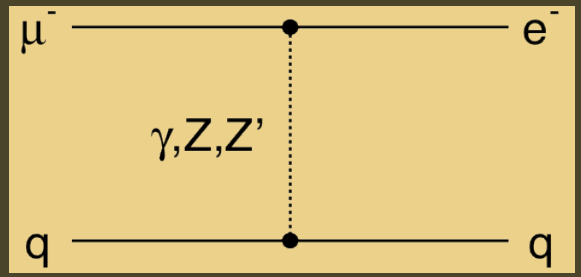

New Heavy Bosons / Anomalous Couplings

μN→eN sensitive to wide array of New Physics models

Mu2e Sensitivity

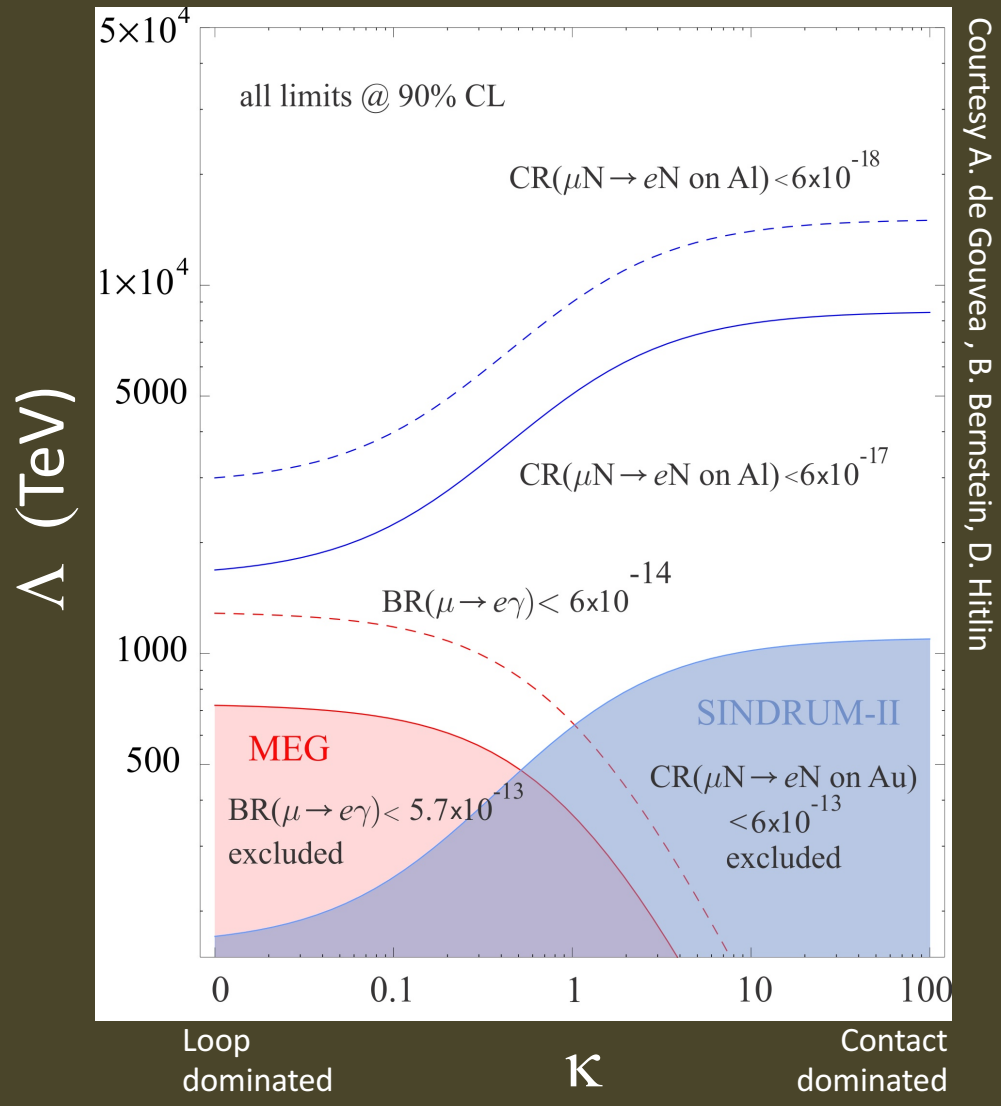

- Mu2e Sensitivity best in all scenarios

Mu2e Sensitivity

W. Altmannshofer, A.J.Buras, S.Gori, P.Paradisi, D.M.Straub

	AC	RVV2	AKM	δLL	FBMSSM	LHT	RS
$D^0 - \bar{D}^0$	★★★	★	★	★	★	★★★	?
ϵ_K	★	★★★	★★★	★	★	★★	★★★
$S_{\psi\phi}$	★★★	★★★	★★★	★	★	★★★	★★★
$S_{\phi K_S}$	★★★	★★	★	★★★	★★★	★	?
$A_{\rm CP}\,(B \to X_s\gamma)$	★	★	★	★★★	★★★	★	?
$A_{7,8}(B \to K^*\mu^+\mu^-)$	★	★	★	★★★	★★★	★★	?
$A_9(B \to K^*\mu^+\mu^-)$	★	★	★	★	★	★	?
$B \to K^{(*)}\nu\bar{\nu}$	★	★	★	★	★	★	★
$B_s \to \mu^+\mu^-$	★★★	★★★	★★★	★★★	★★★	★	★
$K^+ \to \pi^+\nu\bar{\nu}$	★	★	★	★	★	★★★	★★★
$K_L \to \pi^0\nu\bar{\nu}$	★	★	★	★	★	★★★	★★★
$\mu \to e\gamma$	★★★	★★★	★★★	★★★	★★★	★★★	★★★
$\tau \to \mu\gamma$	★★★	★★★	★	★★★	★★★	★★★	★★★
$\mu + N \to e + N$	★★★	★★★	★★★	★★★	★★★	★★★	★★★
d_n	★★★	★★★	★★★	★★	★★★	★	★★★
d_e	★★★	★★★	★★	★	★★★	★	★★★
$(g-2)_\mu$	★★★	★★★	★★	★★★	★★★	★	?

Table 8: "DNA" of flavour physics effects for the most interesting observables in a selection of SUSY and non-SUSY models ★★★ signals large effects, ★★ visible but small effects and ★ implies that the given model does not predict sizable effects in that observable.

★★★ = Discovery Sensitivity

arXiv:0909.1333[hep-ph]

- Mu2e sensitive across the board

Mu2e Sensitivity

W. Altmannshofer, A.J.Buras, S.Gori, P.Paradisi, D.M.Straub

	AC	RVV2	AKM	δLL	FBMSSM	LHT	RS
$D^0 - \bar{D}^0$	★★★	★	★	★	★	★★★	?
ϵ_K	★	★★★	★★★	★	★	★★	★★★
$S_{\psi\phi}$	★★★	★★★	★★★	★	★	★★★	★★★
$S_{\phi K_S}$	★★★	★★	★	★★★	★★★	★	?
$A_{\rm CP}\,(B \to X_s\gamma)$	★	★	★	★★★	★★★	★	?
$A_{7,8}(B \to K^*\mu^+\mu^-)$	★	★	★	★★★	★★★	★★	?
$A_9(B \to K^*\mu^+\mu^-)$	★	★	★	★	★	★	?
$B \to K^{(*)}\nu\bar{\nu}$	★	★	★	★	★	★	★
$B_s \to \mu^+\mu^-$	★★★	★★★	★★★	★★★	★★★	★	★
$K^+ \to \pi^+\nu\bar{\nu}$	★	★	★	★	★	★★★	★★★
$K_L \to \pi^0\nu\bar{\nu}$	★	★	★	★	★	★★★	★★★
$\mu \to e\gamma$	★★★	★★★	★★★	★★★	★★★	★★★	★★★
$\tau \to \mu\gamma$	★★★	★★★	★	★★★	★★★	★★★	★★★
$\mu + N \to e + N$	★★★	★★★	★★★	★★★	★★★	★★★	★★★
d_n	★★★	★★★	★★★	★★	★★★	★	★★★
d_e	★★★	★★★	★★	★	★★★	★	★★★
$(g-2)_\mu$	★★★	★★★	★★	★★★	★★★	★	?

Table 8: "DNA" of flavour physics effects for the most interesting observables in a selection of SUSY and non-SUSY models ★★★ signals large effects, ★★ visible but small effects and ★ implies that the given model does not predict sizable effects in that observable.

★★★ = Discovery Sensitivity

arXiv:0909.1333[hep-ph]

- Mu2e sensitive across the board

How does Mu2e work?

Mu2e Concept

- Generate a beam of low momentum muons (μ^-)
- Stop the muons in a target
  - Mu2e plans to use aluminum
  - Sensitivity goal requires ~10^{18} stopped muons
- The stopped muons are trapped in orbit around the nucleus
  - In orbit around aluminum: τ_μ^{Al} = 864 ns
  - Large τ_μ^{N} important for discriminating background
- Look for events consistent with $\mu N \rightarrow eN$

Mu2e Proton Beam

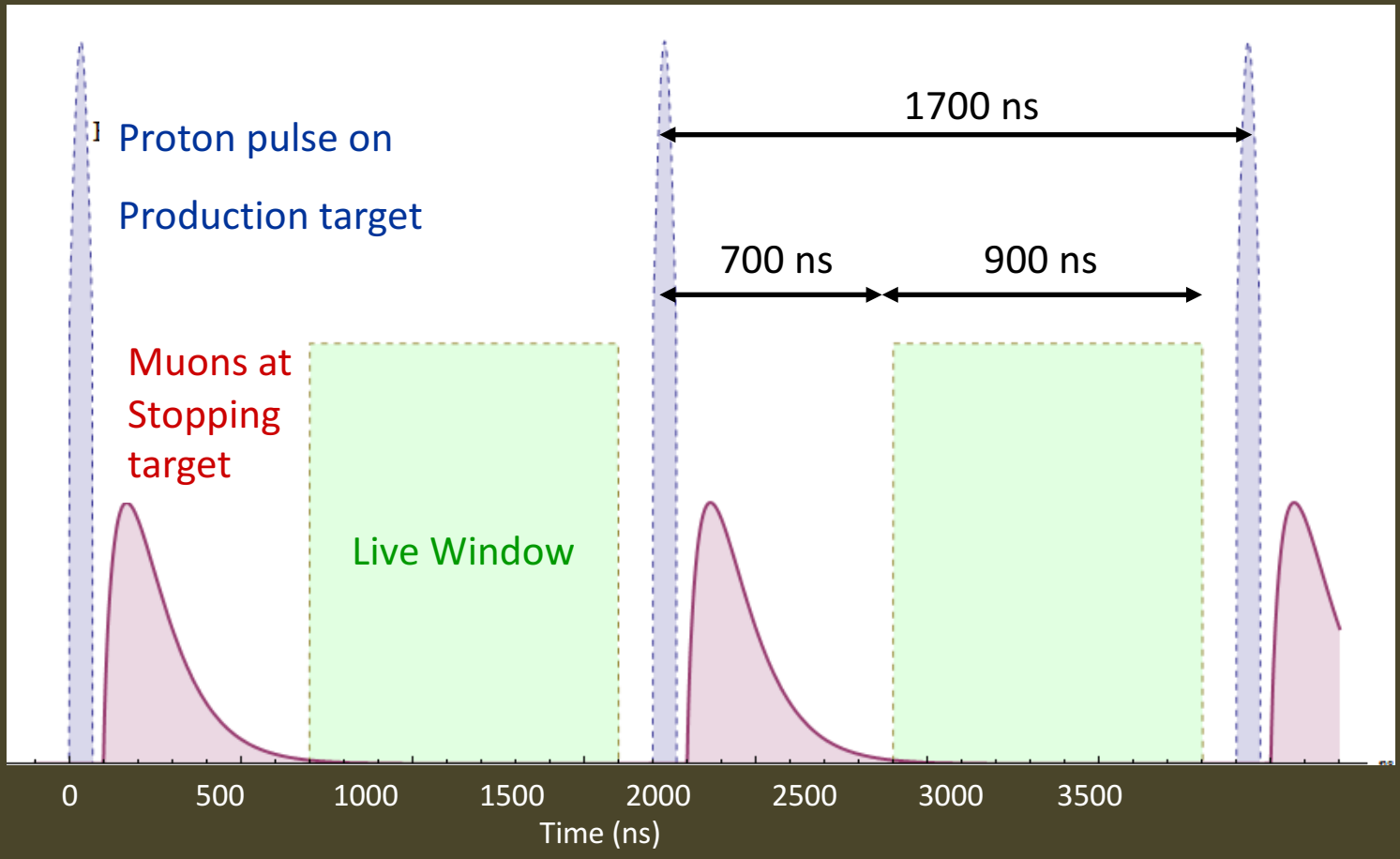

- Mu2e will use a pulsed proton beam and a delayed live gate to suppress prompt backgrounds

Mu2e Concept

- Generate a beam of low momentum muons (μ^-)
- Stop the muons in a target
  - Mu2e plans to use aluminum
  - Sensitivity goal requires ~10^{18} stopped muons
- The stopped muons are trapped in orbit around the nucleus
  - In orbit around aluminum: τ_μ^{Al} = 864 ns
  - Large τ_μ^{N} important for discriminating background
- Look for events consistent with $\mu N \rightarrow eN$

Mu2e Signal

- The process is a coherent one
  - The nucleus is kept intact
- Experimental signature is an electron and nothing else
  - Energy of electron: $E_e = m_\mu - E_{recoil} - E_{1S\text{-}B.E.}$
  - For aluminum: E_e=104.96 MeV
  - Important for discriminating background

Mu2e Sensitivity

- Design goal: single-event-sensitivity of 2.4×10^{-17}
  - Requires about 10^{18} stopped muons
  - Requires about 10^{20} protons on target
  - Requires extreme suppression of backgrounds
- Expected limit: $R_{\mu e} < 6 \times 10^{-17}$ @ 90% CL
  - Factor 10^4 improvement
- Discovery sensitivity: all $R_{\mu e} >$ few $\times 10^{-16}$
  - Covers broad range of new physics theories

Backgrounds

Mu2e Backgrounds

- Intrinsic – scale with no. stopped muons
  - μ Decay-in-Orbit (DIO)
  - Radiative muon capture (RMC)
- Late arriving – scale with no. late protons
  - Radiative pion capture (RPC)
  - μ and π decay-in-flight (DIF)
- Miscellaneous
  - Anti-proton induced
  - Cosmic-ray induced

Mu2e Backgrounds

Category	Source	Events
Intrinsic	μ Decay in Orbit	0.20
	Radiative μ Capture	<0.01
Late Arriving	Radiative π Capture	0.02
	Beam electrons	<0.01
	μ Decay in Flight	<0.01
	π Decay in Flight	<0.01
Miscellaneous	Anti-proton induced	0.05
	Cosmic Ray induced	0.08
Total Background		0.36

(assuming 6.8E17 stopped muons in 6E7 s of beam time)

- Designed to be nearly background free

Mu2e Intrinsic Backgrounds

Once trapped in orbit, muons will:

1) Decay in orbit (DIO): $\mu^- N \rightarrow e^- \nu_\mu \nu_e N$
   - For Al. DIO fraction is 39%
   - Electron spectrum has tail out to 104.96 MeV
   - Accounts for ~55% of total background

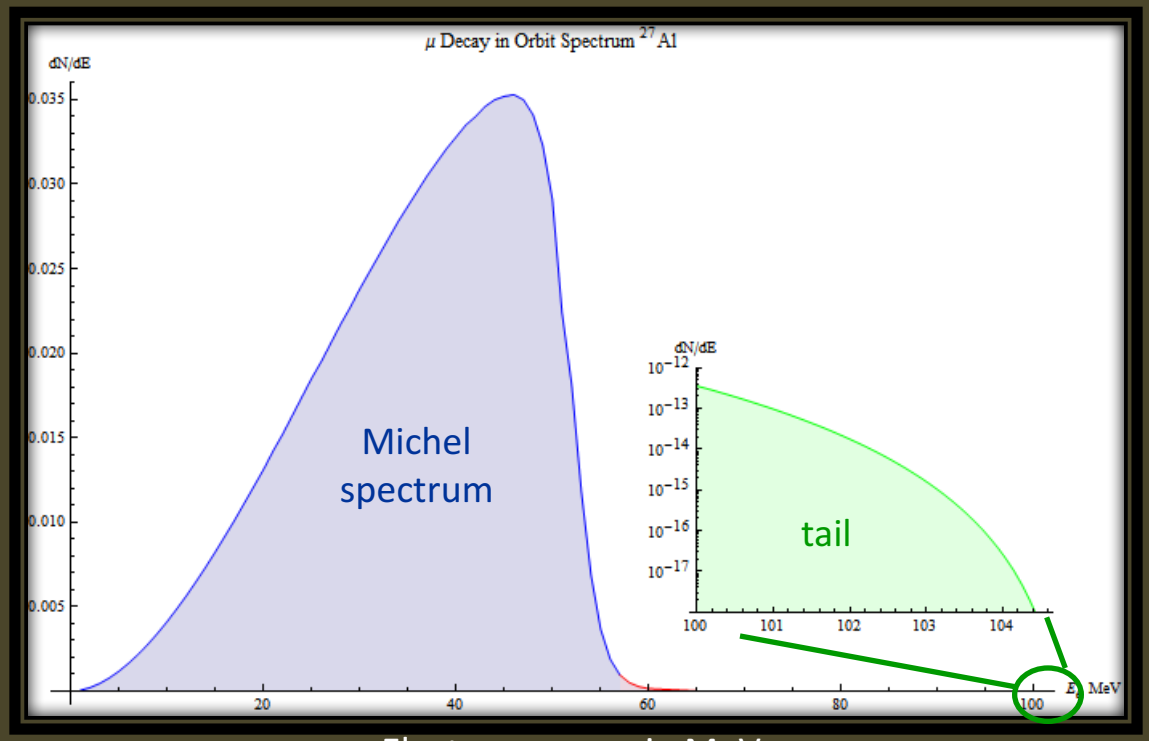

Electron energy in MeV

Mu2e Intrinsic Backgrounds

Once trapped in orbit, muons will:

2) Capture on the nucleus:
   - For Al. capture fraction is 61%
   - Ordinary μ Capture
     - $\mu^- N_Z \rightarrow \nu N^*_{Z-1}$
     - Used for normalization
   - Radiative μ capture
     - $\mu^- N_Z \rightarrow \nu N^*_{Z-1} + \gamma$
     - (# Radiative / # Ordinary) ~ 1 / 100,000
     - E_γ kinematic end-point ~102 MeV
     - Asymmetric $\gamma \rightarrow e^+e^-$ pair production can yield a background electron

Mu2e Late Arriving Backgrounds

- Backgrounds arising from all the other interactions which occur at the production target
  - Overwhelmingly produce a prompt background when compared to $\tau_{\mu}^{Al} = 864$ ns
  - Eliminated by defining a signal timing window starting 700 ns after the initial proton pulse
  - Must eliminate out-of-time ("late") protons, which would otherwise generate these backgrounds in time with the signal window

$$\text{out-of-time protons / in-time protons} < 10^{-10}$$

Mu2e Proton Beam

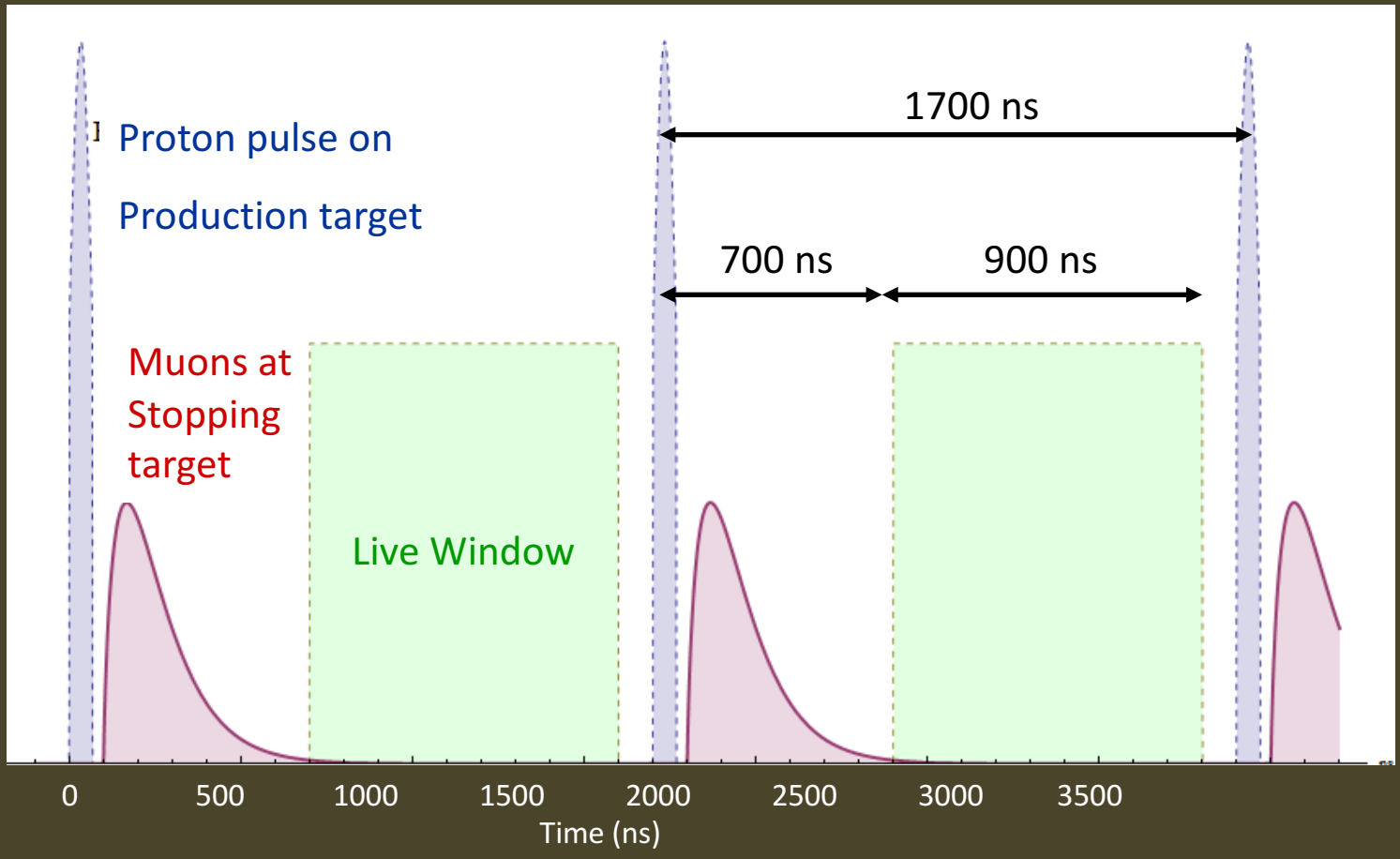

- Protons that arrive late can give rise to prompt backgrounds in the delayed live window.

Mu2e Late Arriving Backgrounds

- Contributions from
  - Radiative π Capture
    - $\pi^- N_Z \rightarrow N^*_{Z-1} + \gamma$
    - For Al. RπC fraction: 2%
    - E_γ extends out to ~m_π
    - Asymmetric γ ––> e^+e^- pair production can yield background electron
  - Beam electrons
    - Originating from upstream π^- and π^0 decays
    - Electrons scatter in stopping target to get into detector acceptance
  - Muon and pion Decay-in-Flight
- Taken together these backgrounds account for ~10% of the total background and scale *linearly* with the number of out-of-time protons

Mu2e Miscellaneous Backgrounds

- Several additional miscellaneous sources can contribute background - most importantly:
  - Anti-protons
    - Proton beam is just above pbar production threshold
    - These low momentum pbars wander until they annihilate
    - A thin mylar window in beamline absorbs most if them
    - Annihilations produce high multiplicity final states e.g. π^- can undergo RπC to yield a background electron
  - Cosmic rays
    - Suppressed by passive and active shielding
    - μ DIF or interactions in the detector material can give an e^- or γ that yield a background electron
    - Background listed assumes veto efficiency of 99.99%

Keys to Mu2e Success

- Excellent momentum resolution (<200 keV/c core)
- Pulsed proton beam
  - Narrow proton pulses (< +/- 125 ns)
  - Very few out-of-time protons (< 10^{-10})
- Avoid trapping particles… B-field requirements
  - Further mitigates beam-related backgrounds
- Thin anti-proton annihilation window(s)
- High CR veto efficiency (>99.99%)

The Mu2e Beamlines

The Mu2e Proton Beam

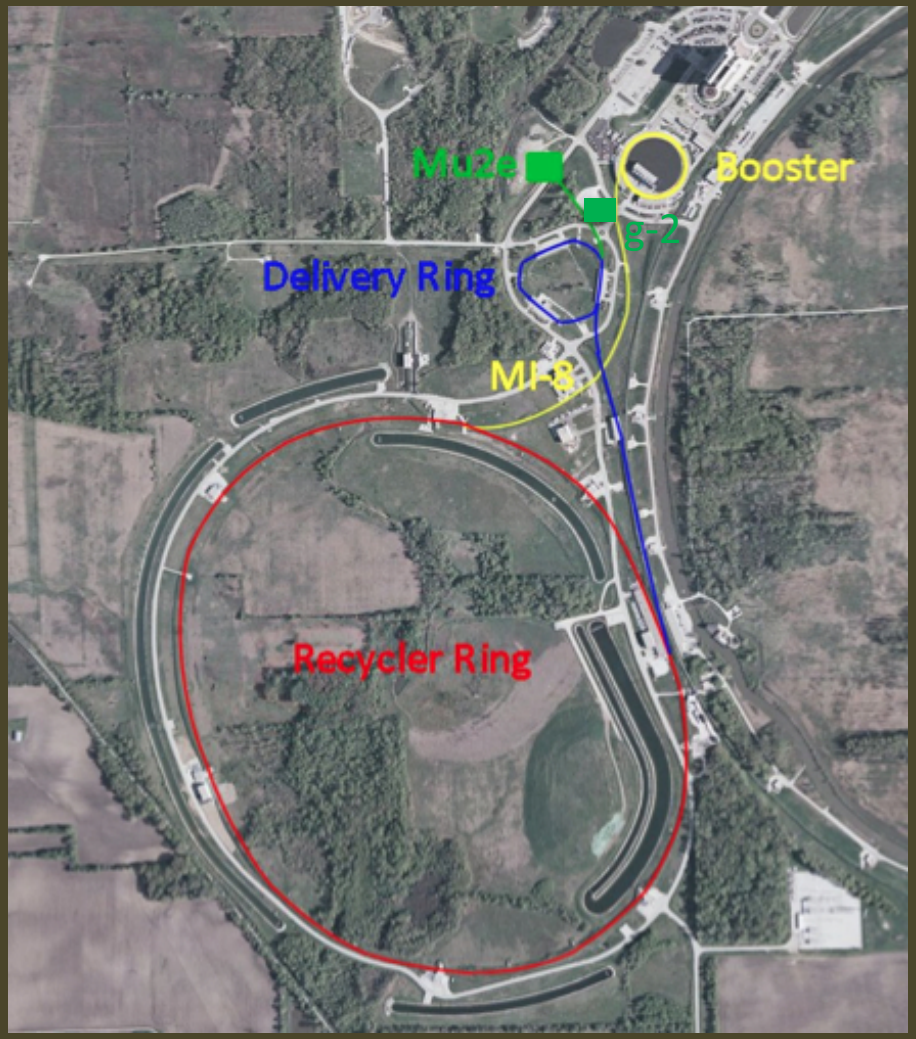

- Mu2e begins by using protons to produce pions
- Mu2e will repurpose much of the Tevatron anti-proton complex to instead produce muons.
- Mu2e can (and will) run simultaneously with NOvA and BNB.

The Mu2e Proton Beam

Quantity	Value	Units
MI-RR Cycle Time	1400.0	msec
Number of Spills per MI-RR Cycle	8	
Spill Duration	43.12	msec
Reset (Beam Off) Time Between Spills	5	msec
Number of Pulses per Spill	25.4k	
Pulse Spacing	1695	ns
Protons on Target (POT) Per Pulse	39×10^{6}	POT
Instantaneous Rate	24×10^{12}	POT/s
Average Rate	6×10^{12}	POT/s
Duty Factor	25%	
Proton Beam Energy	8	GeV

- Mu2e will use 8kW of 8 GeV proton beam

Mitigating out-of-time protons

- The RF structure of the Recycler provides some “intrinsic” extinction:
  - Extinction (Intrinsic) = few 10^{-5}
- A custom-made AC dipole placed just upstream of the production target provides additional “external” extinction:
  - Extinction (AC dipole) = 10^{-6} – 10^{-7}
- Together they provide a total extinction:
  - Extinction (Total) = few 10^{-11} – 10^{-12}

Mu2e Experimental Apparatus

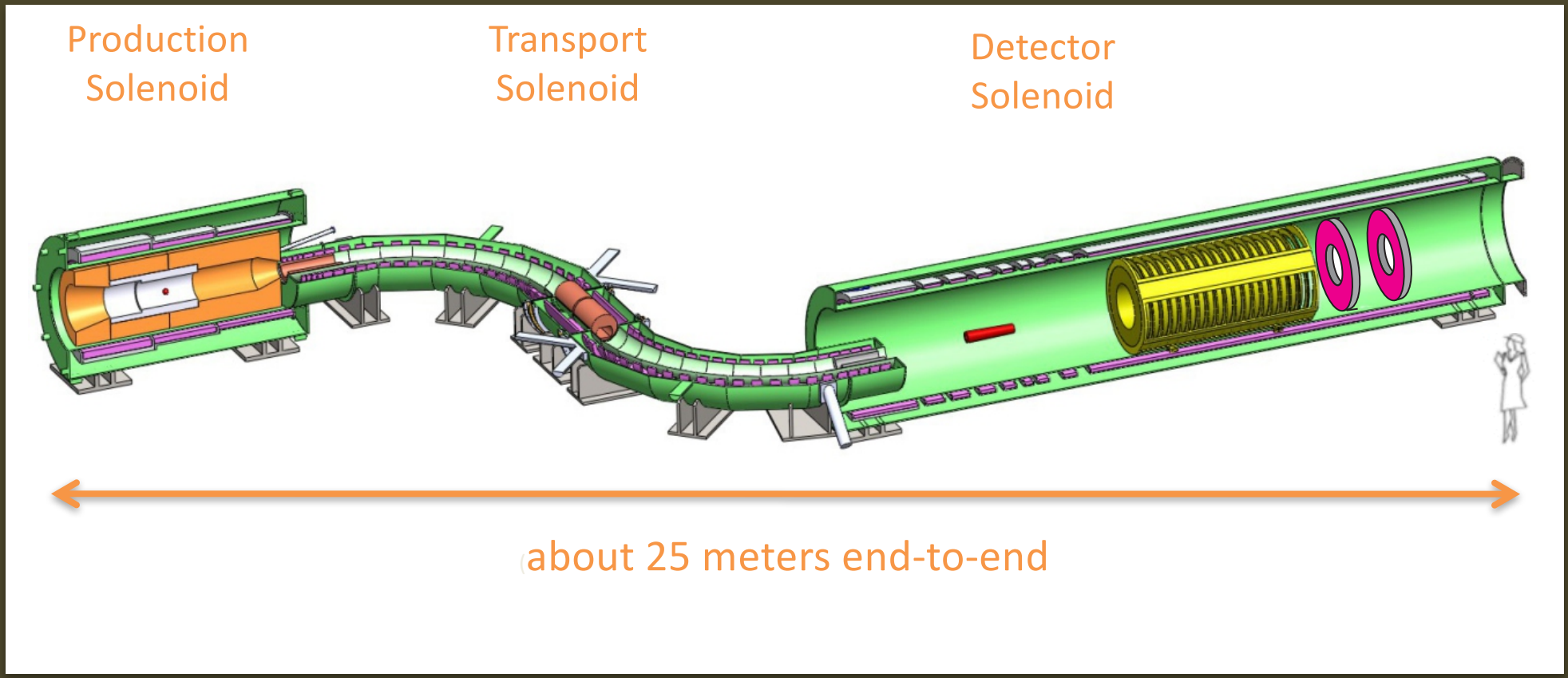

- Consists of 3 solenoid systems

Mu2e Experimental Apparatus

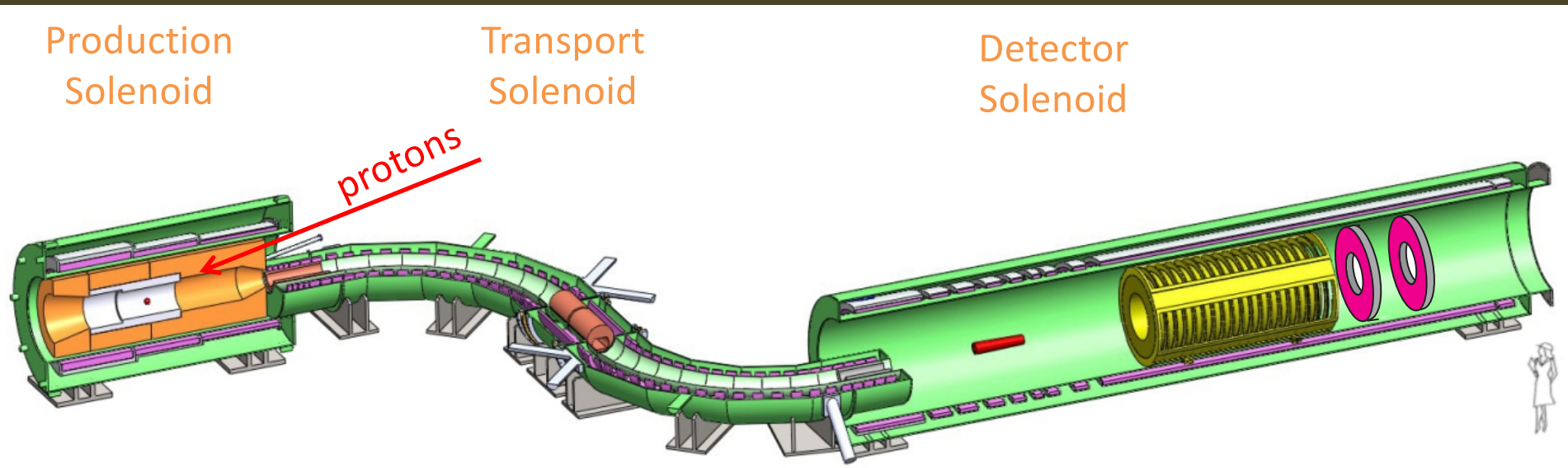

Production Solenoid:
8 GeV protons interact with a tungsten target to produce μ^- (from π^- decay)

- Consists of 3 solenoid systems

Mu2e Experimental Apparatus

Production Solenoid

Transport Solenoid

Detector Solenoid

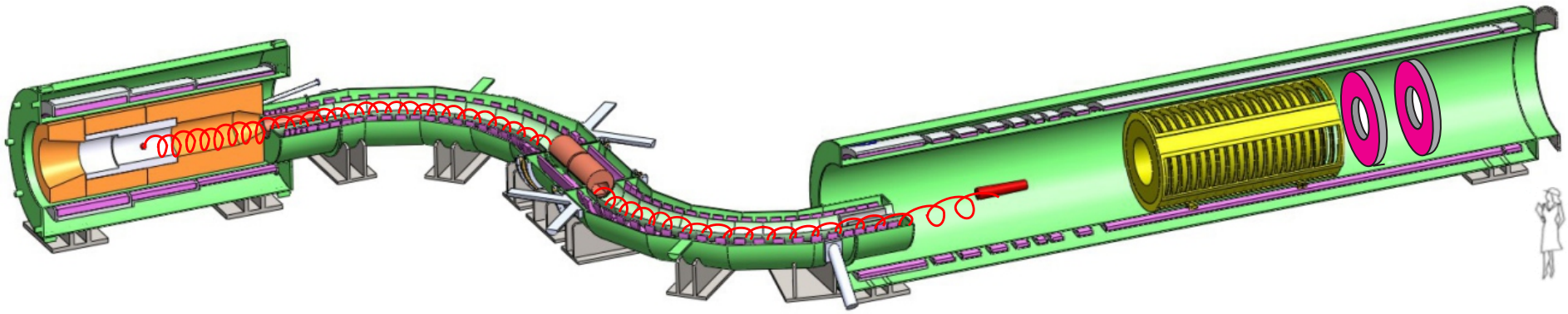

Transport Solenoid:
Captures π- and subsequent μ-; momentum- and sign-selects beam

- Consists of 3 solenoid systems

Mu2e Experimental Apparatus

Production Solenoid

Transport Solenoid

Detector Solenoid

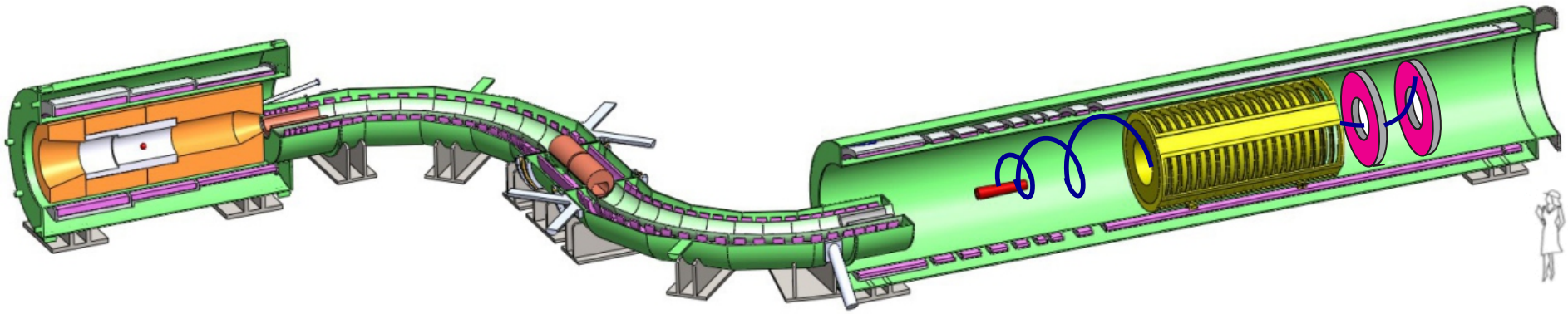

Detector Solenoid:
Upstream – Al. stopping target, Downstream – tracker, calorimeter
(not shown – cosmic ray veto system, extinction monitor, target monitor)

- Consists of 3 solenoid systems

Mu2e Experimental Apparatus

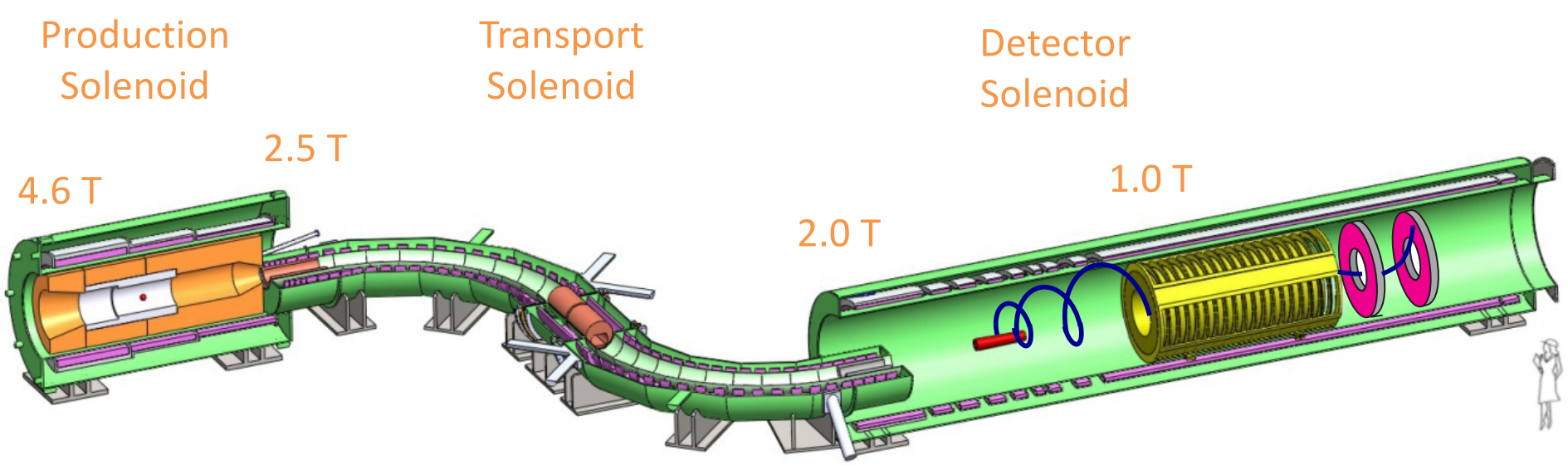

Graded fields important to suppress backgrounds, to increase muon yield, and to improve geometric acceptance for signal electrons

- Consists of 3 solenoid systems

Mu2e Experimental Apparatus

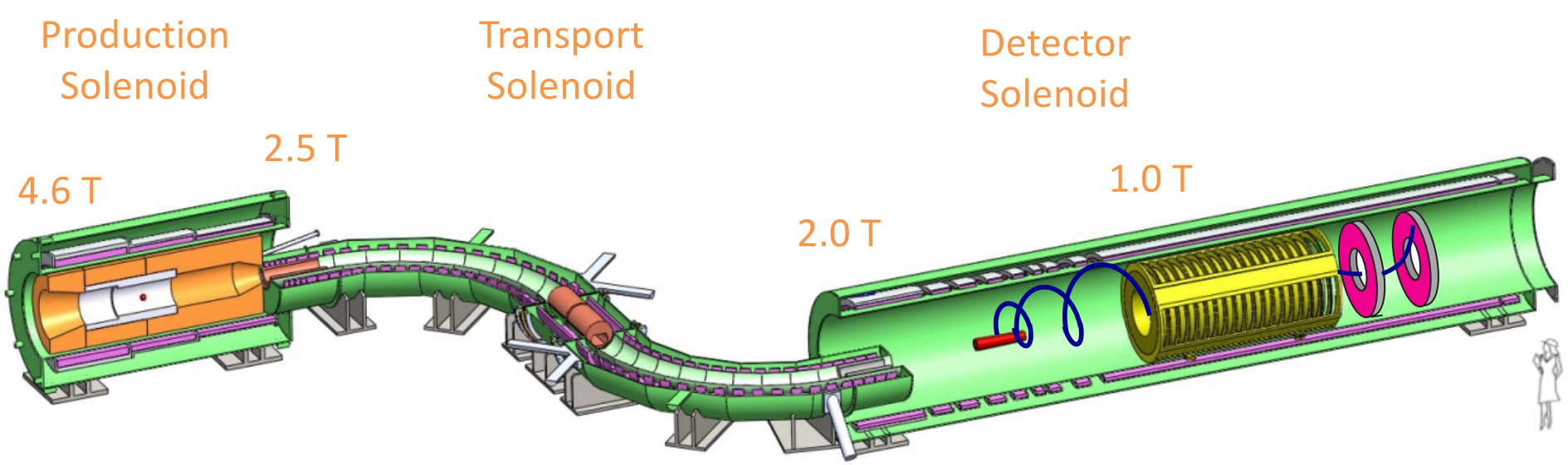

Graded fields important to suppress backgrounds, to increase muon yield, and to improve geometric acceptance for signal electrons

- Derived from MELC concept originated by Lobashev and Djilkibaev in 1989

Mu2e Conductor R&D

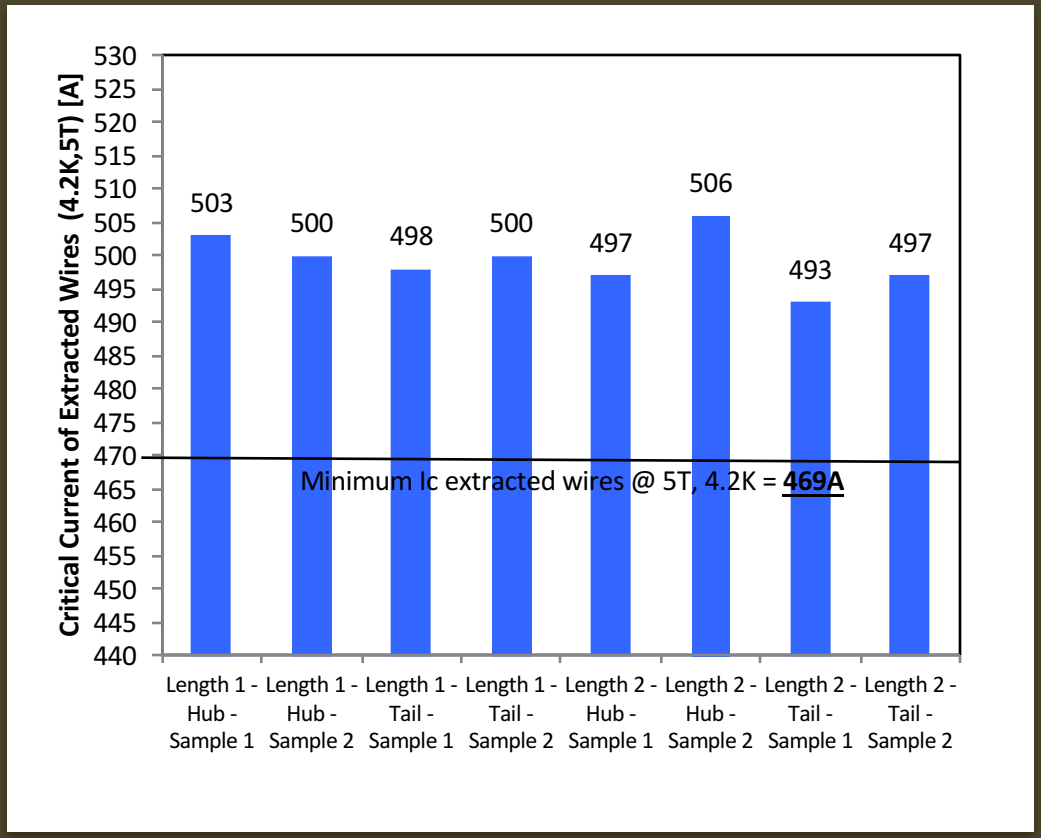

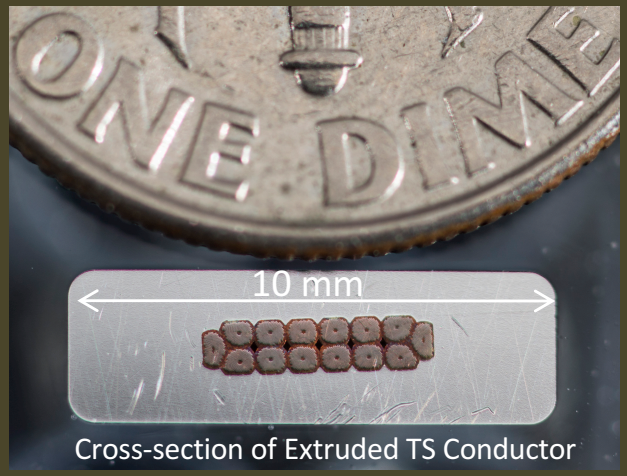

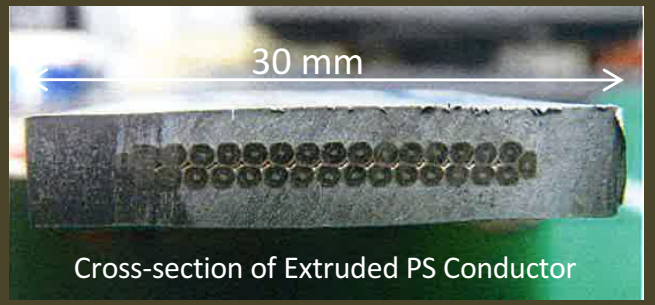

- Conductor production is well along
  - TS and DS conductor done, PS expected end 2016
  - Need ~75 km total (incl. spares); about 85% done.

Mu2e Solenoid Summary

	PS	TS	DS
Length (m)	4	13	11
Diameter (m)	1.7	0.4	1.9
Field @ start (T)	4.6	2.5	2.0
Field @ end (T)	2.5	2.0	1.0
Number of coils	3	52	11
Conductor (km)	14	44	17
Operating current (kA)	10	3	6
Stored energy (MJ)	80	20	30
Cold mass (tons)	11	26	8

- PS, DS will be built by General Atomics
- TS will be built by ASG + Fermilab

Mu2e Solenoid Summary


TS Coil Module prototype at Fermilab

- Designs are finalized.
- TS fabrication has begun.
- PS, DS fabrication will begin this winter.

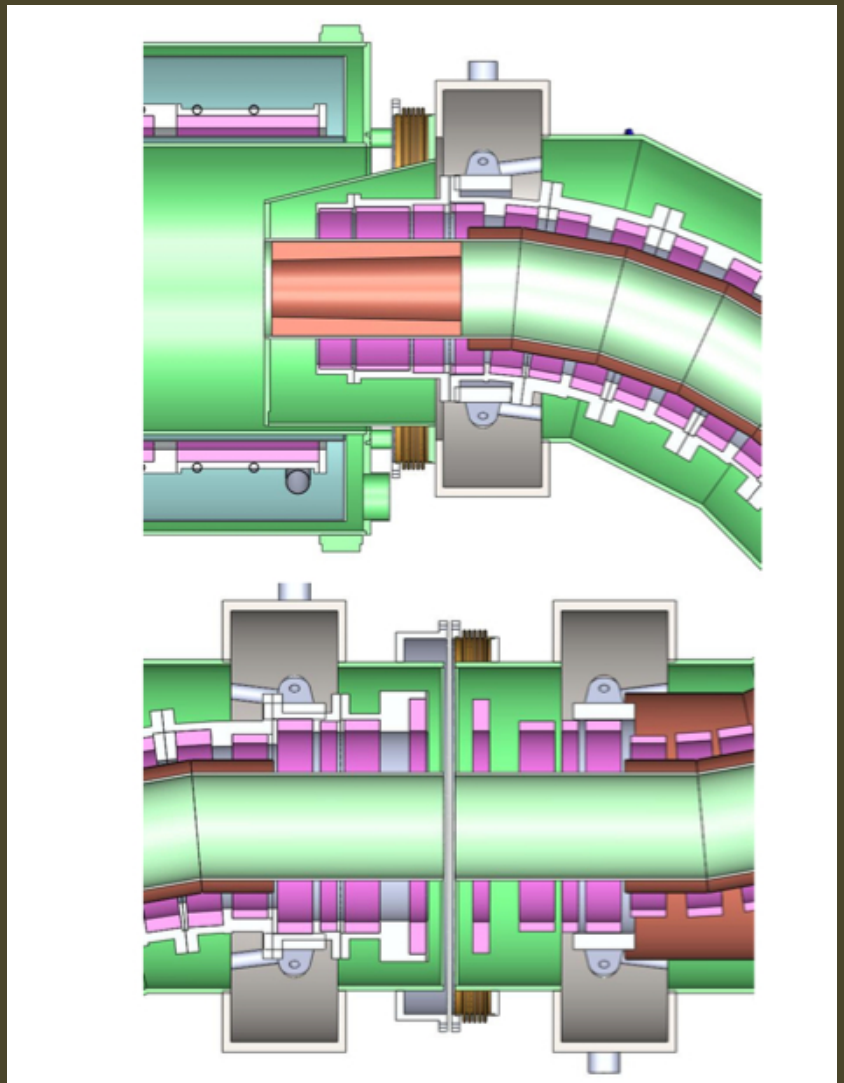
Figure 7.25. TSu Cryostat Interfaces. Top: TSu-PS interface; Bottom; TSu-TSd interface.

Mu2e Solenoid Summary

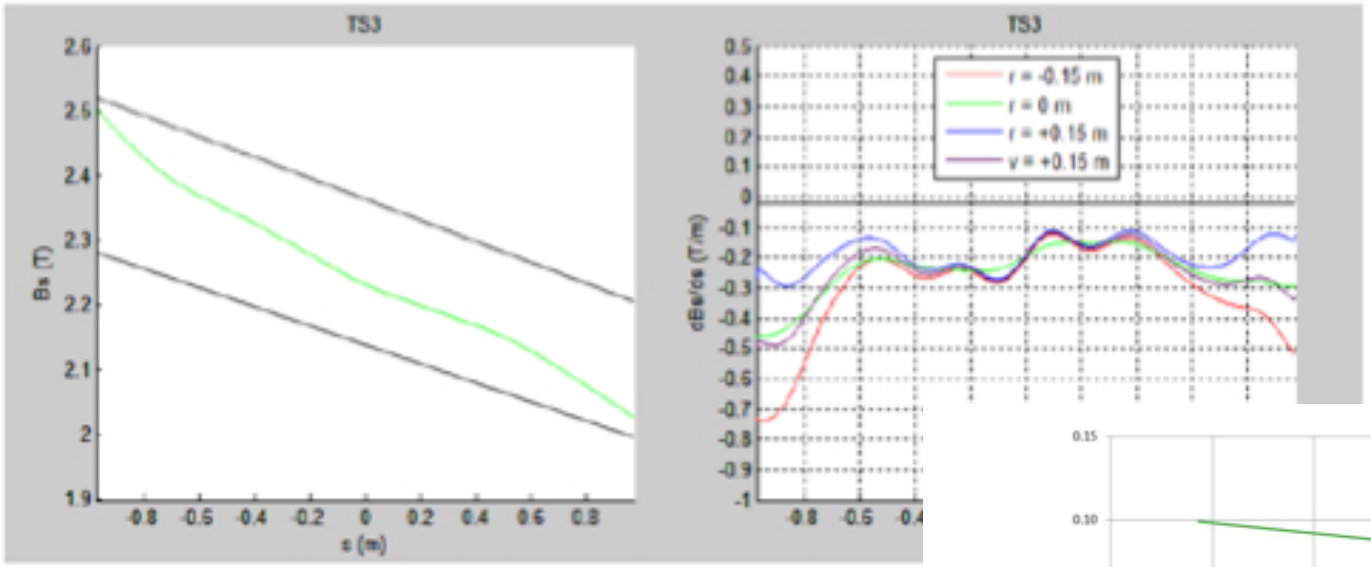

Figure 7.28. Axial field distribution at the center of TS3 (le
(right).

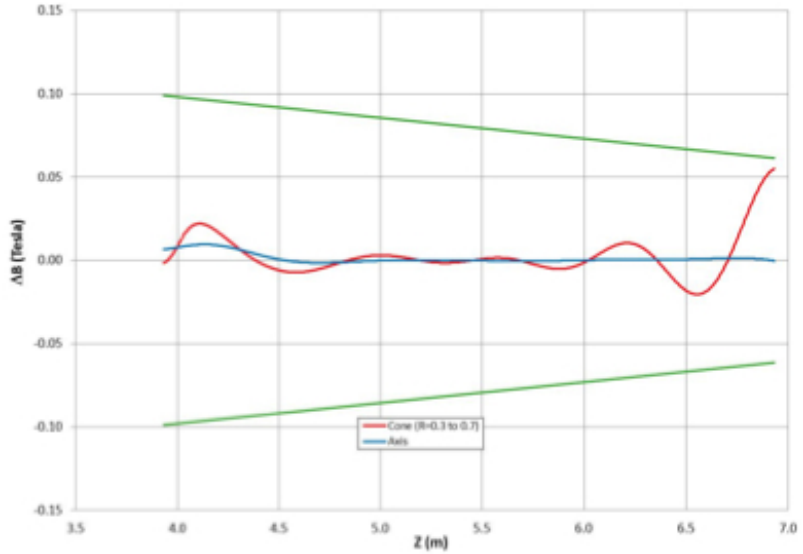

Figure 7.39. Comparison of the magnetic field with the field requirements in the DS gradient section (DS1 Gradient). Field requirements from Table 7.2 are shown in green. ΔB is relative to uniform gradient of -0.25 T/m and a field value of 1. 5 T at the stopping target on axis (blue); on a radial cone from 0.3m to 0.7 m starting at the upstream end of DS1 section (red).

- Designs meet field specs (including fabrication and design tolerances).

Some Mu2e numbers

- Every 1 second Mu2e will
  - Send 7,000,000,000,000 protons to the Production Solenoid
  - Send 26,000,000,000 μs through the Transport Solenoid
  - Stop 13,000,000,000, μs in the Detector Solenoid
- By the time Mu2e is done…

Total number of stopped muons

1,000,000,000,000,000,000

Some Perspective

1,000,000,000,000,000,000

= number of stopped Mu2e muons

= number of grains of sand on earth's beaches

The Mu2e Detectors

The Mu2e Detector

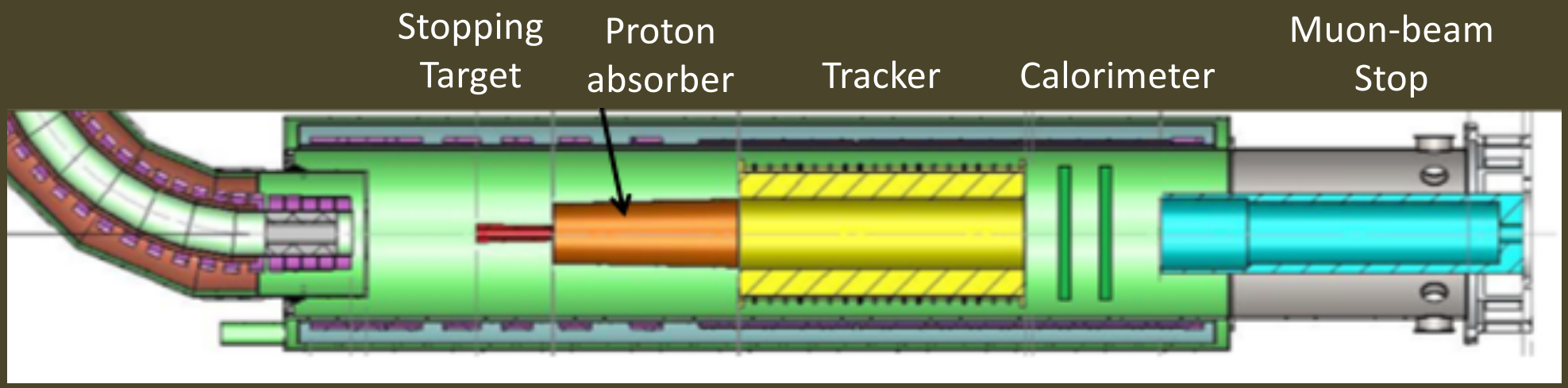

- I am going to focus on the principle elements:
  - Tracker, Calorimeter, Cosmic-Ray Veto

The Mu2e Tracker

- Will employ straw technology
  - Low mass
  - Can reliably operate in vacuum
  - Robust against single-wire failures

- 5 mm diameter straw
- Spiral wound
- Walls: 12 μm Mylar + 3 μm epoxy + 200 Å Au + 500 Å Al
- 25 μm Au-plated W sense wire
- 33 – 117 cm in length
- 80/20 Ar/CO2 with HV < 1500 V

The Mu2e Tracker

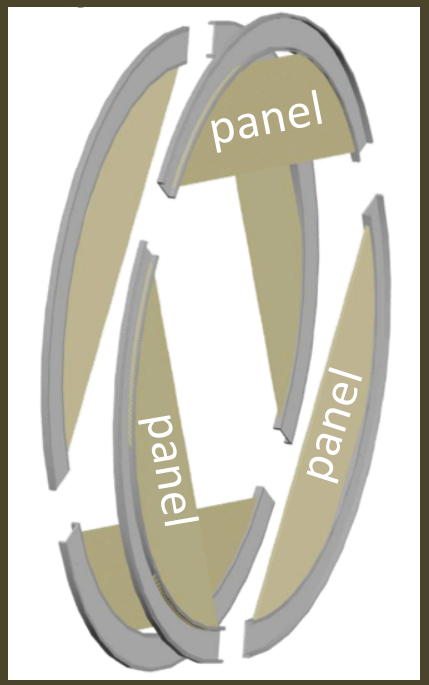

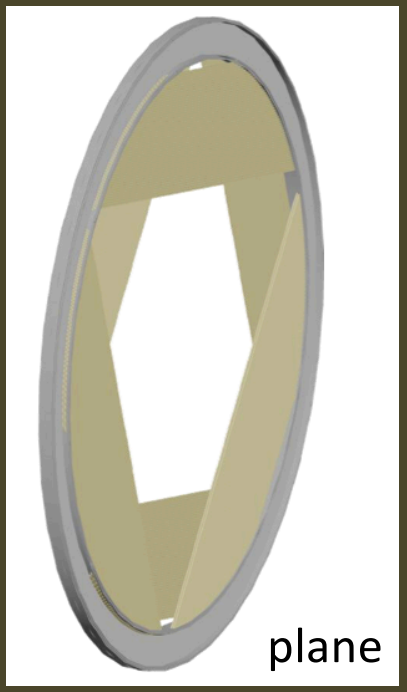

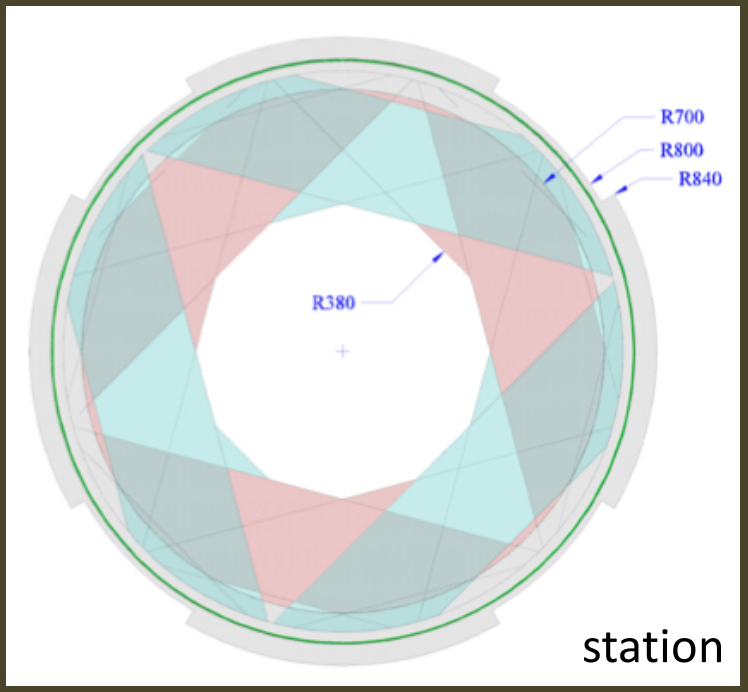

- Self-supporting “panel” consists of 100 straws
- 6 panels assembled to make a “plane”
- 2 planes assembled to make a “station”
- Rotation of panels and planes improves stereo information
- >20k straws total

First Prototype Panel

- Starting pre-production prototype now

The Mu2e Tracker

- 18 “stations” with straws transverse to the beam
- Naturally moves readout and support to large radii, out of the active volume

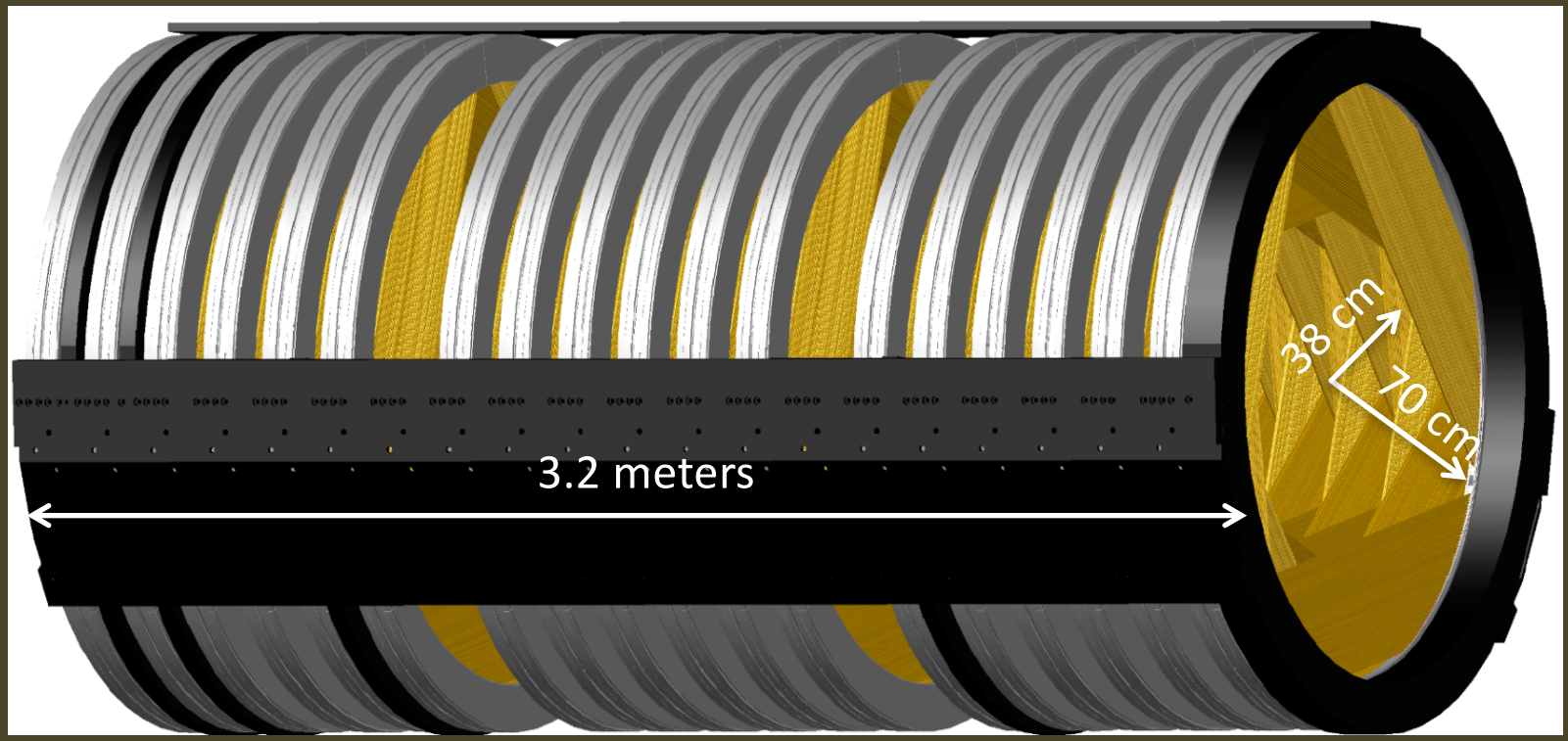

The Mu2e Tracker

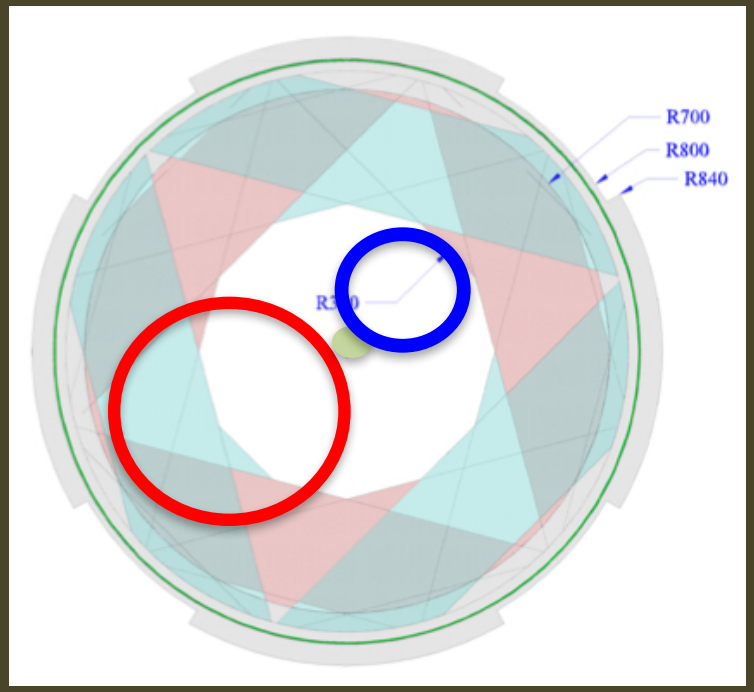

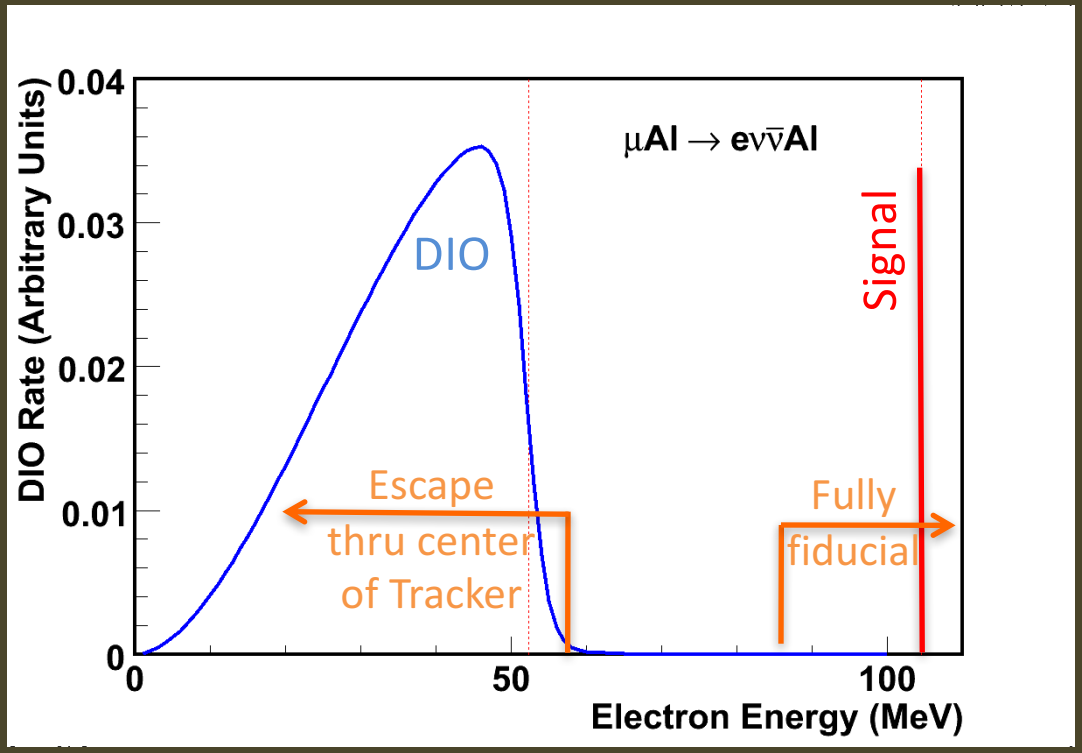

- Inner 38 cm is purposefully un-instrumented
  - Blind to beam flash
  - Blind to >99% of DIO spectrum

Mu2e Track Reconstruction

- Straw-hit rates
  - From beam flash (0-300 ns): ~1000 kHz/cm^2
    - Need to survive this, but won't collect data
  - Later, near live window (>500 ns)
    - Peak ~ 10 kHz/cm^2 (inner straws)
    - Average ~ 3 kHz/cm^2 (over all straws)

8 Channel Prototype

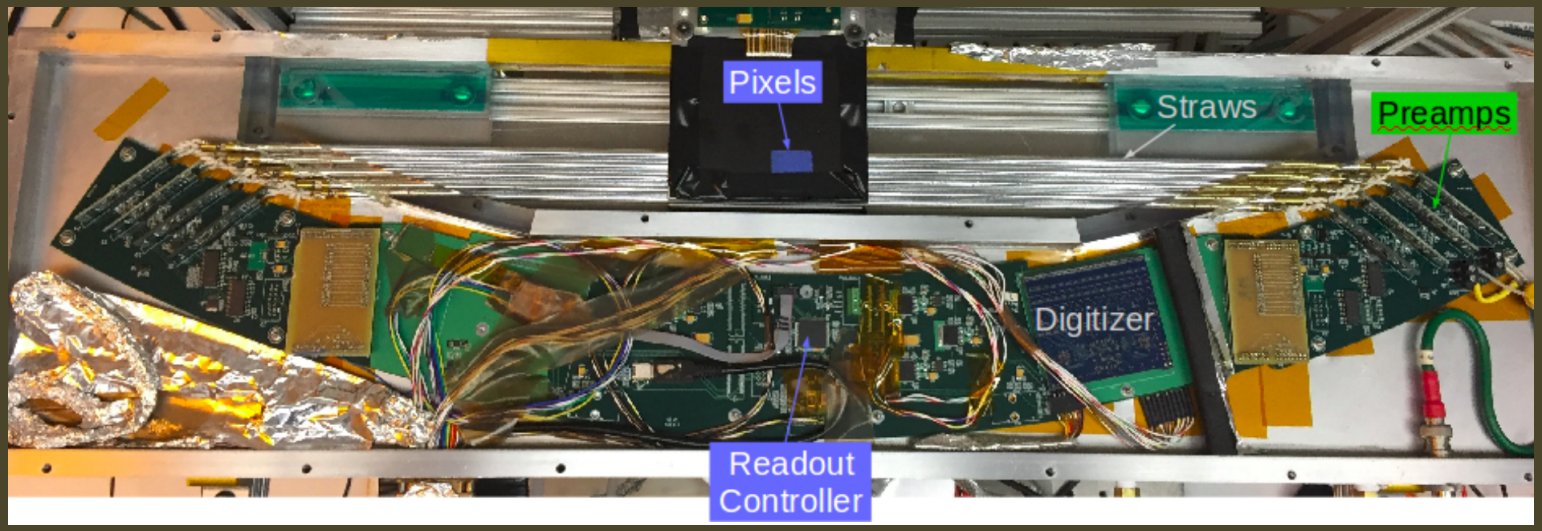

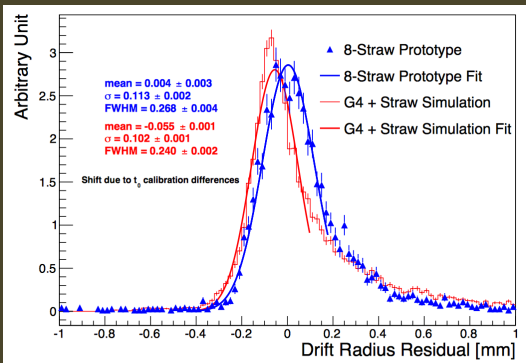

Transverse Resolution
(Data vs MC)
$\sigma_{data} = 0.113 \pm 0.002$ mm
$\sigma_{MC} = 0.102 \pm 0.001$ mm

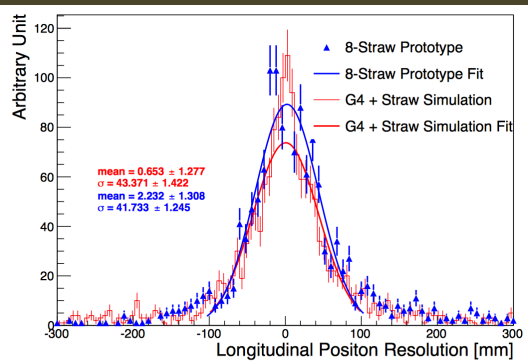

Longitudinal Resolution
(Data vs MC)
$\sigma_{data} = 42 \pm 1$ mm
$\sigma_{MC} = 43 \pm 1$ mm

Parameter	Value	Reference
N electrons per ionization	$< N >= 2$	NIMA 301, 202(1991)
Energy per ionization electron	39 eV	NIST (27-100 eV) and G4
Avg. Straw Gain	70k	Prototype (PAM, ^{55}Fe)
Threshold Value	12 mV	Prototype (DVM, ^{55}Fe)
Threshold Noise	3 mV	Spice Sim. (V. Rusu)
Shaping Time	22 ns	Prototype (^{55}Fe)

- Measured gain, crosstalk, resolution, …

Mu2e Pattern Recognition

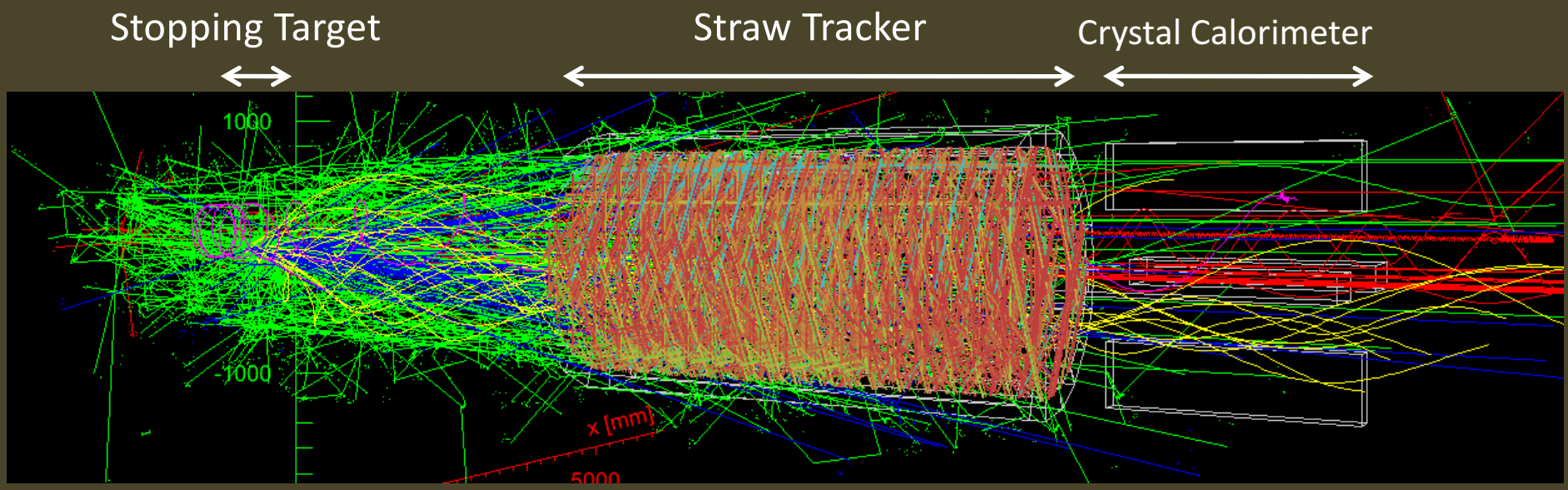

- A signal electron, together with all the other "stuff" occurring simultaneously, integrated over 500-1695 ns window

Mu2e Pattern Recognition

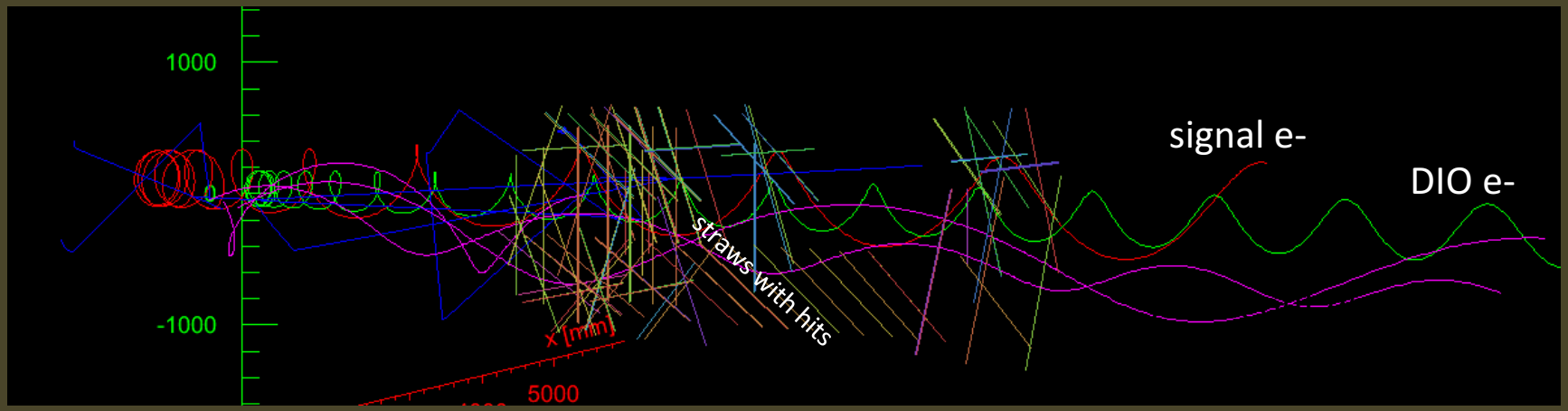

(particles with hits within +/-40 ns of signal electron t_{mean})

- We use timing information to look in +/- 40 ns windows – significant reduction in occupancy and significant simplification for Patt. Rec.

Mu2e Spectrometer Performance

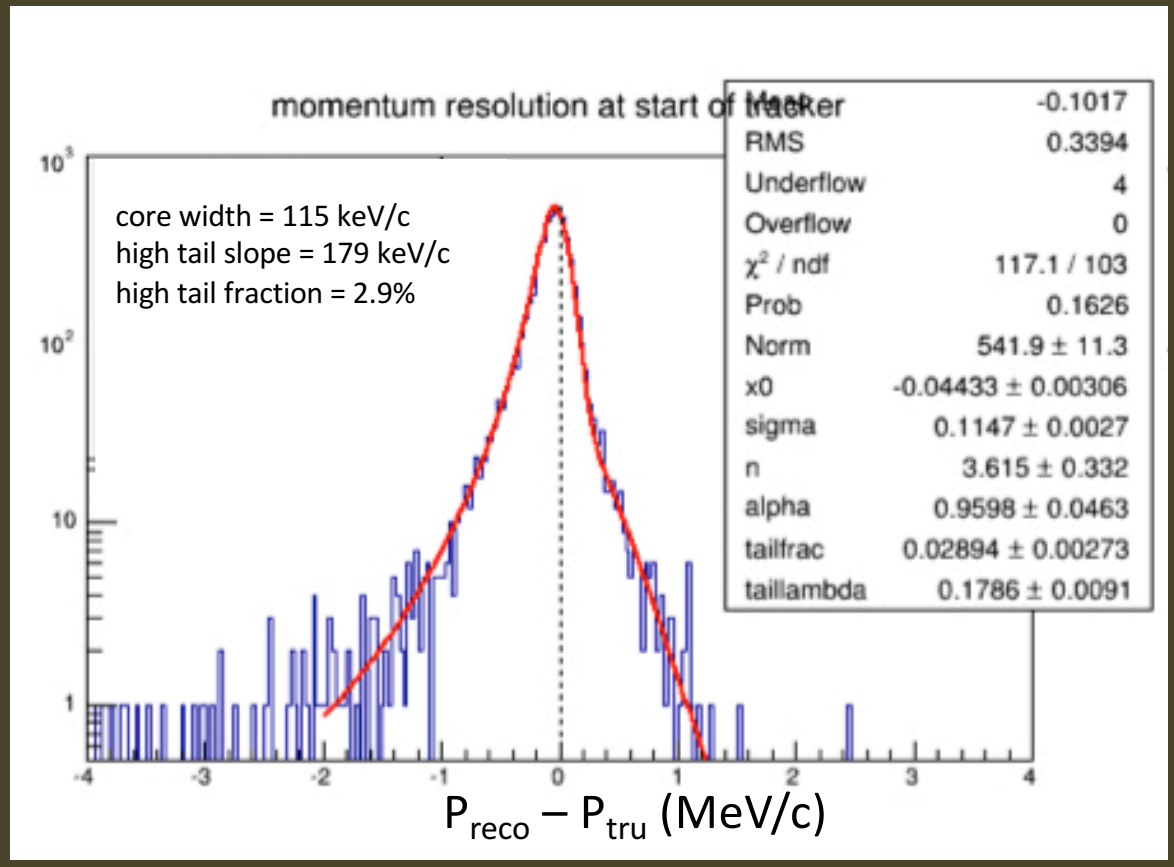

- Performance well within physics requirements

After all analysis requirements

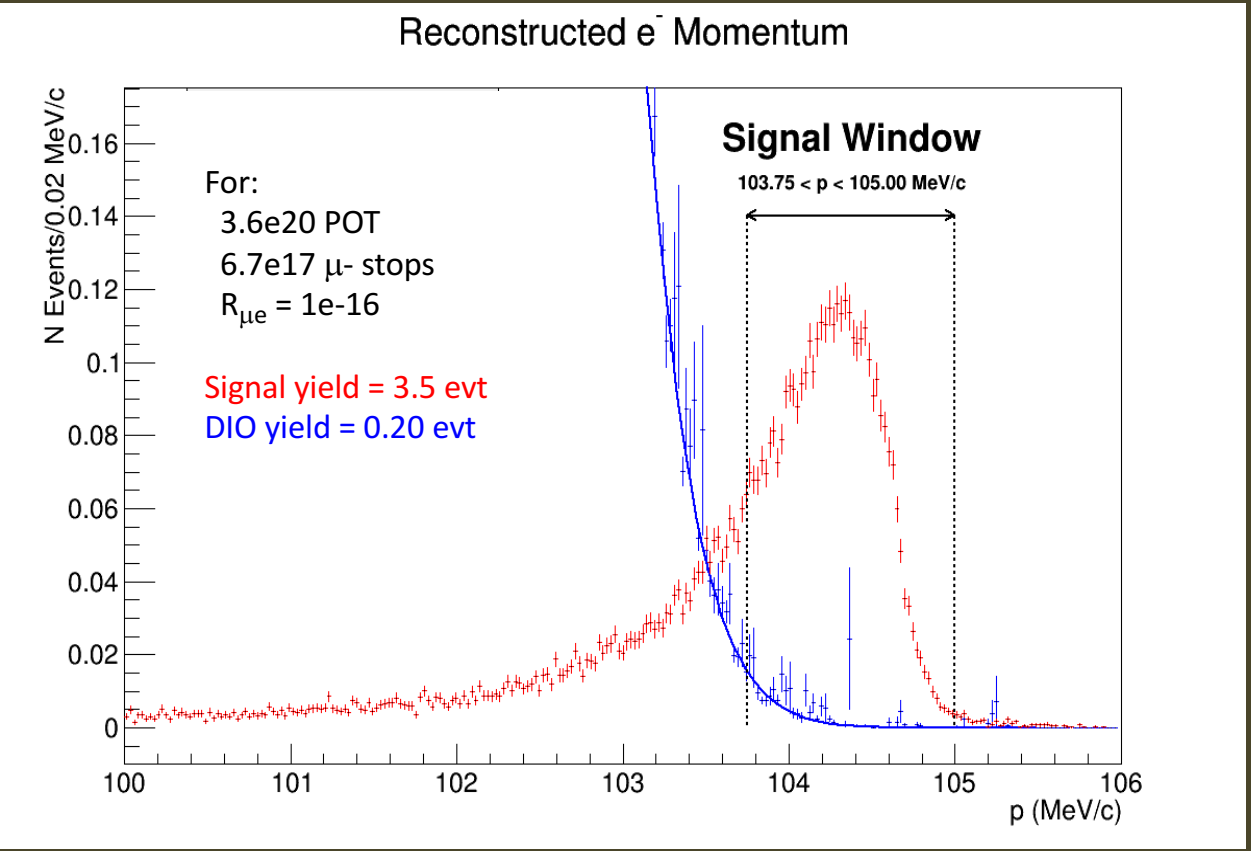

- Single-event-sensitivity = 2.9 x 10^{-17} (SES goal 2.4 x 10^{-17})
- Total background < 0.5 events

Track Reconstruction and Selection

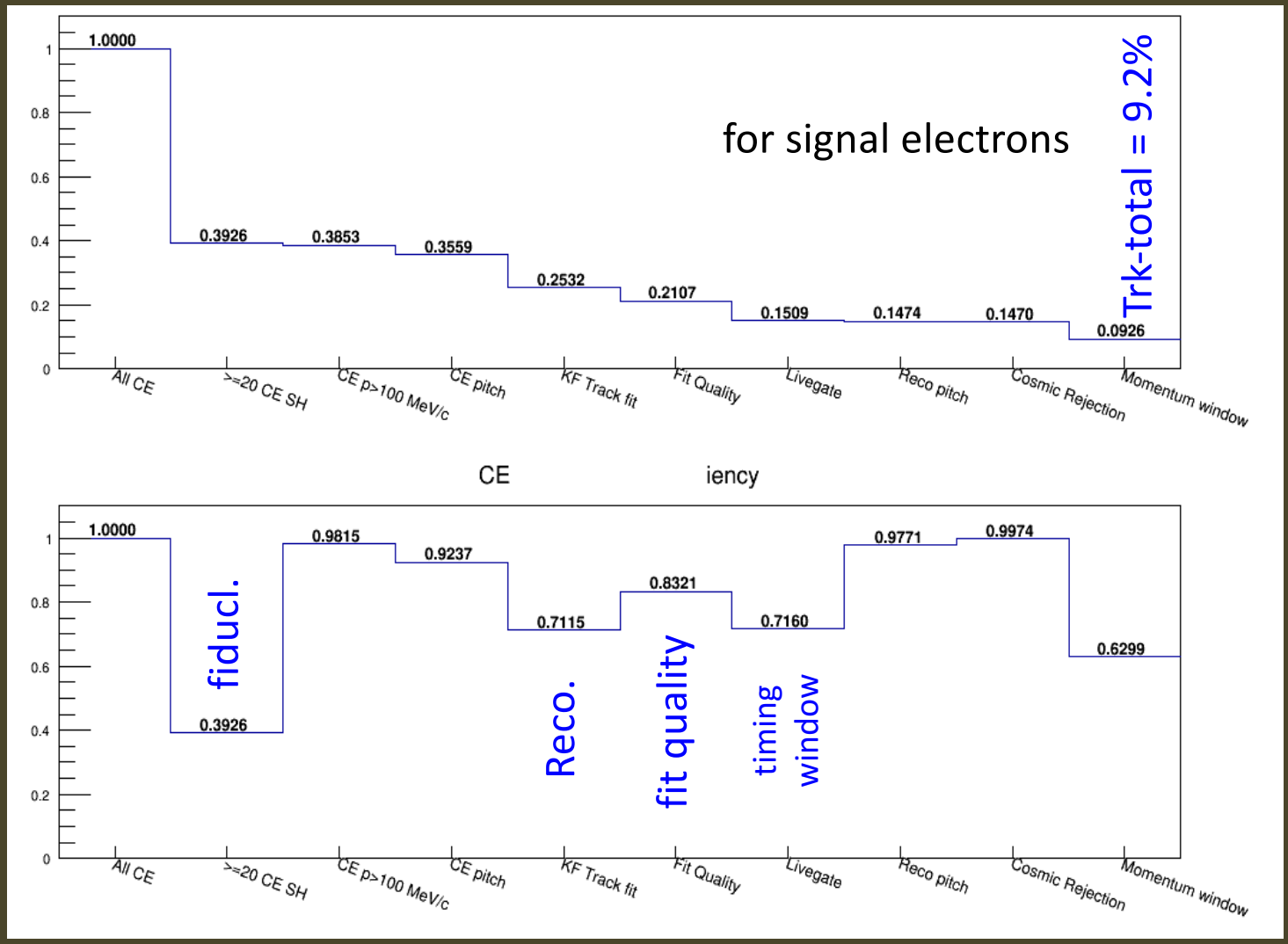

Inefficiency dominated by geometric acceptance

After calorimeter PID and CRV deadtime, Total = 8.5%

Mu2e Performance

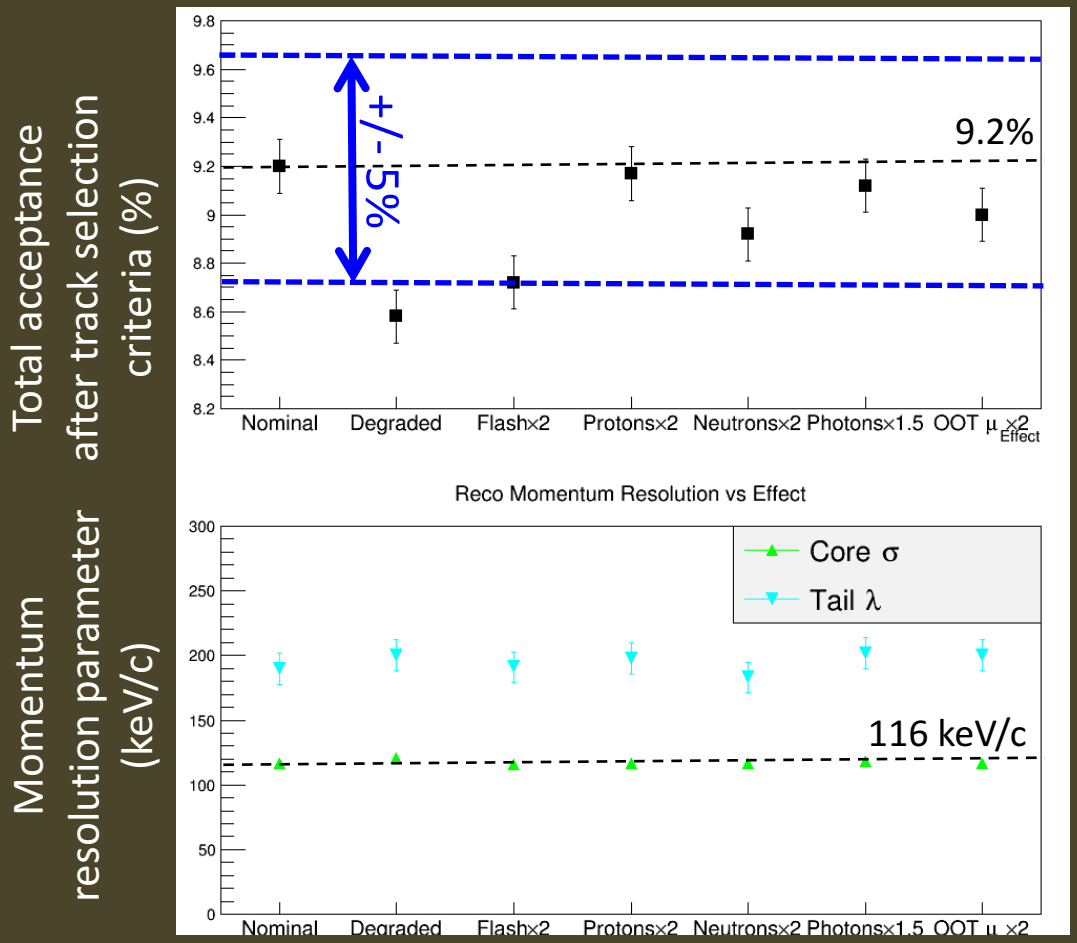

Variations in accidental hit rate

- Robust against increases in rate

Mu2e Calorimeter

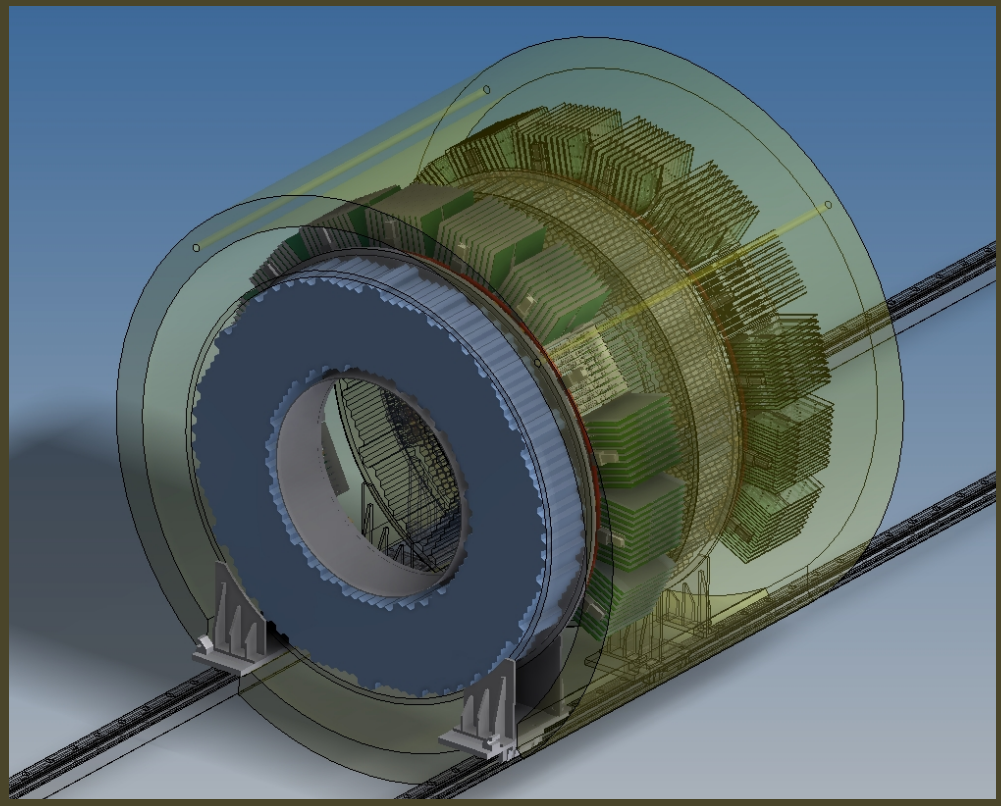

- Crystal calorimeter
  - Compact
  - Radiation hard
  - Good timing and energy resolution

Mu2e Calorimeter

- Baseline design : Cesium Iodine (CsI)
  - Radiation hard, fast, non-hygroscopic

	CsI
Density (g/cm3)	4.51
Radiation length (cm)	1.86
Moliere Radius (cm)	3.57
Interaction length (cm)	39.3
dE/dX (MeV/cm)	5.56
Refractive index	1.95
Peak luminescence (nm)	310
Decay time (ns)	26
Light yield (rel. to NaI)	3.6%
Variation with temperature	-1.4% / deg-C

Mu2e Calorimeter

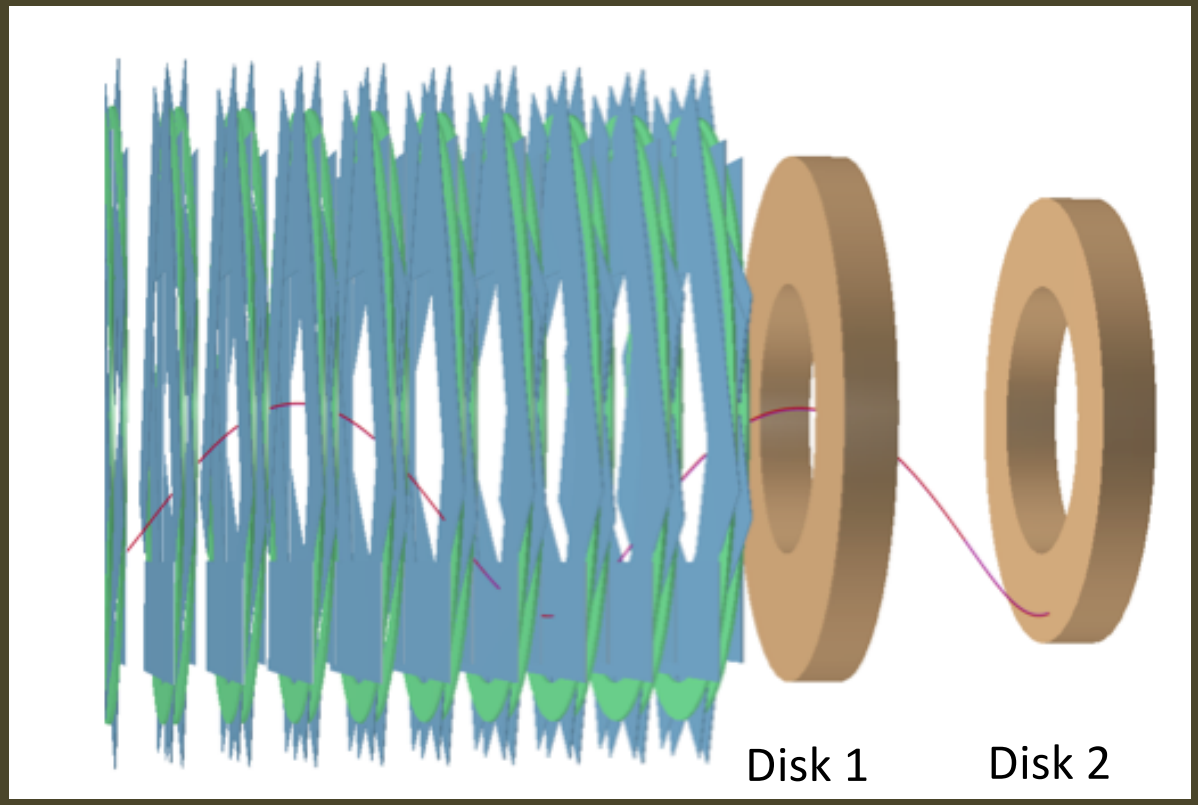

- Will employ 2 disks (radius = 37-66 cm)
- ~1400 crystals with square cross-section
  - ~3 cm diameter, ~20 cm long (10 X_0)
- Two photo-sensors/crystal on back (MPPCs)

3x3 Prototype

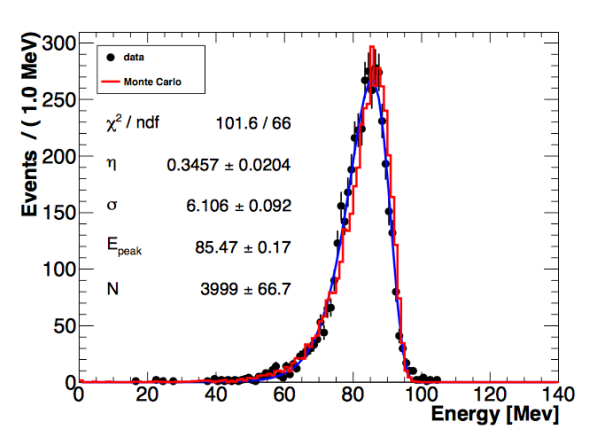

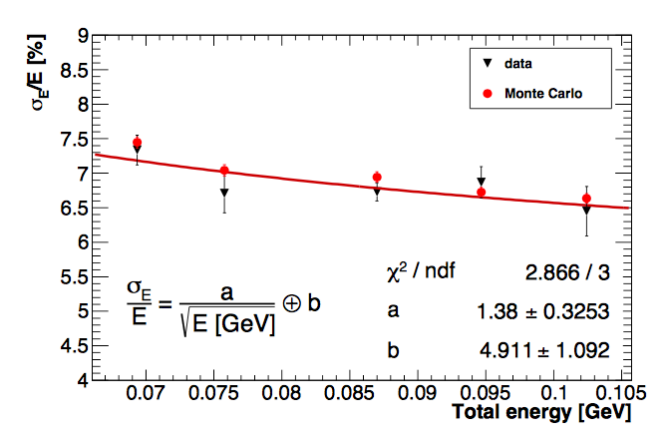

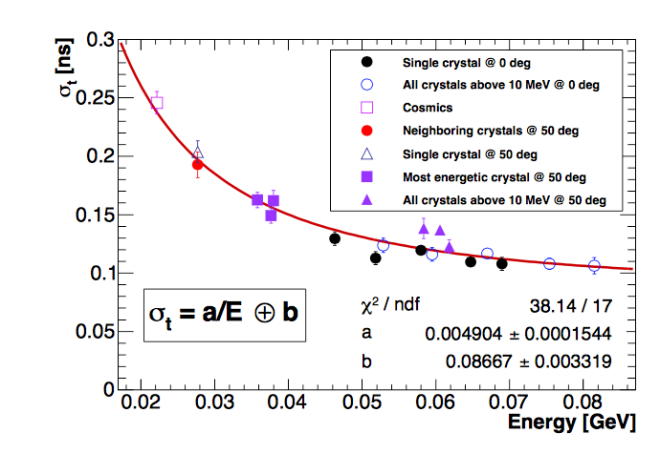

- Data well described by the Monte Carlo

- Energy Resolution vs E
- σ_E ~ 6-7% at 100 MeV
- For this small matrix, there is a significant contribution from leakage

- Time Resolution vs E
- σ_t ~ 110 ps at 100 MeV

- Test beam with e^- at E = 80-120 MeV

Mu2e Calorimeter

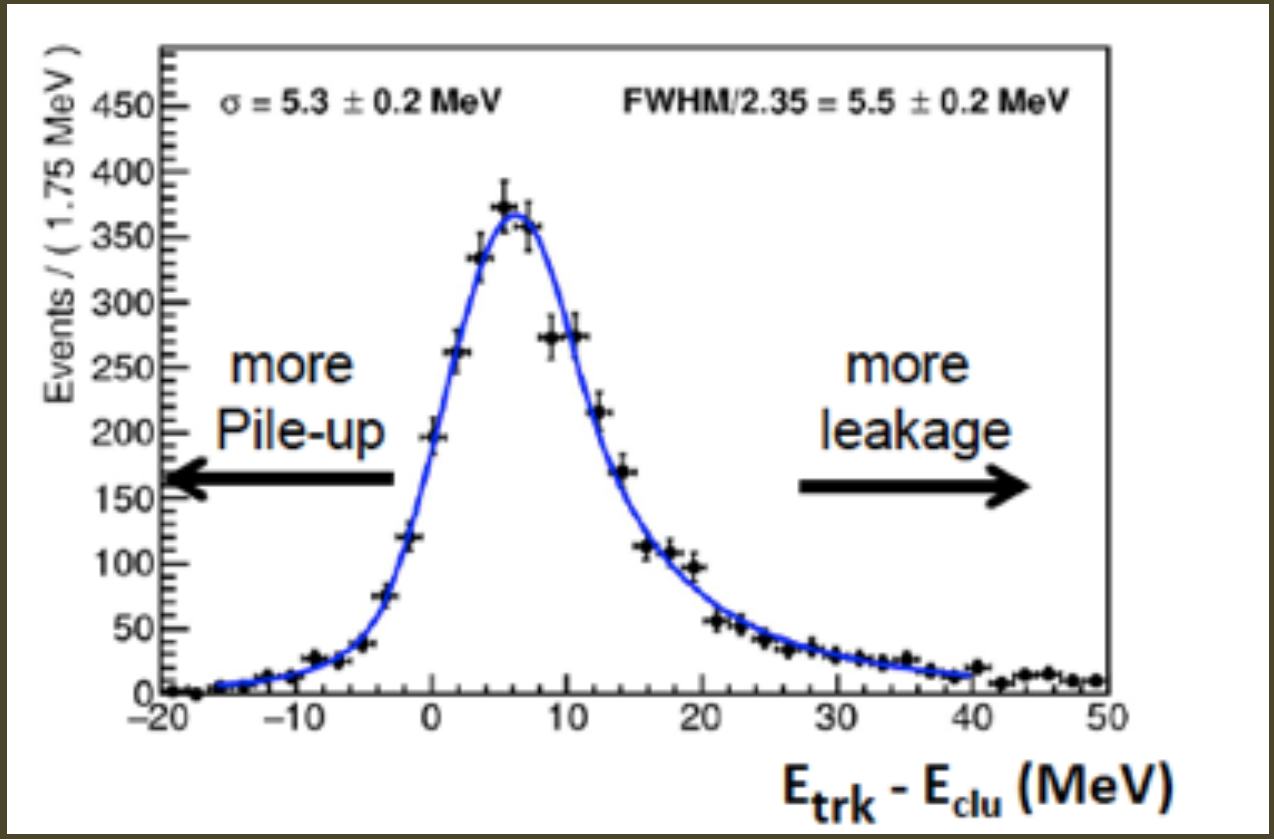

- With 60 ns integration, expect to achieve an energy resolution ~5% for 105 MeV electrons
  - Performance a weak function of rate in relevant range

Calorimeter Particle ID

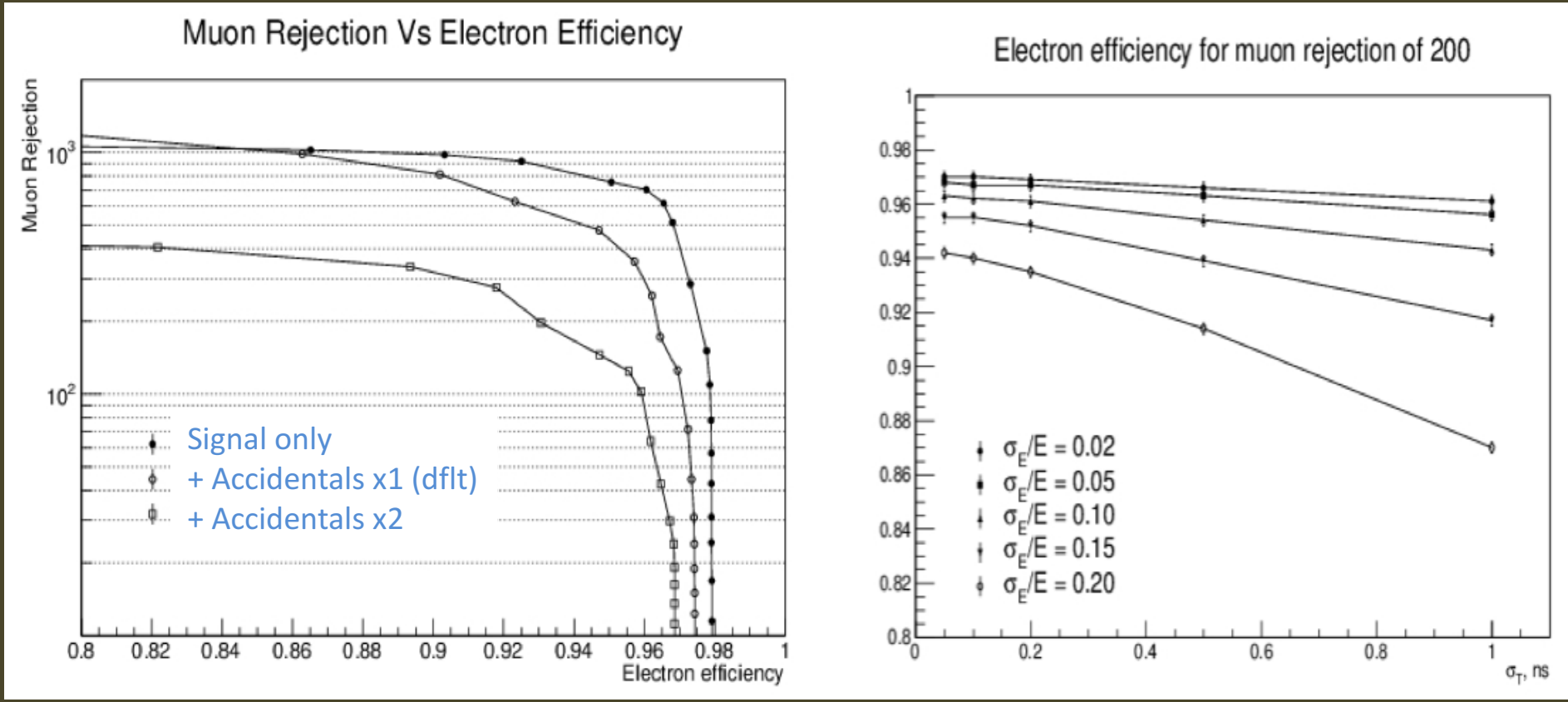

- Combine TOF and E/P information in LLR
  - 96% electron efficiency for muon rejection x200

Mu2e Cosmic-Ray Veto

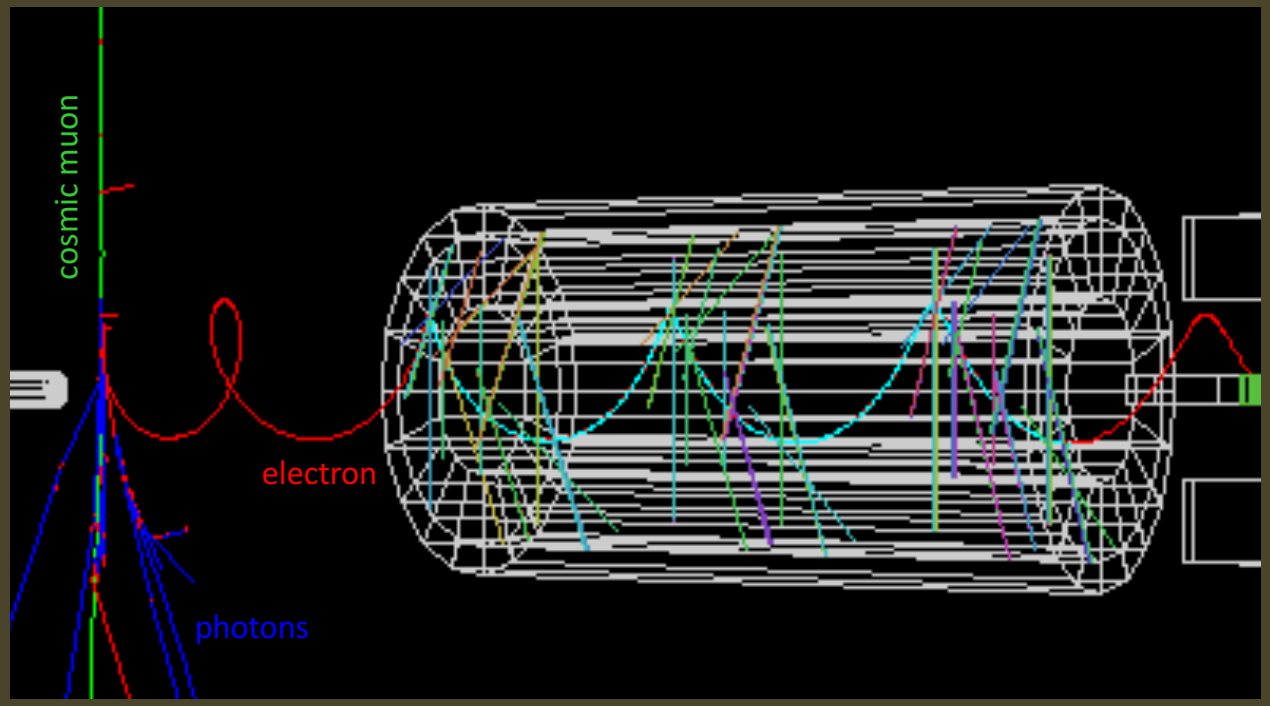

- Cosmic μ can generate background events via decay, scattering, or material interactions

Mu2e Cosmic-Ray Veto

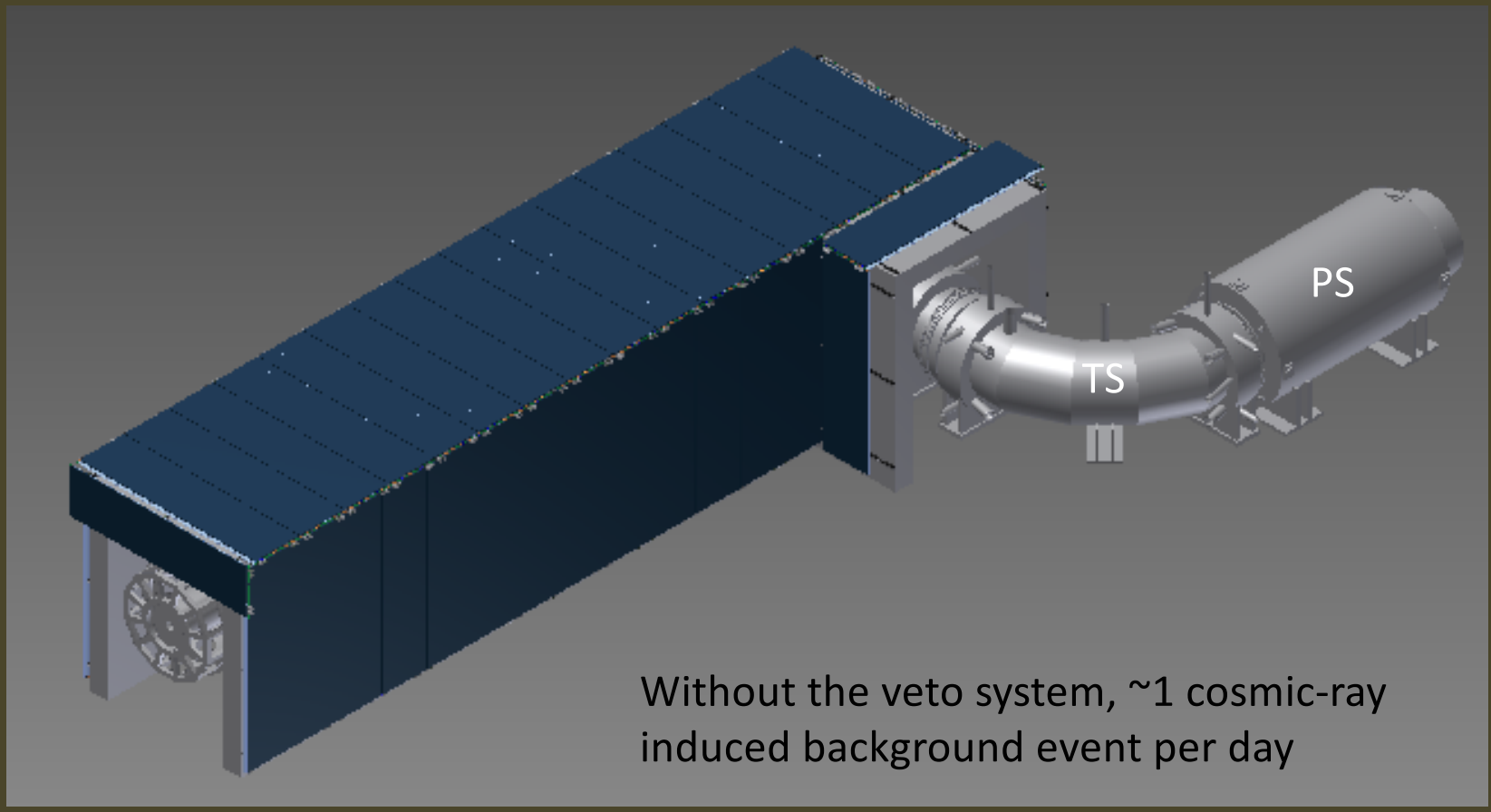

- Veto system covers entire DS and half TS

Mu2e Cosmic-Ray Veto

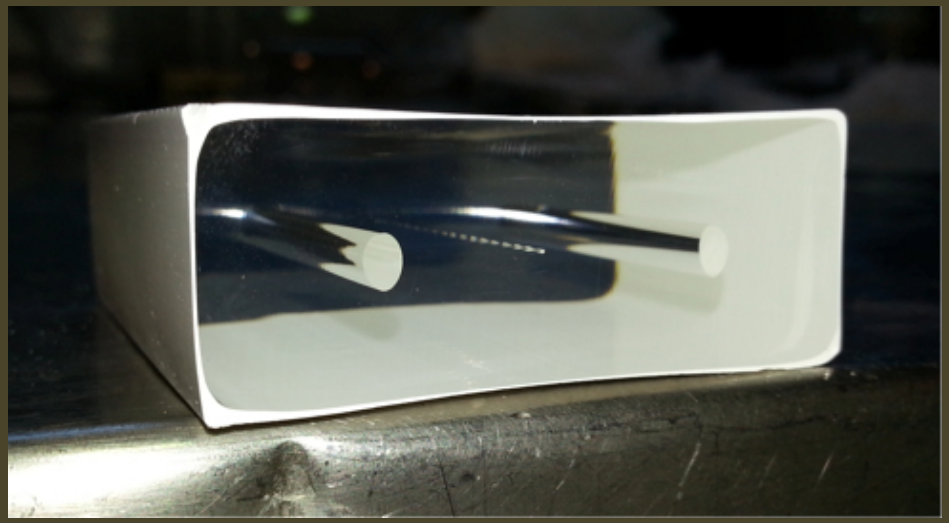

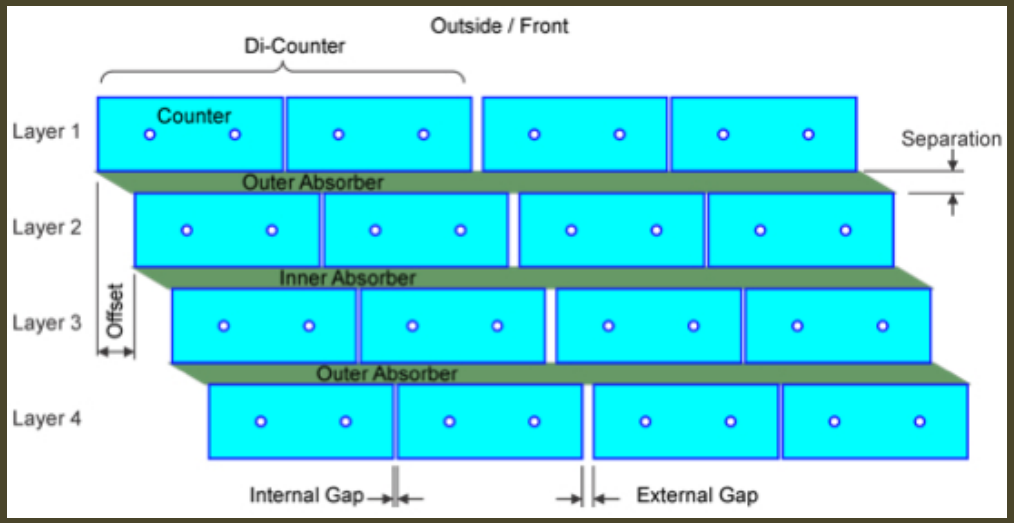

- Will use 4 overlapping layers of scintillator
  - Each bar is 5 x 2 x ~450 cm^3
  - 2 WLS fibers / bar
  - Read-out both ends of each fiber with SiPM
  - Have achieved $\varepsilon > 99.4\%$ (per layer) in test beam

Cosmic Ray Veto

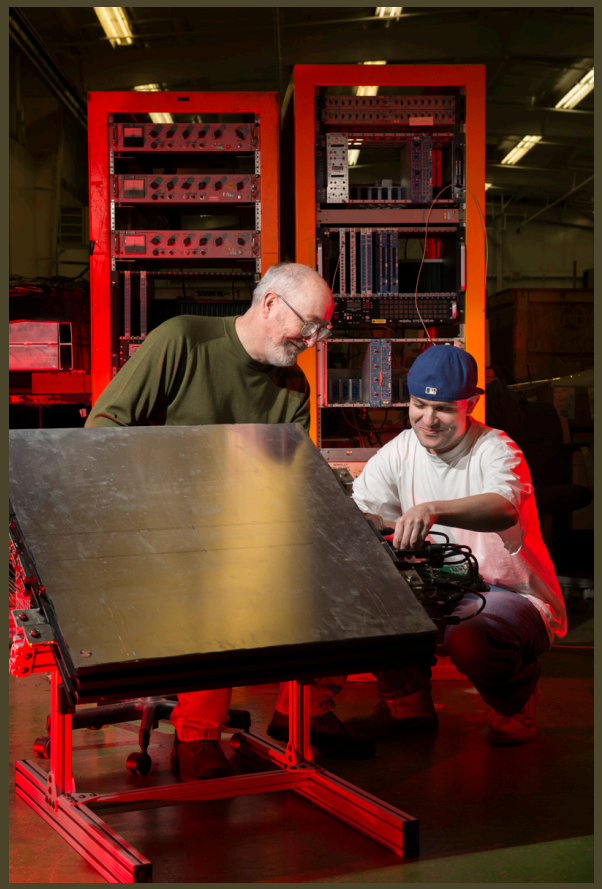

Typical light yield from CRV counter prototype – 20 cm from RO end

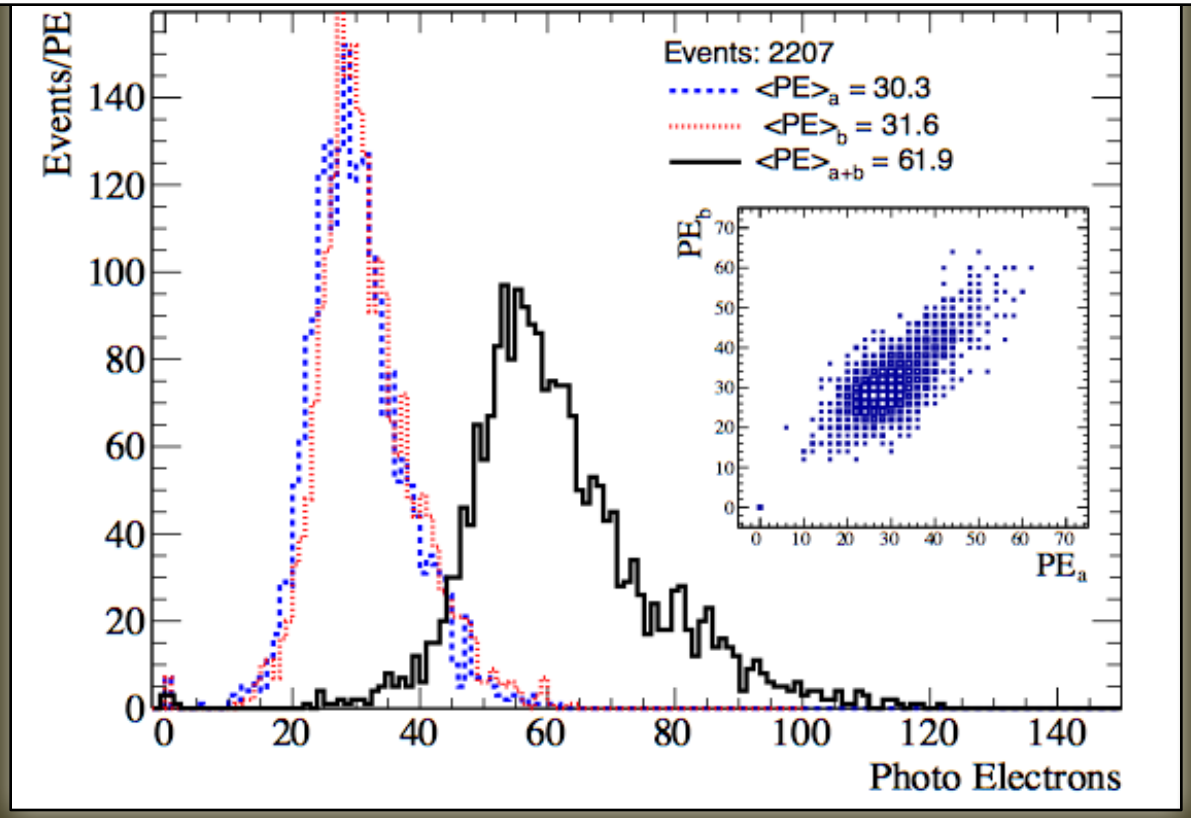

- Test beam data to vet design/performance

Mu2e Detector Hall


East Face, September 2016

- Structurally complete. Outfitting well along.

Mu2e Detector Hall


North Face, September 2016

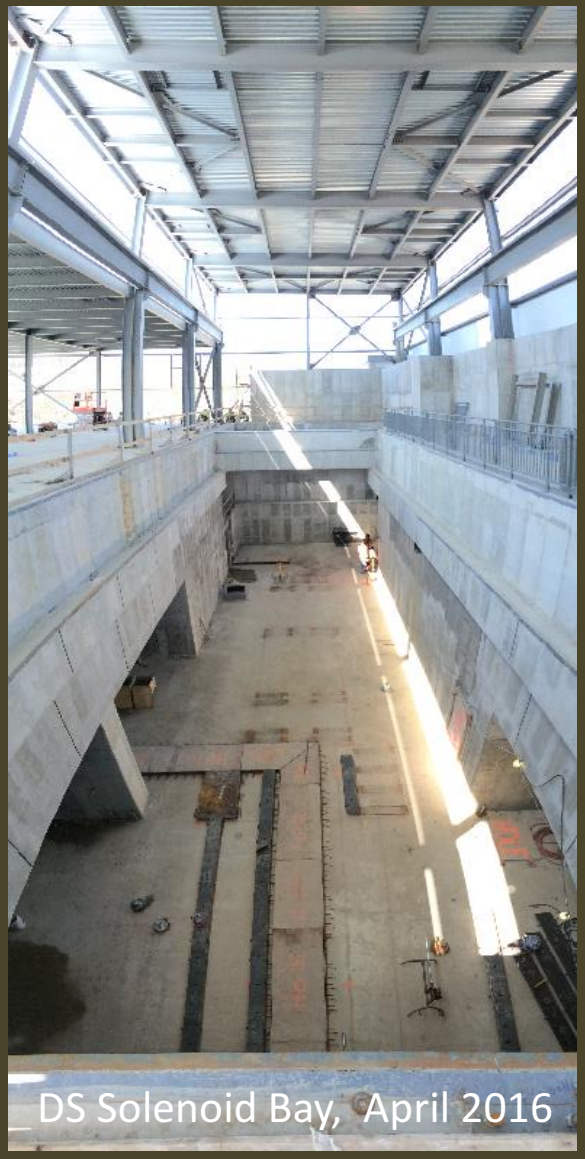
DS Solenoid Bay, April 2016

- Beneficial Occupancy expected Nov/Dec 2016

Details, details, details

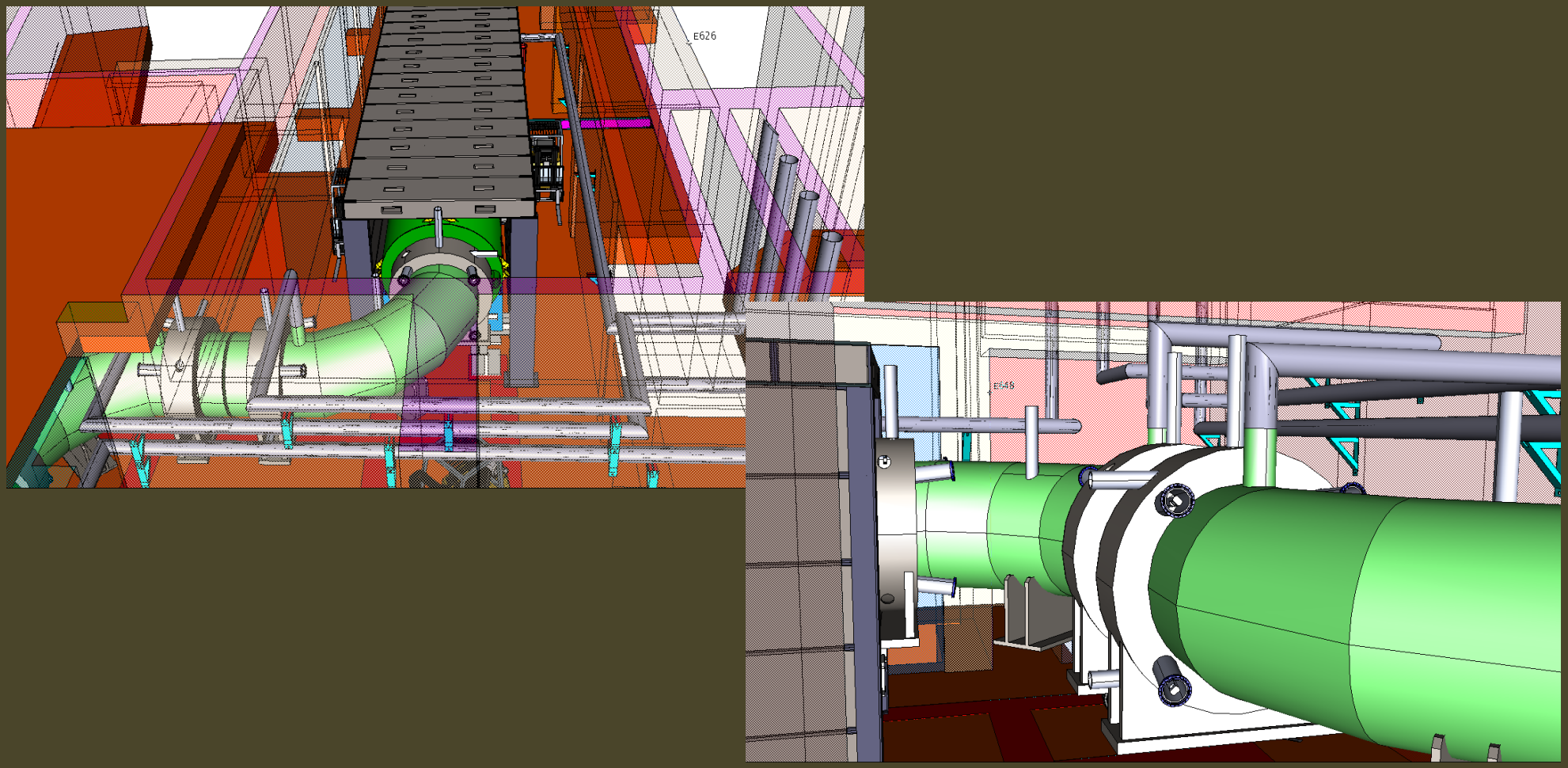

- Working to identify and resolve interface issues

Mu2e Schedule

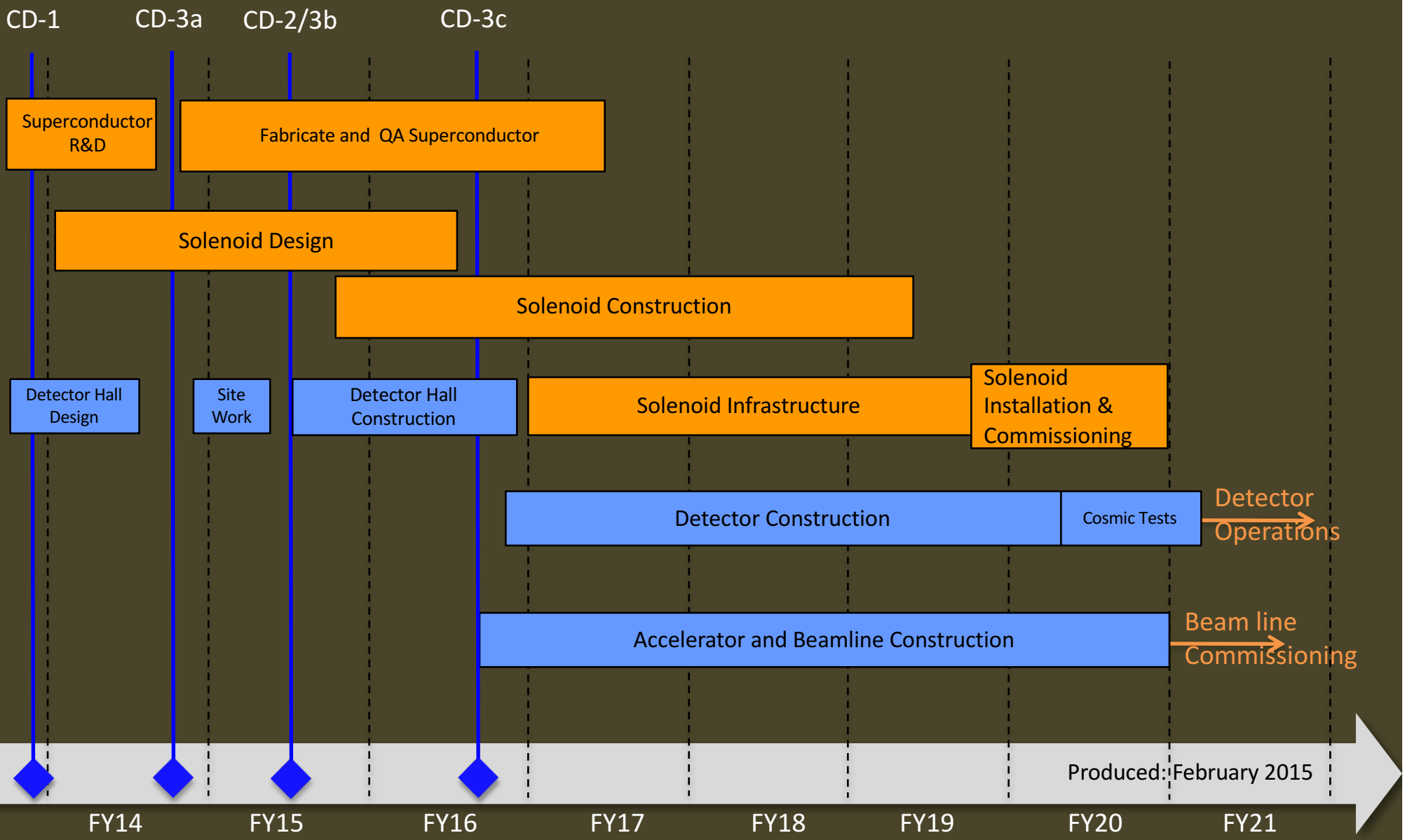

Mu2e Schedule

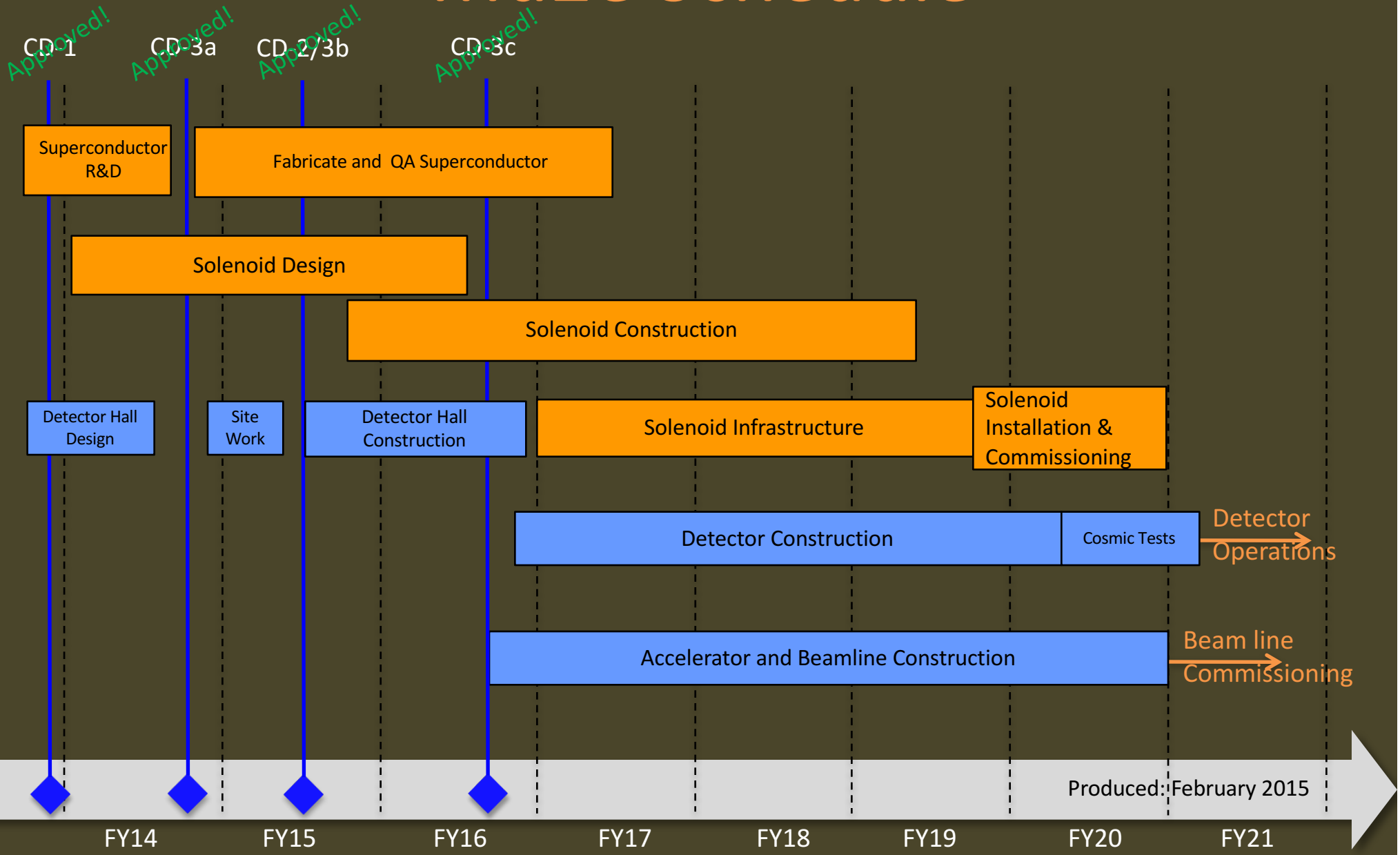

What next?

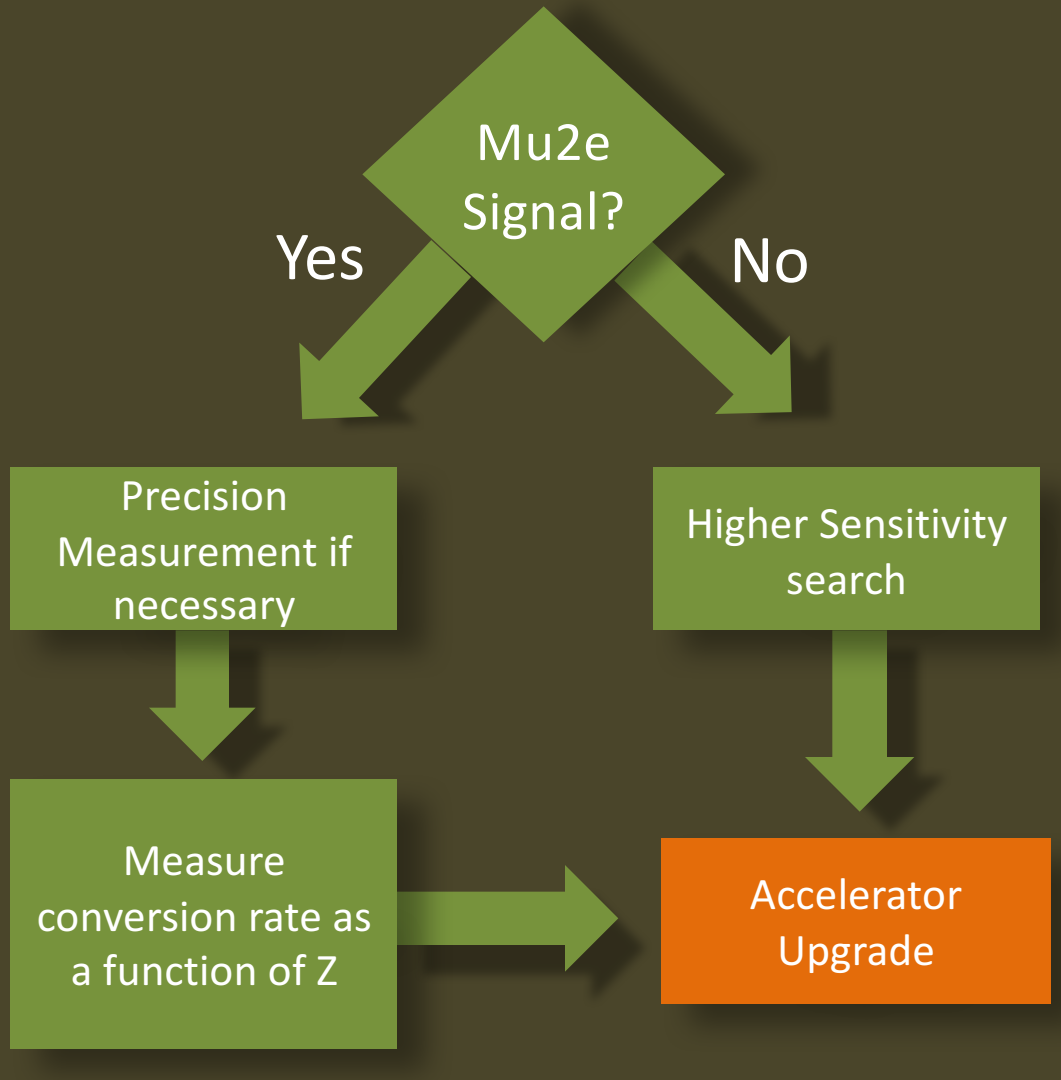

- A next-generation Mu2e experiment makes sense in all scenarios
  - Push sensitivity or
  - Study underlying new physics
  - Will need more protons → upgrade accelerator
  - Snowmass white paper, arXiv:1307.1168

μN→eN vs stopping-target Z

- By measuring the ratio of rates using different stopping targets Mu2e can unveil underlying new-physics mechanism

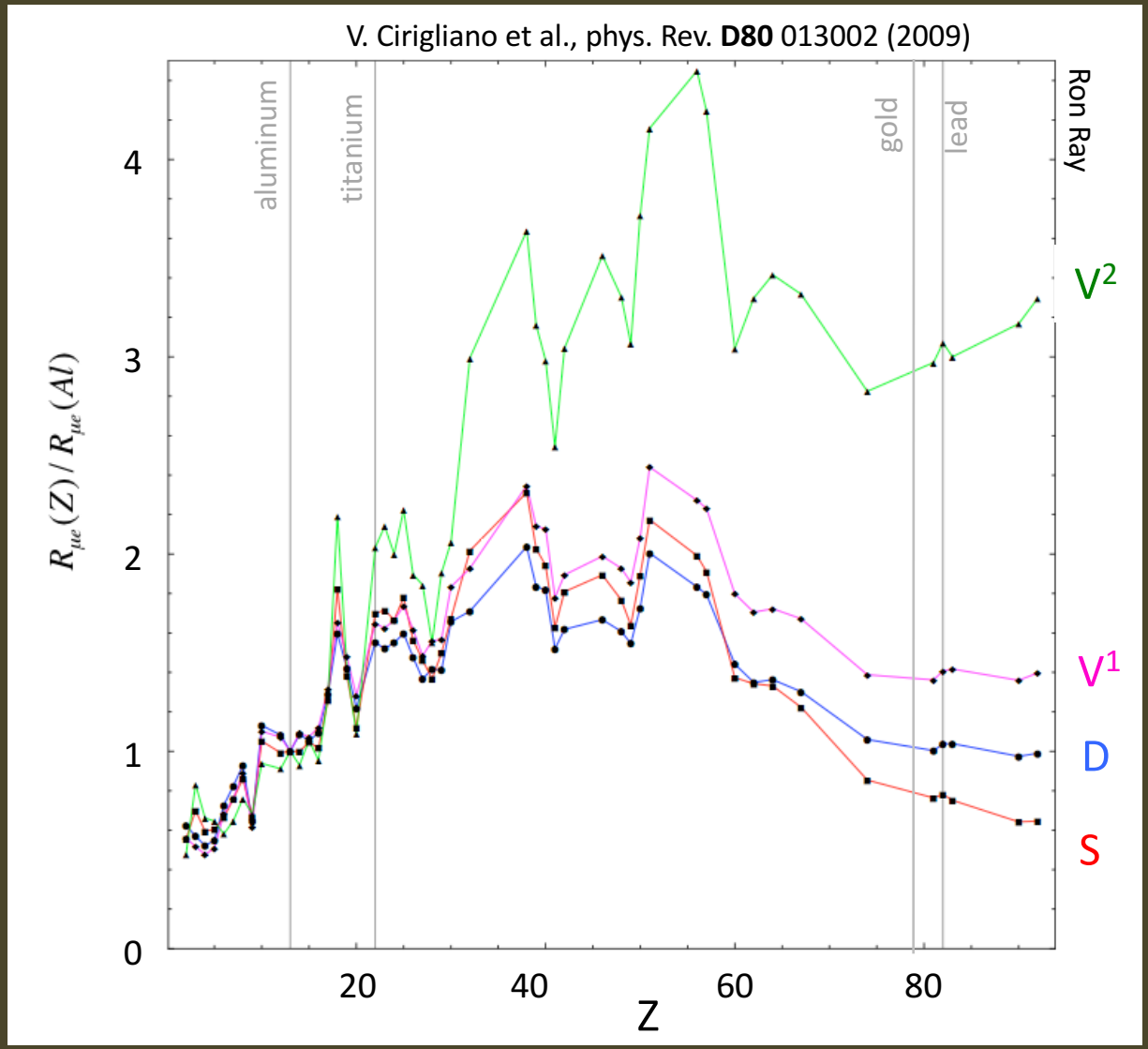

Concluding remarks

Summary

The Mu2e experiment:

- Improves sensitivity by a factor of 10^4
- Provides *discovery capability* over wide range of New Physics models
- Is complementary to LHC, heavy-flavor, dark matter, and neutrino experiments
- Is progressing on schedule… will begin commissioning in 2020

Interested in learning more?

- Technical Design Report
  - http://arXiv.org/abs/1501.05241
- Experiment web site
  - http://mu2e.fnal.gov

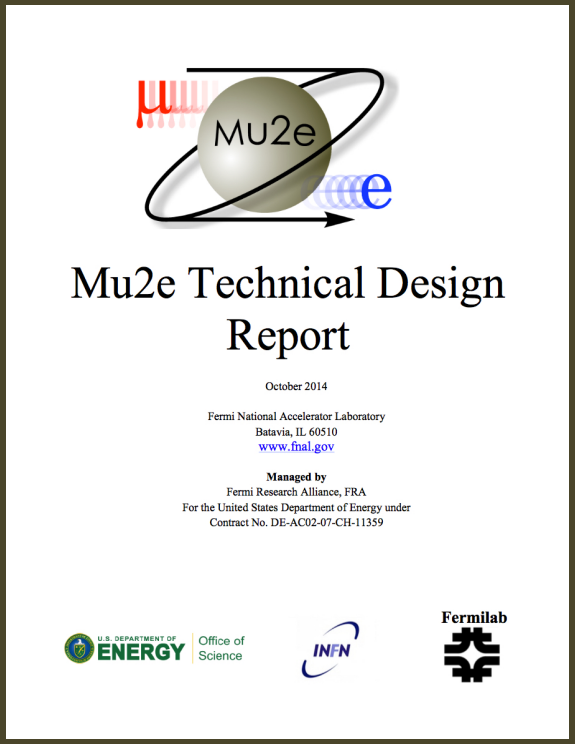

The Mu2e Collaboration


The Mu2e Collaboration, Oct. 2015



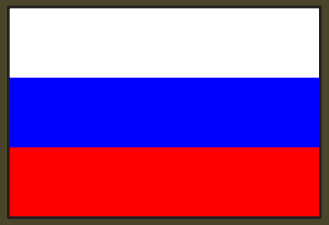

~200 Scientists from 35 Institutions

Argonne National Laboratory, Boston University, Brookhaven National Laboratory, University of California Berkeley, University of California Irvine, California Institute of Technology, City University of New York, Joint Institute of Nuclear Research Dubna, Duke University, Fermi National Accelerator Laboratory, Laboratori Nazionale di Frascati, University of Houston, Helmholtz-Zentrum Dresden-Rossendorf, University of Illinois, INFN Genova, Lawrence Berkeley National Laboratory, INFN Lecce, University Marconi Rome, Kansas State University, Lewis University, University of Louisville, University of Minnesota, Muons Inc., Northwestern University, Institute for Nuclear Research Moscow, Northern Illinois University, INFN Pisa, Purdue University, Novosibirsk State University/Budker Institute of Nuclear Physics, Rice University, University of South Alabama, Sun Yat-Sen University, University of Virginia, University of Washington, Yale University

Additional Slides

Mu2e Experimental Apparatus

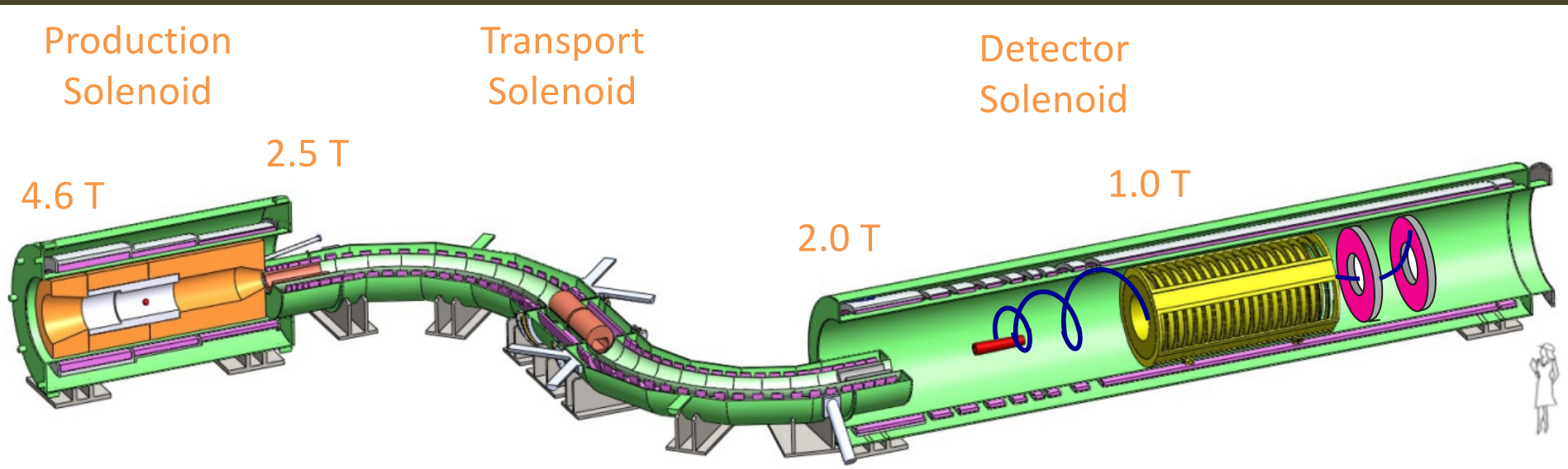

Graded fields important to suppress backgrounds, to increase muon yield, and to improve geometric acceptance for signal electrons

- Derived from MELC concept originated by Lobashev and Djilkibaev in 1989

Constraints from μ→e Experiments

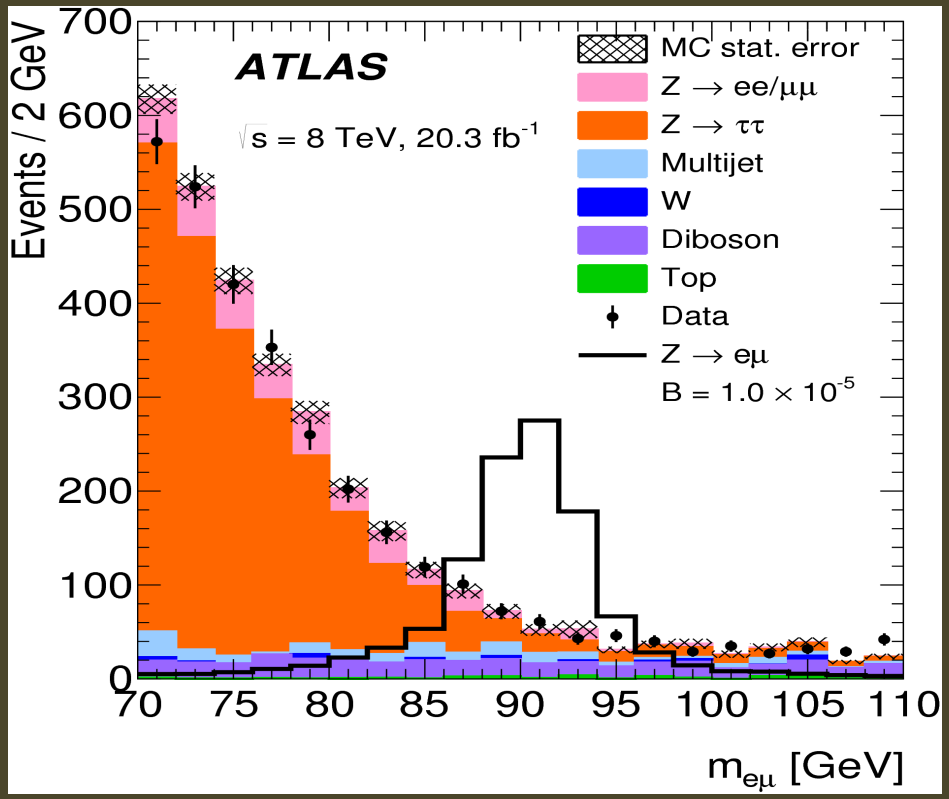

Constraints on LFV Z couplings

μ→eee: B(Z→μe) <5x10^{-13}* (now)

CMS : B(Z→μe) < 7.3 x 10^{-7}

ATLAS: B(Z→μe) < 7.5 x 10^{-7} (now)

* S. Nussinov, R.D. Peccei, and X.M. Zhang, Phys. Rev. D63 (2001) 016003 (arXiv:0004153 [hep-ph]).

Constraints from μ→e Experiments

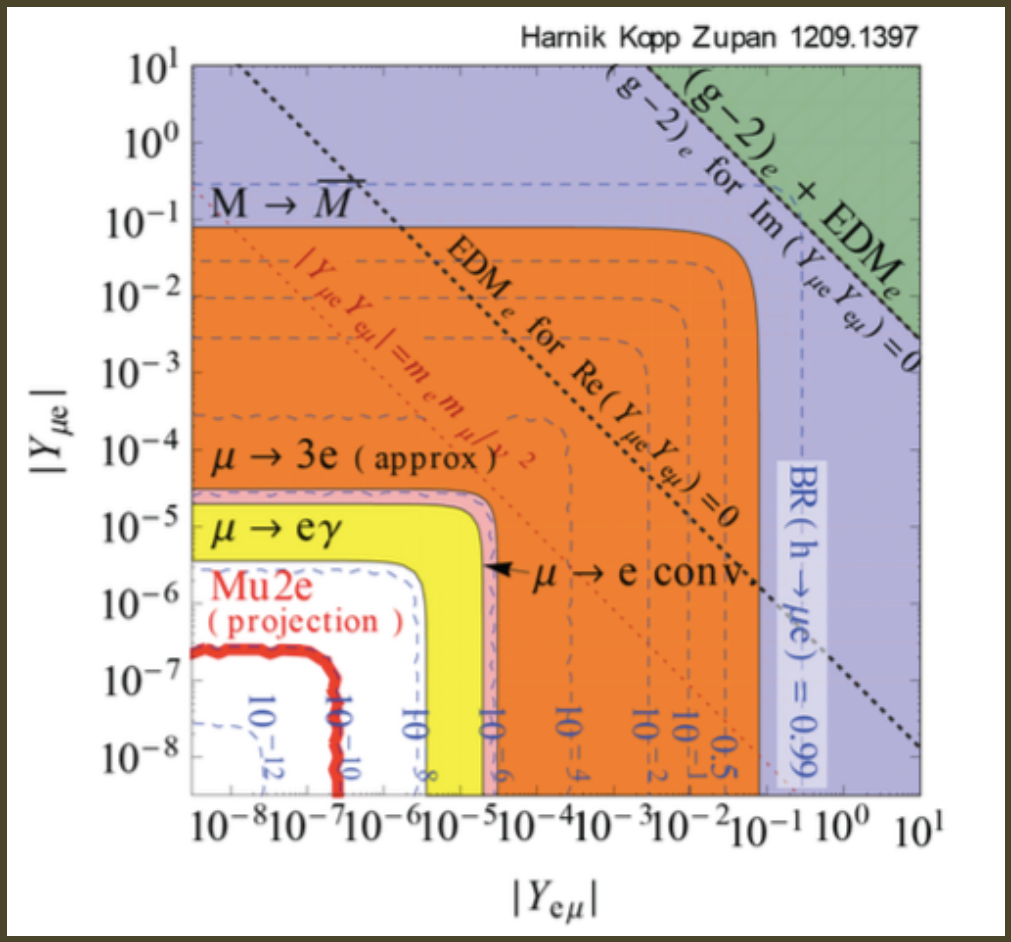

Constraints on LFV Yukawa couplings

μ→eγ : B(h→μe) < 10^{-8}* (now)

μN→eN : B(h→μe) < 10^{-10} (future)

Collider reach
LHC : B(h→μe) < 10^{-2} -10^{-3}

* R. Harnik, J. Kopp, and J. Zupan, JHEP 03 (2013) 026 (arXiv:1209.1397 [hep-ph]).

Constraints from τ→e,μ Experiments

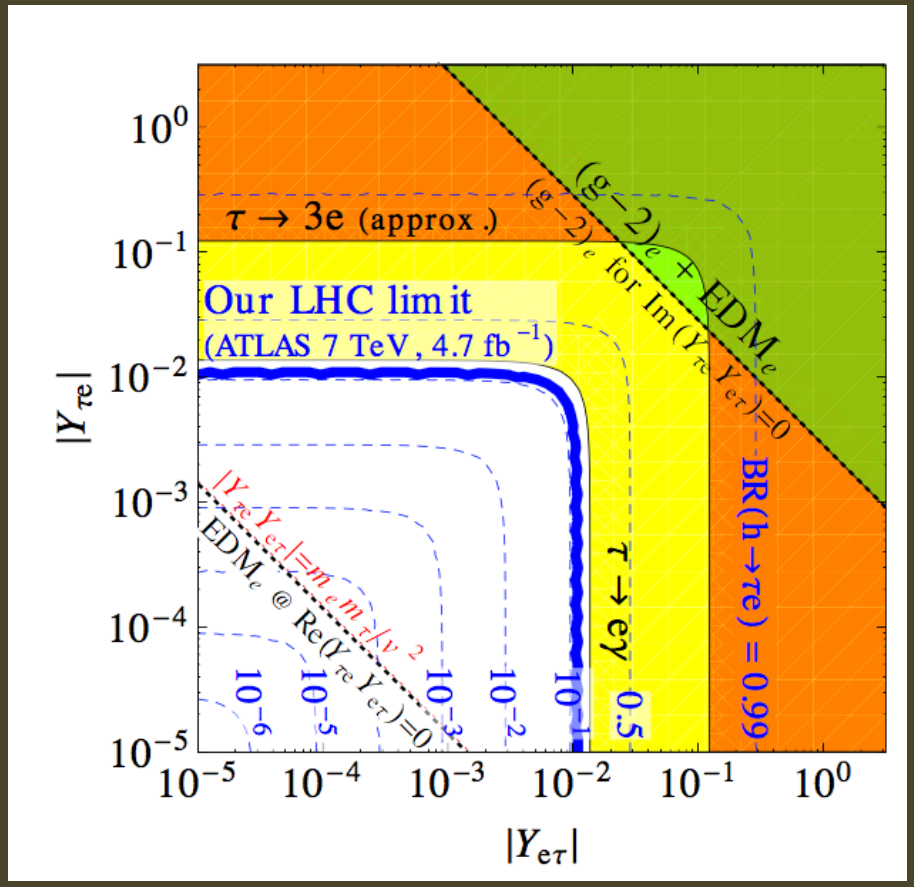

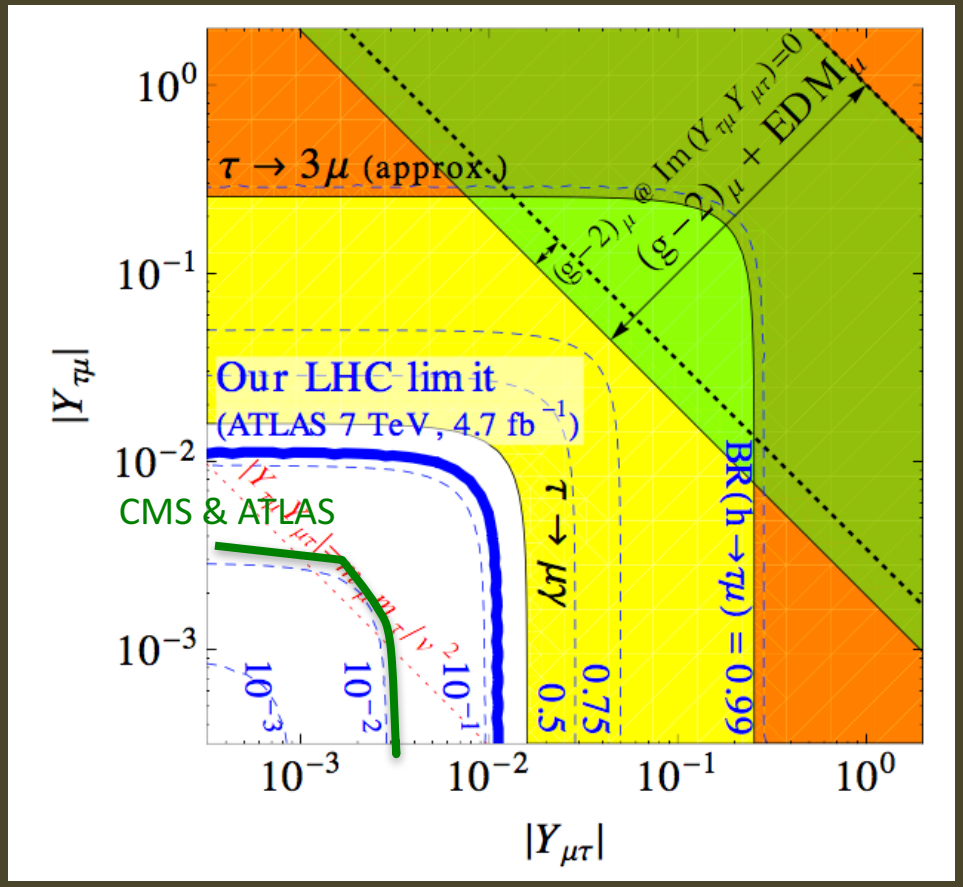

- cLFV using τ correspond to B(h→τe, τμ) ~ 10%
- CMS and ATLAS already exploring B(h→τμ) ~ 1%

h→τ constraints from μ→e cLFV

τμ-τe couplings can contribute to μ→e transitions. As an example:

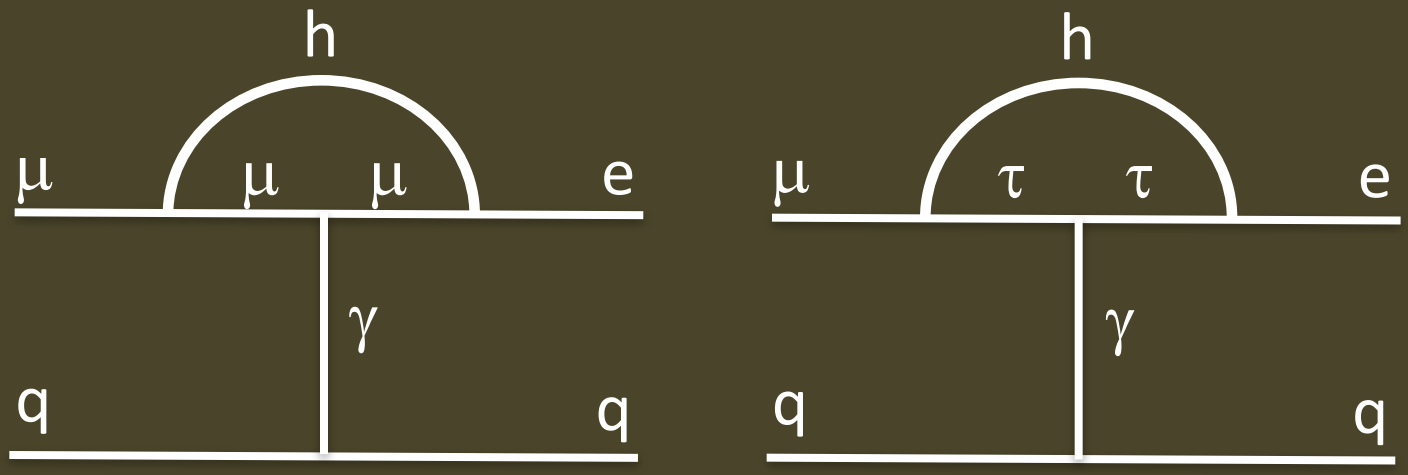

- μ→eγ constrains dipole contributions
- $\mu^- N \rightarrow e^- N$ constrains vector contributions
- Future improvements in $\mu^- N \rightarrow e^- N$ will probe $B(h\rightarrow\tau\mu)B(h\rightarrow\tau e) < 10^{-7}$

cf. I.Dorsner, S. Fajfer, A. Greljo, J. Kamenik, N, Kosnik, I. Nisandzic (1502.07784)
R. Harnik, J. Kopp, J. Supan (1209.1397)

Direct Searches for cLFV h decays

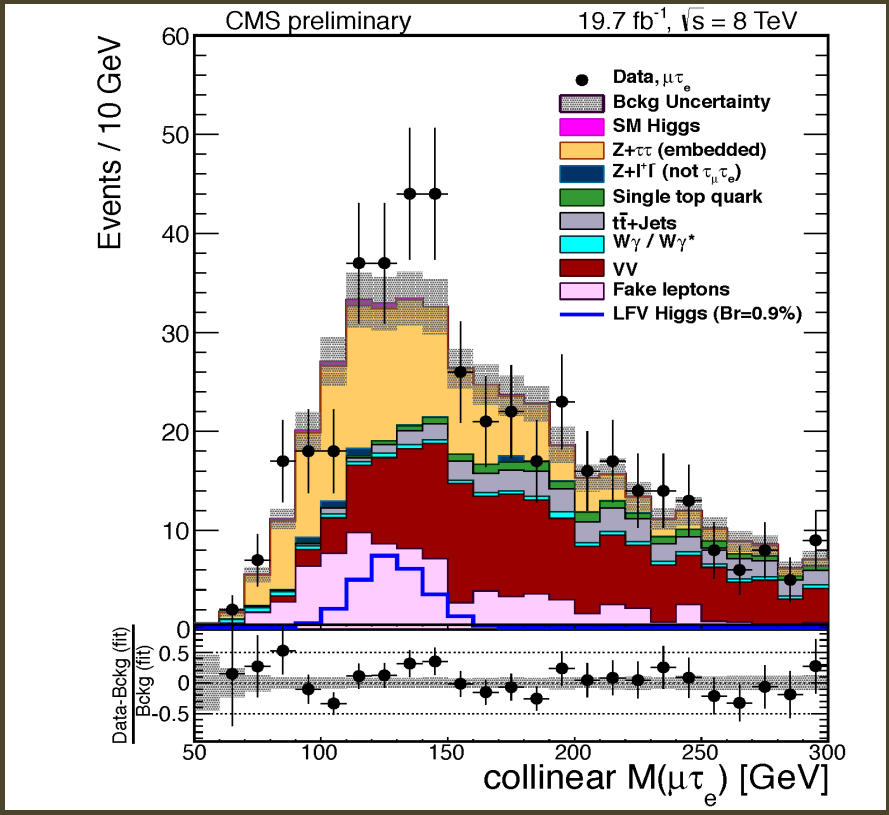

CMS

$B(h \rightarrow \tau\mu) < 1.51 \times 10^{-2}$

Best fit : (0.84 +/- 0.40)%

ATLAS

$B(h \rightarrow \tau\mu) < 1.43 \times 10^{-2}$

Best fit : (0.53 +/- 0.51)%

- Looking forward to more data…

Mu2e Sensitivity

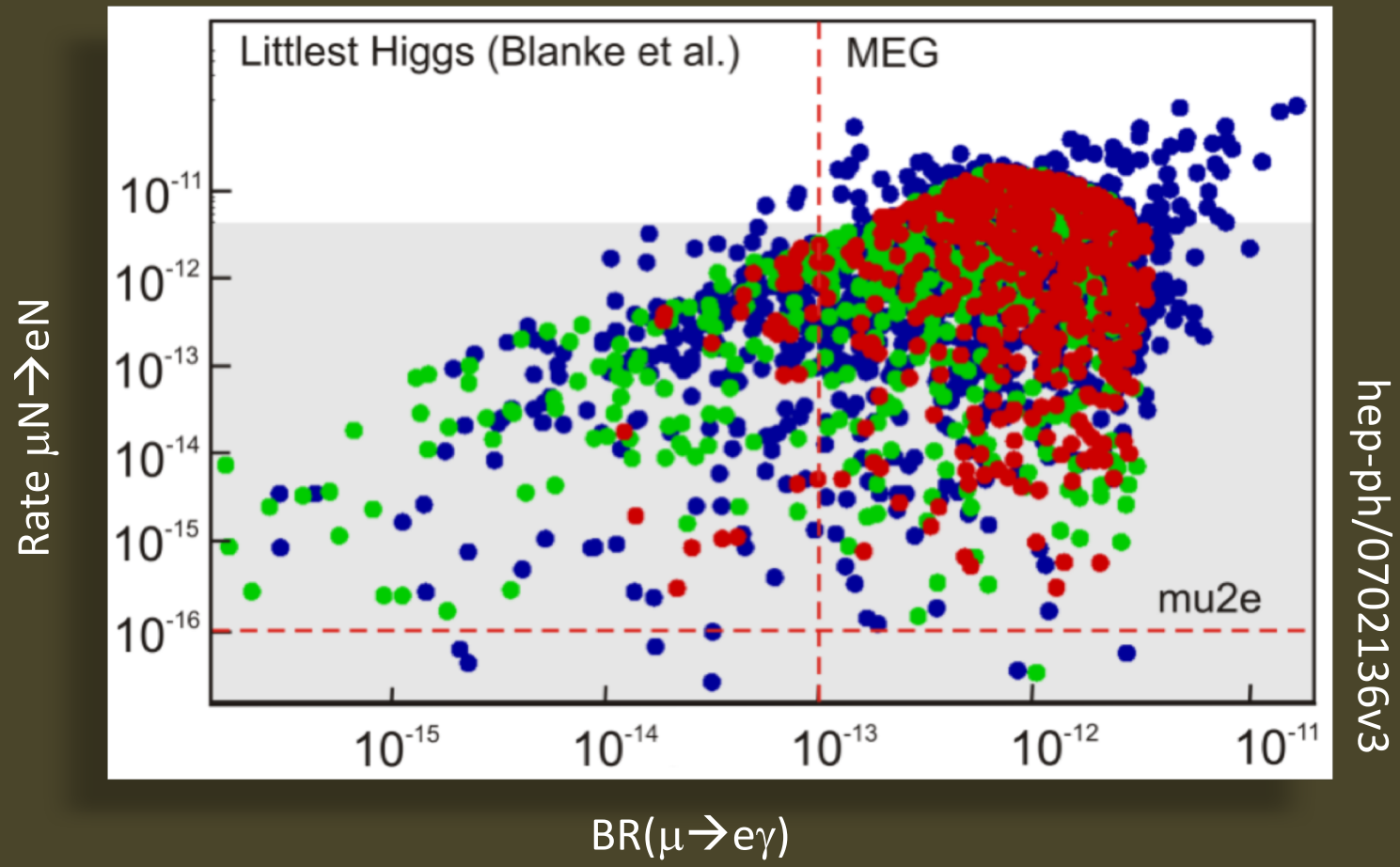

- Mu2e will cover the entire space

Mu2e Sensitivity

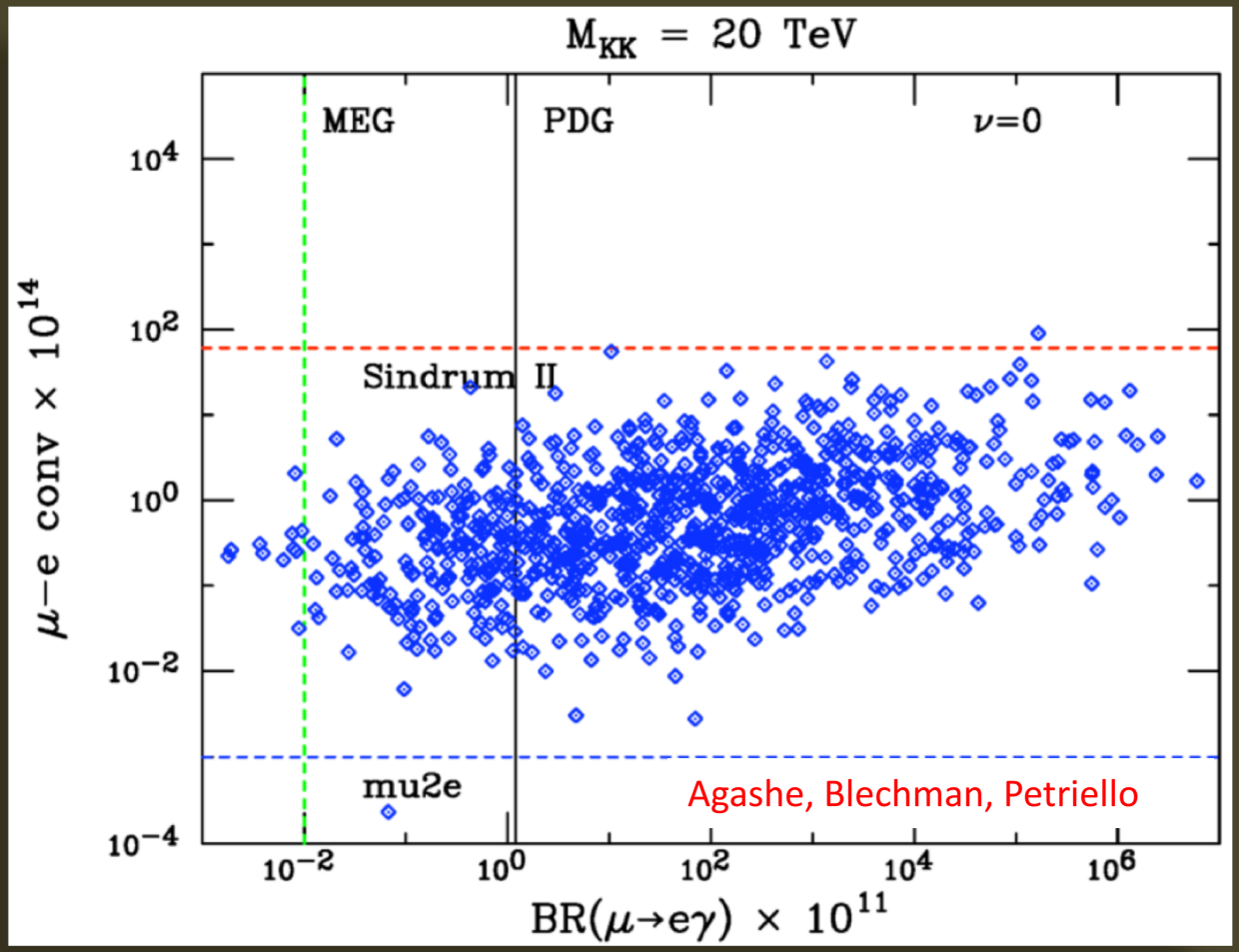

hep-ph/0606021v2

- Mu2e, MEG will each cover entire space

Mu2e Sensitivity

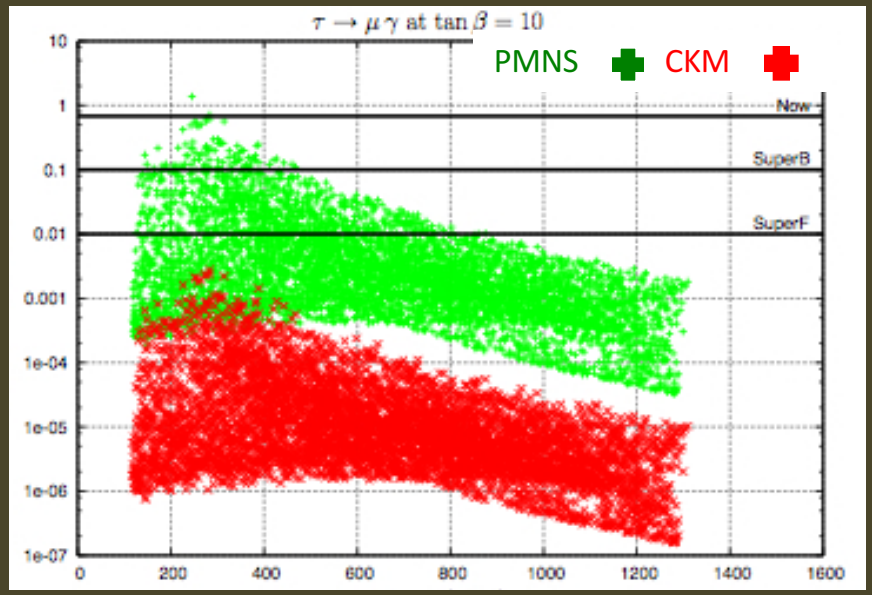

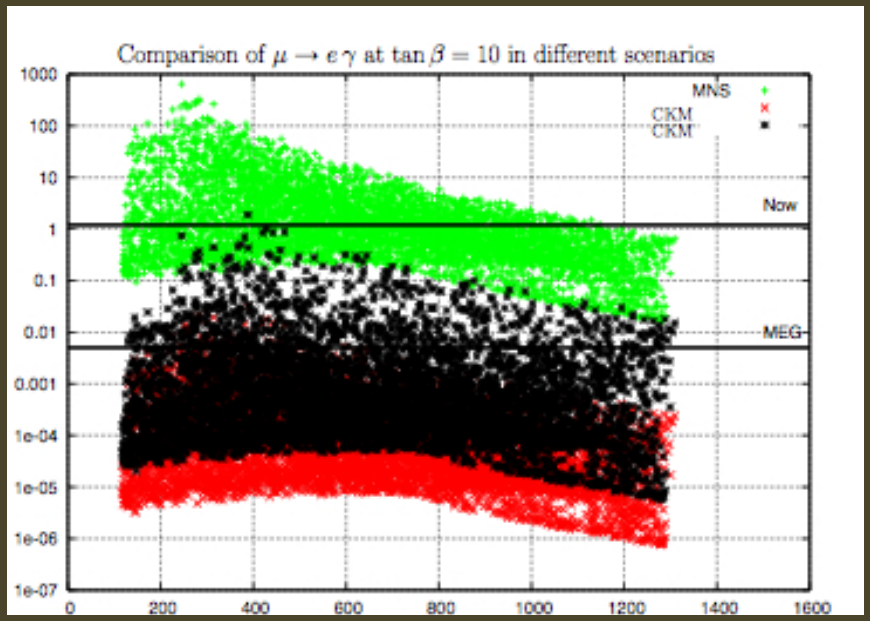

- $\mu\to e\gamma$, $\tau\to\mu\gamma$ will begin to probe this space

Mu2e Sensitivity

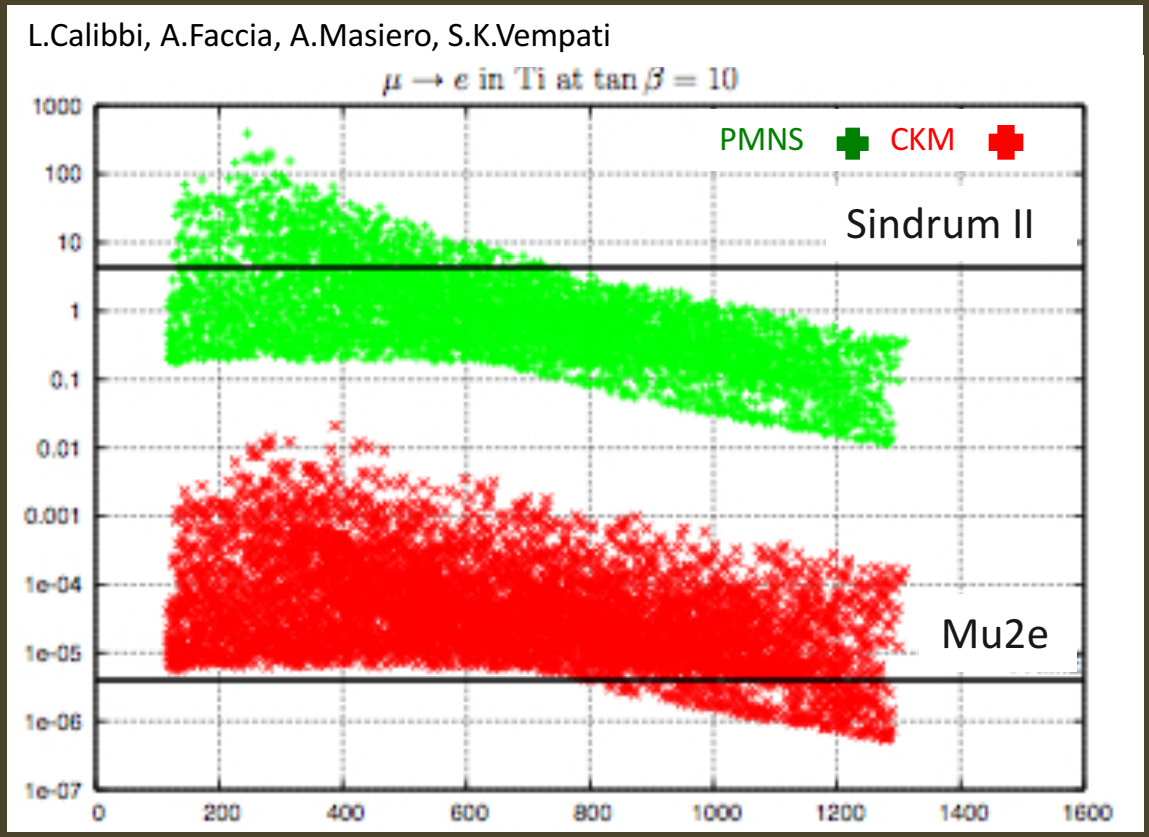

Rate μN → eN / 10^{-12}

$M_{1/2}$ (GeV/c^2)

hep-ph/0605139v2

- Mu2e will cover (almost) entire space

Mu2e Sensitivity

A. Vicente & C.E. Yaguna – Scotogenic model, N_1-N_1 annihilation region

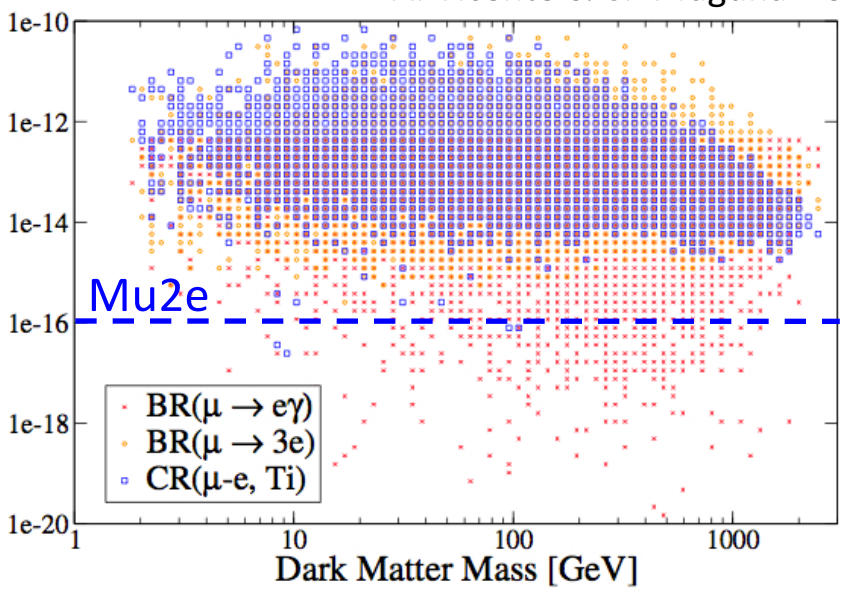

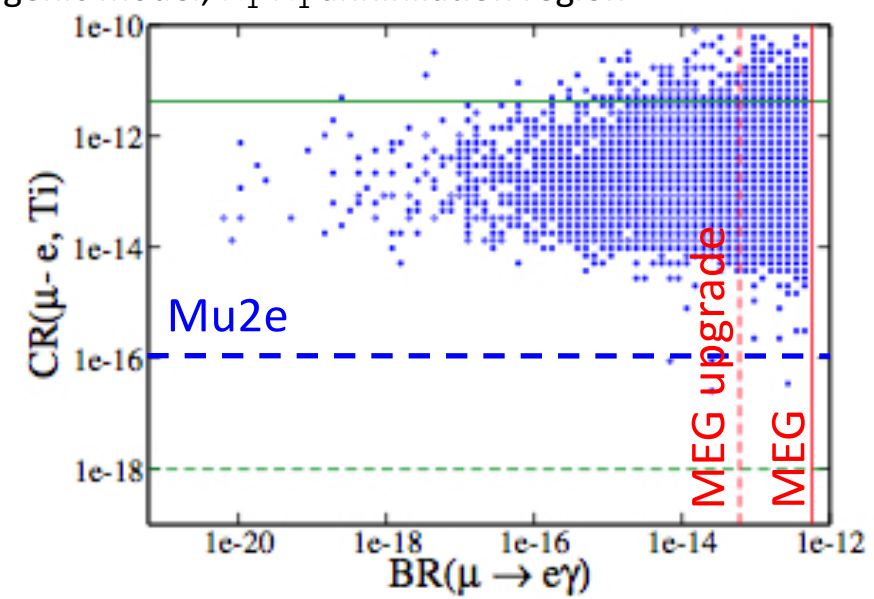

arXiv: 1412.2545 [hep-ph]

- Mu2e will explore a significant fraction of the parameter space

Mu2e Sensitivity

TABLE XII: LFV rates for points **SPS 1a** and **SPS 1b** in the CKM case and in the $U_{e3} = 0$ PMNS case. The processes that are within reach of the future experiments (MEG, SuperKEKB) have been highlighted in boldface. Those within reach of post–LHC era planned/discussed experiments (PRISM/PRIME, Super Flavour factory) highlighted in italics.

	SPS 1a		SPS 1b		SPS 2		SPS 3		Future
Process	CKM	$U_{e3} = 0$	CKM	$U_{e3} = 0$	CKM	$U_{e3} = 0$	CKM	$U_{e3} = 0$	Sensitivity
BR($\mu \to e\,\gamma$)	$\mathbf{3.2 \cdot 10^{-14}}$	$\mathbf{3.8 \cdot 10^{-13}}$	$\mathbf{4.0 \cdot 10^{-13}}$	$\mathbf{1.2 \cdot 10^{-12}}$	$1.3 \cdot 10^{-15}$	$8.6 \cdot 10^{-15}$	$1.4 \cdot 10^{-15}$	$1.2 \cdot 10^{-14}$	$\mathcal{O}(10^{-14})$
BR($\mu \to e\,e\,e$)	$2.3 \cdot 10^{-16}$	$2.7 \cdot 10^{-15}$	$2.9 \cdot 10^{-16}$	$8.6 \cdot 10^{-15}$	$9.4 \cdot 10^{-18}$	$6.2 \cdot 10^{-17}$	$1.0 \cdot 10^{-17}$	$8.9 \cdot 10^{-17}$	$\mathcal{O}(10^{-14})$
CR($\mu \to e$ in Ti)	$\mathit{2.0 \cdot 10^{-15}}$	$\mathit{2.4 \cdot 10^{-14}}$	$\mathit{2.6 \cdot 10^{-15}}$	$\mathit{7.6 \cdot 10^{-14}}$	$\mathit{1.0 \cdot 10^{-16}}$	$\mathit{6.7 \cdot 10^{-16}}$	$\mathit{1.0 \cdot 10^{-16}}$	$\mathit{8.4 \cdot 10^{-16}}$	$\mathcal{O}(10^{-18})$
BR($\tau \to e\,\gamma$)	$2.3 \cdot 10^{-12}$	$6.0 \cdot 10^{-13}$	$3.5 \cdot 10^{-12}$	$1.7 \cdot 10^{-12}$	$1.4 \cdot 10^{-13}$	$4.8 \cdot 10^{-15}$	$1.2 \cdot 10^{-13}$	$4.1 \cdot 10^{-14}$	$\mathcal{O}(10^{-8})$
BR($\tau \to e\,e\,e$)	$2.7 \cdot 10^{-14}$	$7.1 \cdot 10^{-15}$	$4.2 \cdot 10^{-14}$	$2.0 \cdot 10^{-14}$	$1.7 \cdot 10^{-15}$	$5.7 \cdot 10^{-17}$	$1.5 \cdot 10^{-15}$	$4.9 \cdot 10^{-16}$	$\mathcal{O}(10^{-8})$
BR($\tau \to \mu\,\gamma$)	$5.0 \cdot 10^{-11}$	$\mathbf{1.1 \cdot 10^{-8}}$	$7.3 \cdot 10^{-11}$	$\mathbf{1.3 \cdot 10^{-8}}$	$2.9 \cdot 10^{-12}$	$\mathit{7.8 \cdot 10^{-10}}$	$2.7 \cdot 10^{-12}$	$\mathit{6.0 \cdot 10^{-10}}$	$\mathcal{O}(10^{-9})$
BR($\tau \to \mu\,\mu\,\mu$)	$1.6 \cdot 10^{-13}$	$3.4 \cdot 10^{-11}$	$2.2 \cdot 10^{-13}$	$3.9 \cdot 10^{-11}$	$8.9 \cdot 10^{-15}$	$2.4 \cdot 10^{-12}$	$8.7 \cdot 10^{-15}$	$1.9 \cdot 10^{-12}$	$\mathcal{O}(10^{-8})$

- These are SuSy benchmark points for which LHC has discovery sensitivity
- Some of these will be observable by MEG/SuprB
- All of these will be observable by Mu2e

Mu2e at Fermilab

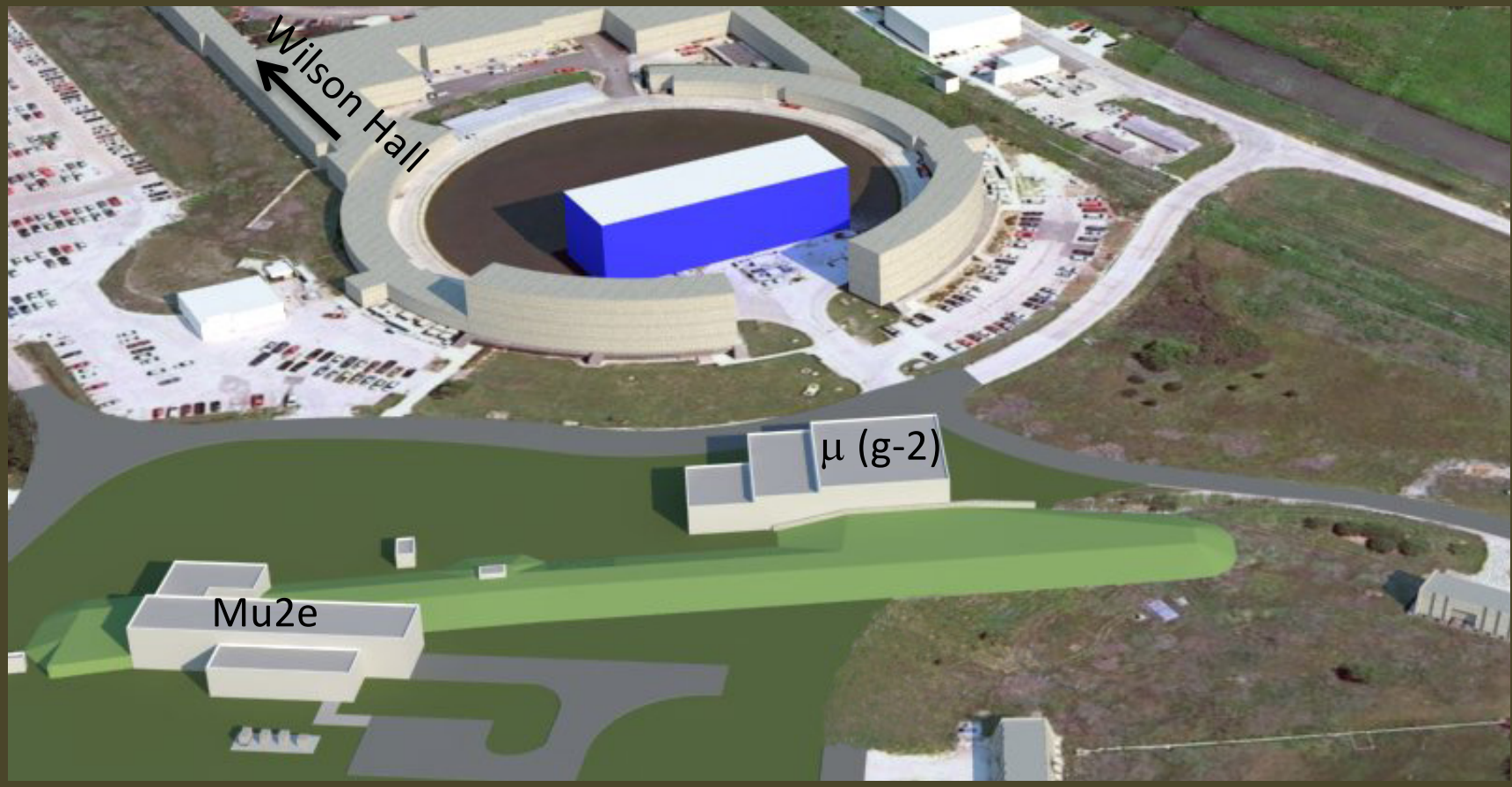

- Mu2e is located together with Muon (g-2) just south of Wilson Hall.

Trigger and DAQ System

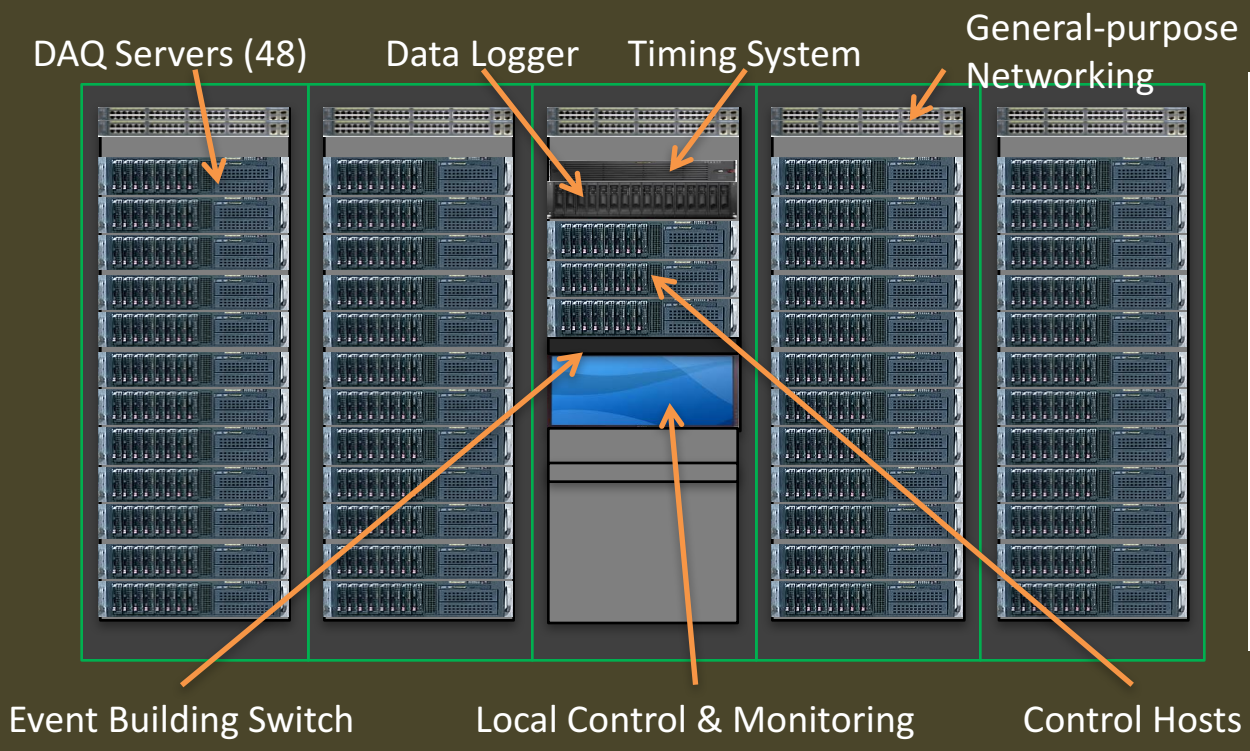

Parameter	Value
DAQ Servers	36
Detector Optical Links	216
System Bandwidth	40 GBytes/sec
Online Processing	40 TFLOPS
Input Event Size (average)	120 KBytes
Input Event Rate	192 KHz
Input Data Rate	30 GBytes/sec
Rejection Factor	≥ 100
Output Event Size (average)	130 KBytes
Output Event Rate	≤ 2000 Hz
Output Data Rate	≤ 260 MBytes/sec
Offline Storage	~7 PByte/year

- Stream data in time slices to cpu farm. Employ software trigger filters to identify good events.

Calorimeter Radiation Tolerance

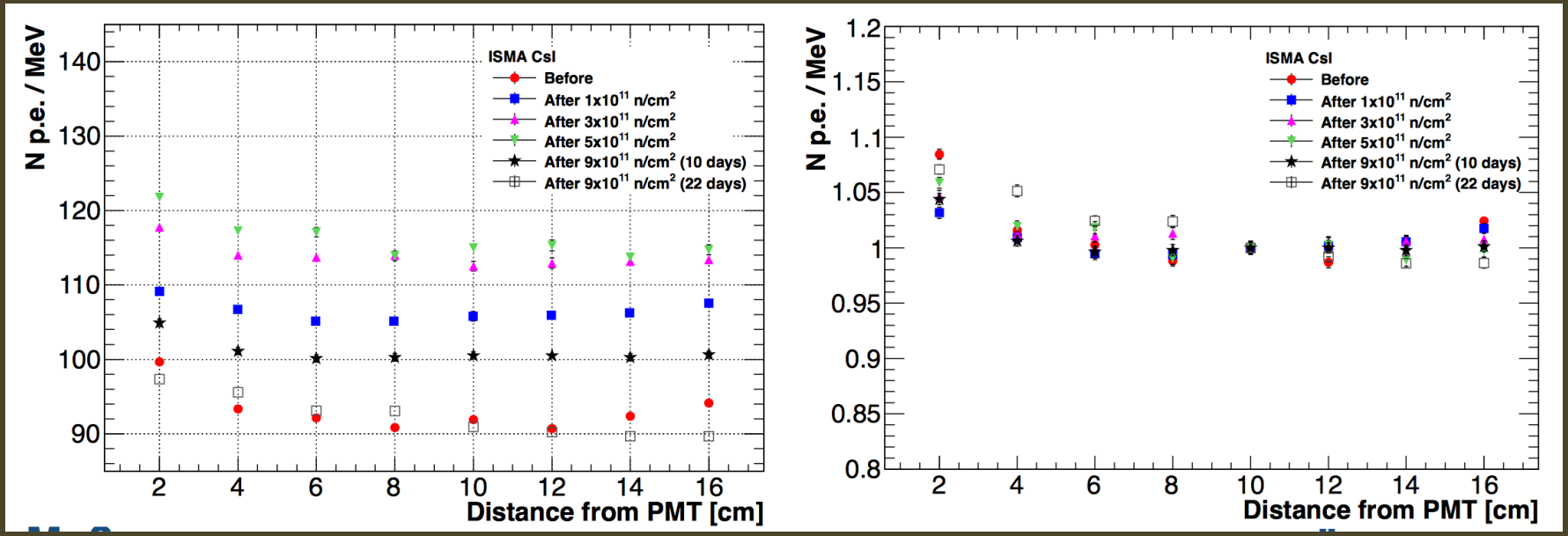

- Expect maximum of 10^{11} n/cm^2 over lifetime of the experiment

Calorimeter Radiation Tolerance

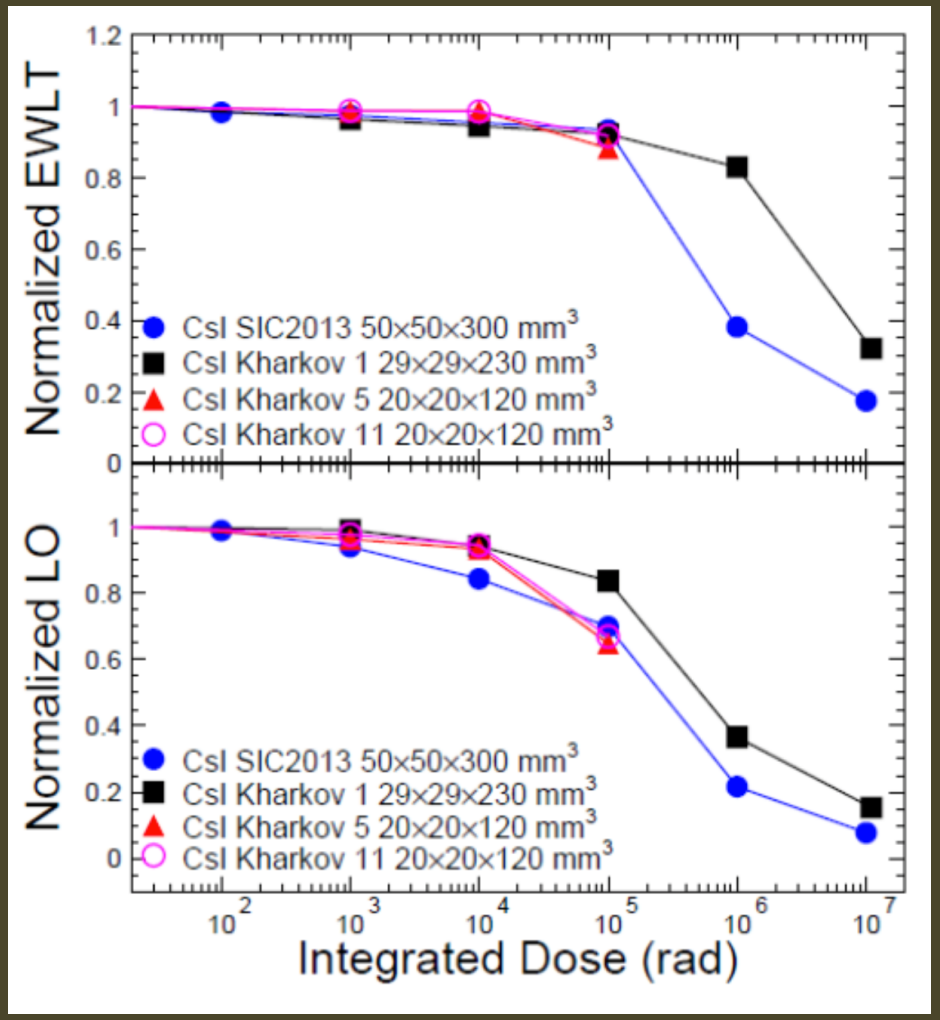

- Expect maximum (average) of 20 (3) kRad over lifetime of the experiment

Selection Requirements

Parameter	Requirement
Track quality and background rejection criteria	
Kalman Fit Status	Successful Fit
Number of active hits	$N_{active} \geq 25$
Fit consistency	$\chi 2$ consistency $> 2 \times 10^{-3}$
Estimated reconstructed momentum uncertainty	$\sigma_p < 250$ keV/c
Estimated track t_0 uncertainty	$\sigma_t < 0.9$ nsec
Track t_0 (livegate)	700 ns $< t_0 <$ 1695 ns
Polar angle range (pitch)	$45° < \theta < 60°$
Minimum track transverse radius	-80 mm $< d_0 <$ 105 mm
Maximum track transverse radius	450 mm $< d_0 + 2/\omega <$ 680 mm
Track momentum	103.75 $< p <$ 105.0 MeV/c
Calorimeter matching and particle identification criteria	
Track match to a calorimeter cluster	$E_{cluster} > 10$ MeV $\chi 2$ (track-calo match) < 100
Ratio of cluster energy to track momentum	$E/P < 1.15$
Difference in track t_0 to calorimeter t_0	$\Delta t = \lvert t_{track} - t_{calo} \rvert < 3$ ns from peak
Particle identification	$\log(L(e)/L(\mu)) < 1.5$

- Full set of selection criteria employed to estimate backgrounds and sensitivity reported in TDR (Summer 2014)

Estimated background yields

Table 3.4 A summary of the estimated background yields using the selection criteria of Section 3.5.3. The total run time and corresponding number of protons on target are provided in Table 3.5. An extinction of 10^{-10}, a cosmic ray veto inefficiency of 10^{-4}, and particle-identification with a muon-rejection of 200 are used. 'Intrinsic' backgrounds are those that scale with the number of stopped muons, 'Late Arriving' backgrounds are those with a strong dependence on the achieved extinction, and 'Miscellaneous' backgrounds are those that don't fall into the previous two categories.

Category	Background process	Estimated yield (events)
Intrinsic	Muon decay-in-orbit (DIO)	0.199 ± 0.092
	Muon capture (RMC)	$0.000\ ^{+0.004}_{-0.000}$
Late Arriving	Pion capture (RPC)	0.023 ± 0.006
	Muon decay-in-flight (μ-DIF)	<0.003
	Pion decay-in-flight (π-DIF)	$0.001 \pm <0.001$
	Beam electrons	0.003 ± 0.001
Miscellaneous	Antiproton induced	0.047 ± 0.024
	Cosmic ray induced	0.082 ± 0.018
	Total	0.36 ± 0.10

Single event sensitivity = $(2.87+0.35-0.29) \times 10^{-17}$

(goal = 2.4×10^{-17})

Systematic Uncertainties

Effect	Uncertainty in DIO background yield	Uncertainty in CE single-event-sensitivity ($\times 10^{-17}$)
MC Statistics	±0.02	±0.07
Theoretical Uncertainty	±0.04	-
Tracker Acceptance	±0.002	±0.03
Reconstruction Efficiency	±0.01	±0.15
Momentum Scale	+0.09, -0.06	±0.07
μ-bunch Intensity Variation	±0.007	±0.1
Beam Flash Uncertainty	±0.011	±0.17
μ-capture Proton Uncertainty	±0.01	±0.016
μ-capture Neutron Uncertainty	±0.006	±0.093
μ-capture Photon Uncertainty	±0.002	±0.028
Out-Of-Target μ Stops	±0.004	±0.055
Degraded Tracker	-0.013	+0.191
Total (in quadrature)	+0.10, -0.08	+0.35, -0.29

- Evaluated for all background sources

Mu2e Proton Timing

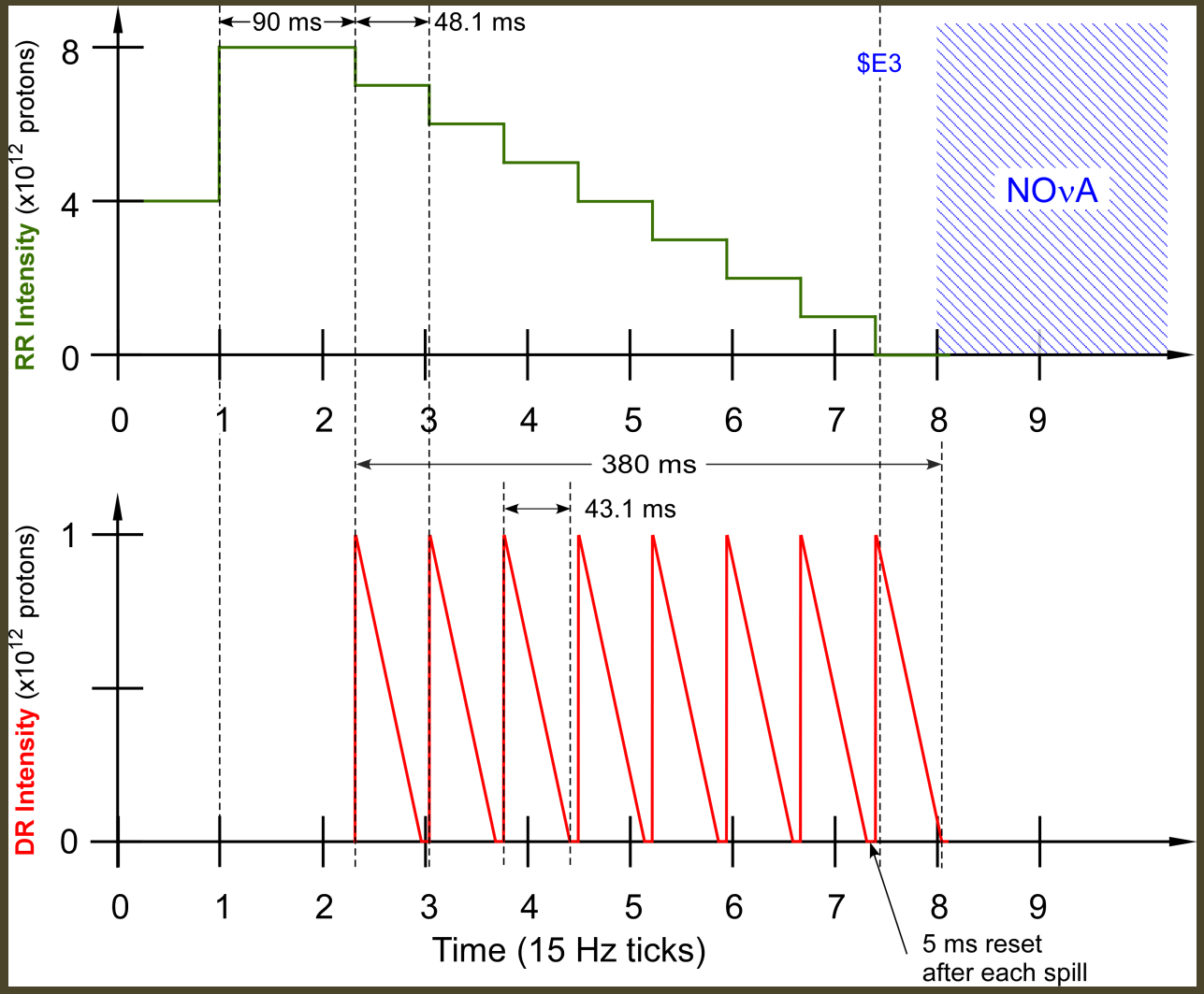

- Mu2e will run simultaneously with NOvA, BNB, etc.

Tracker Occupancy

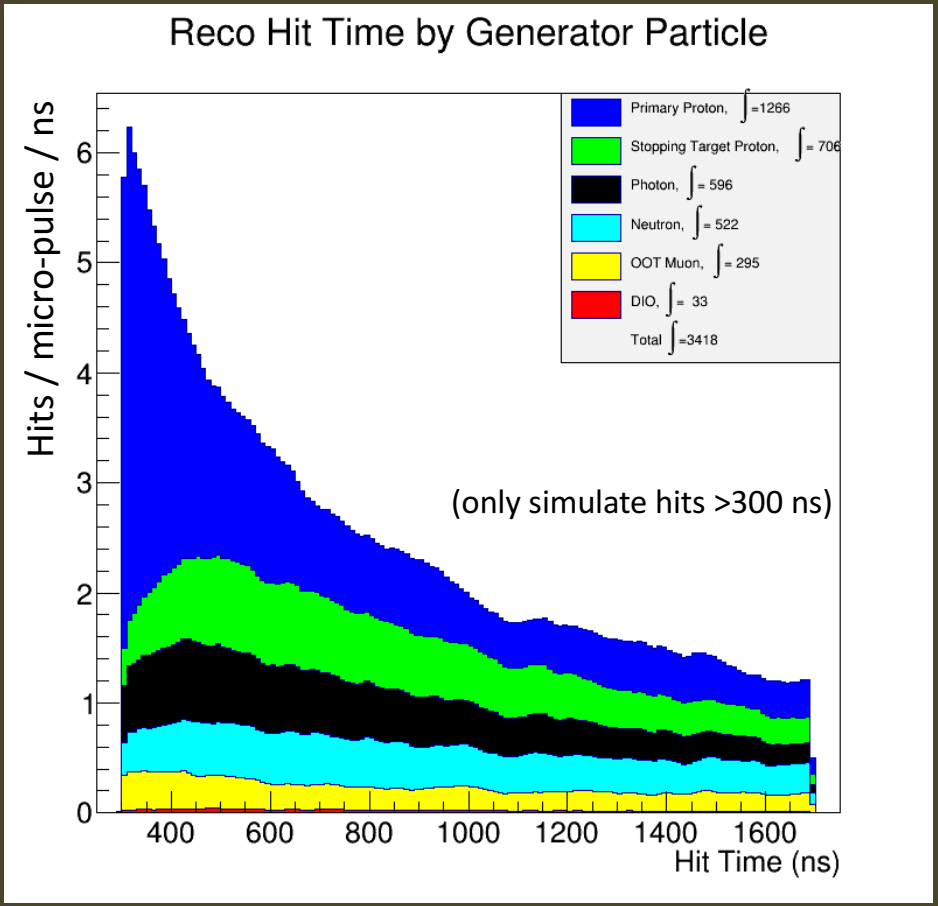

- Accidental occupancy from beam flash, μ capture products, out-of-target μ stops, etc.

Signal Momentum Spectrum

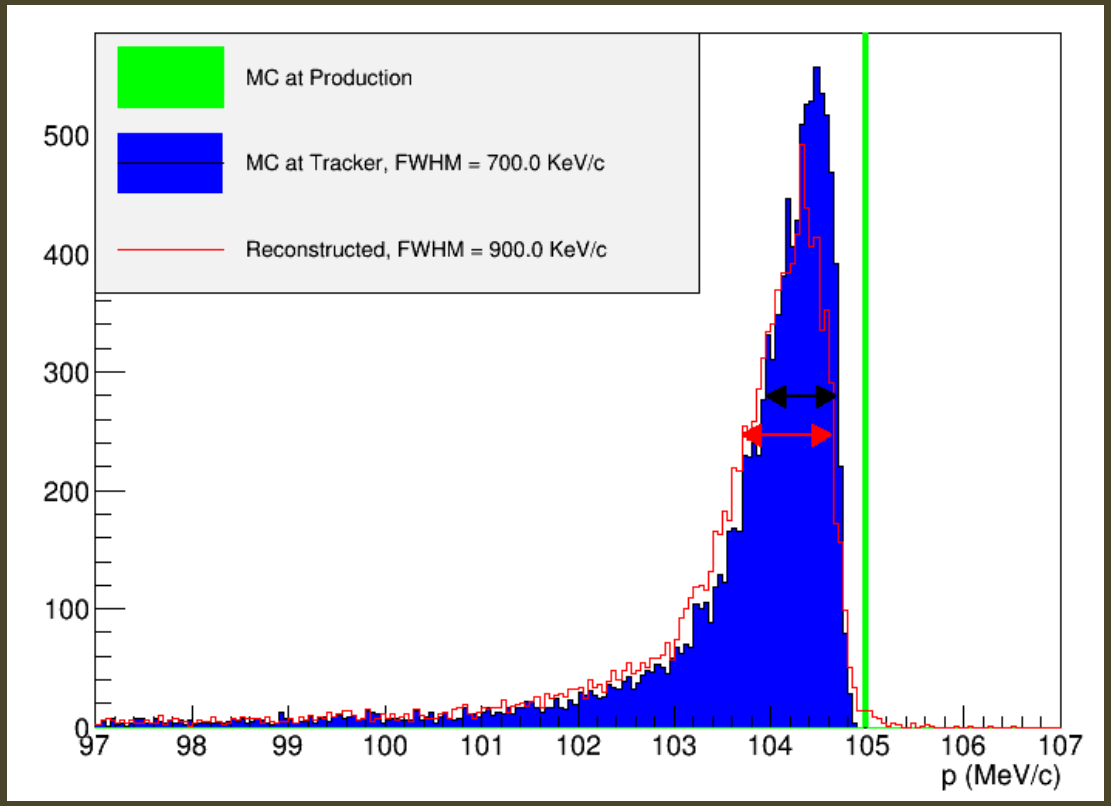

- Smearing dominated by interactions in stopping target and in (neutron/proton) absorbers upstream of tracker

Calorimeter Particle ID

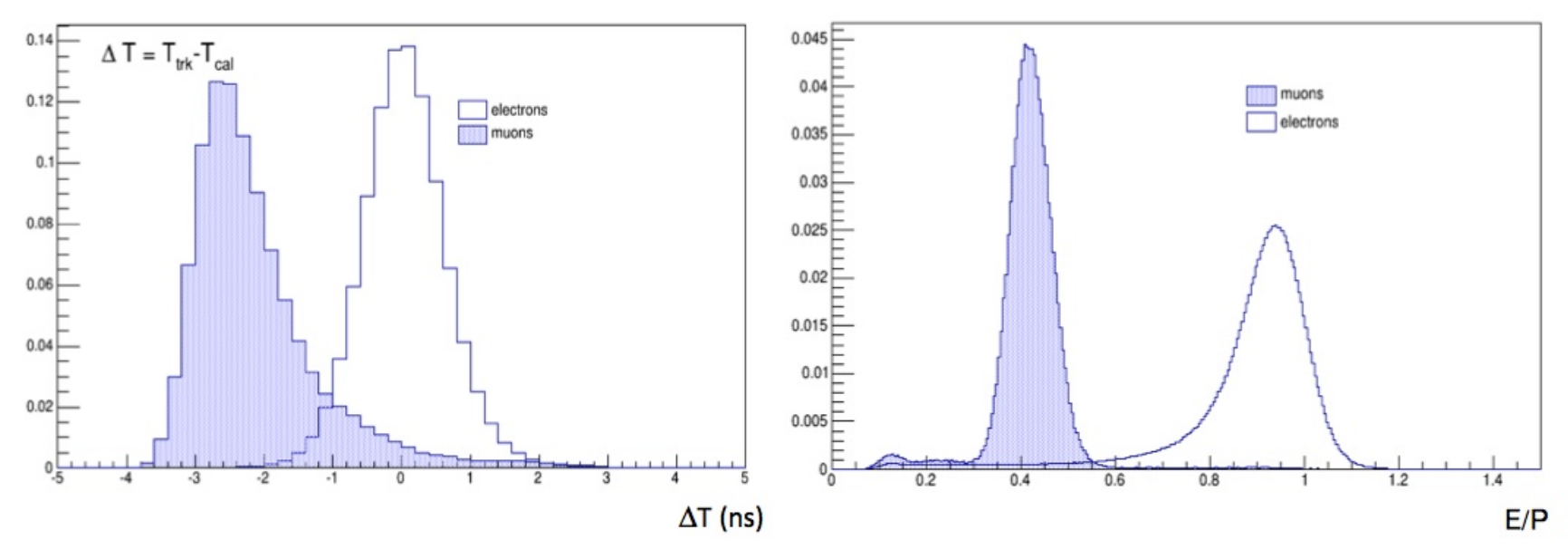

- Electrons and muons well separated

False vetoes in CRV

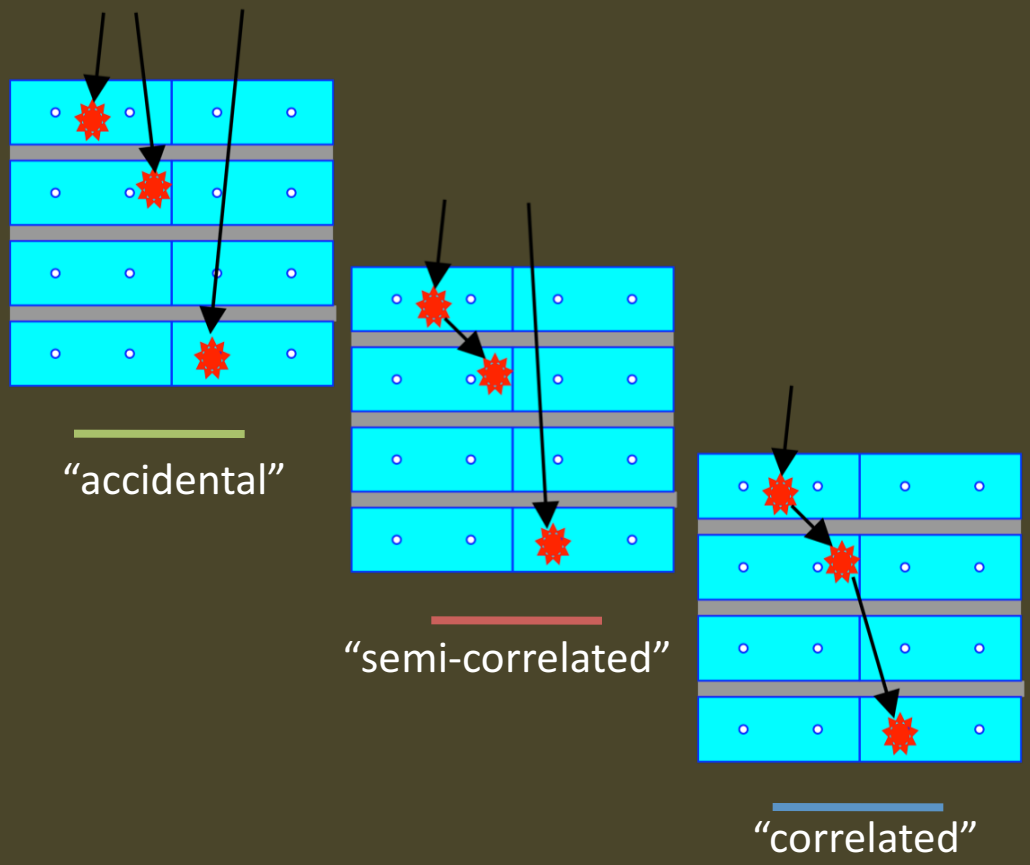

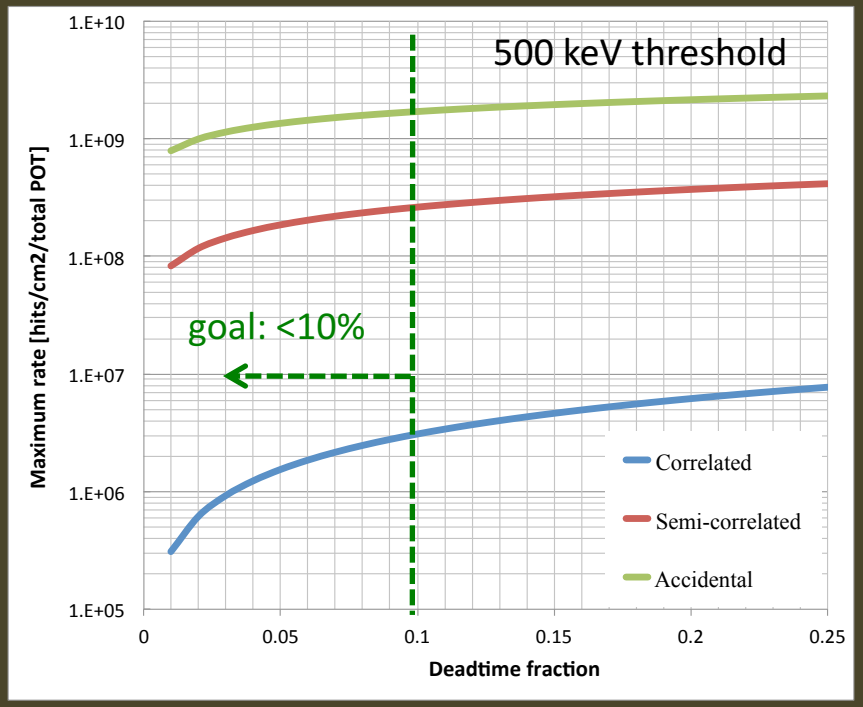

- We need to understand contributions from accidentals and correlated-accidentals
  - For neutrons and photons as a function of time, energy, timing resolution, and read-out threshold

Estimated dead time from CRV vetos – dominated by n/γ background

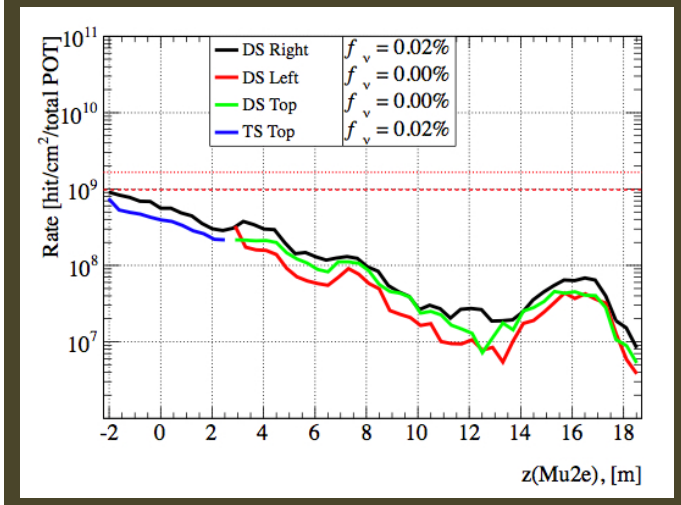

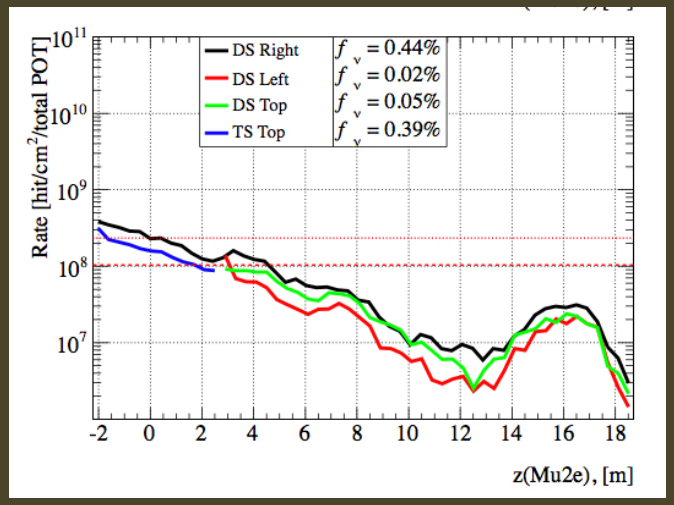

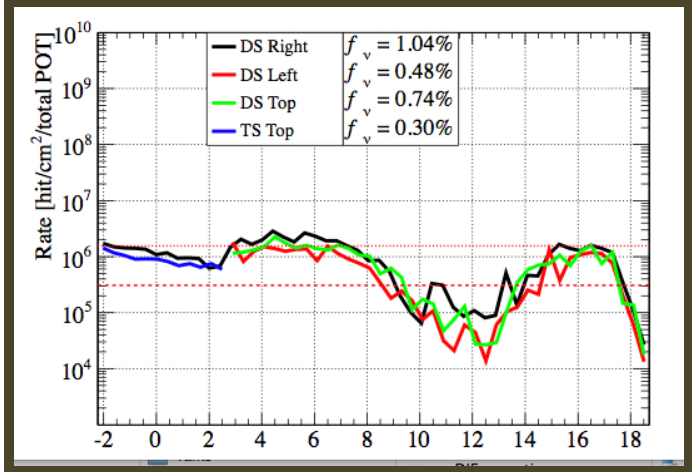

accidental semi-correlated correlated

- Total dead time from neutron/photon "noise" = 5%
  - For 500 keV readout threshold
  - Increasing to 1 MeV reduces to 2%
  - Cross-check with a separate physics generator (MARS) yields dead time within 50%

Mu2e Neutron Shielding

- Several copious sources of neutrons
  - Production target, stopping target, collimators
- Lots of neutrons and subsequent photons (from n- capture and activation processes)
  - Generate false vetoes in CRV… if rate high enough becomes a source of significant deadtime
  - Cause radiation damage to the read-out electronics (esp. SiPMs)

Mu2e Neutron Shielding

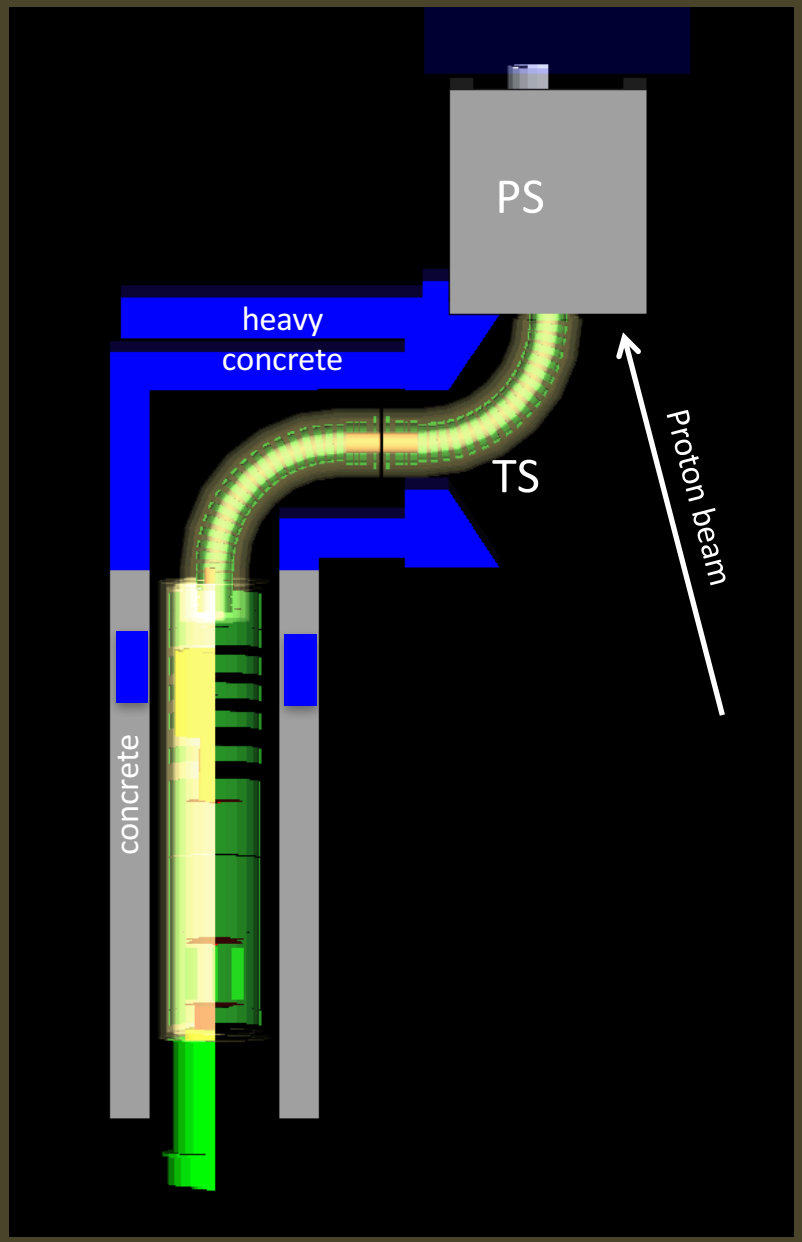

- Have identified a cost effective shielding solution
- Non-trivial optimization required
- Reduces rates of neutrons and photons at CRV to acceptable level

PS Heat and Radiation Shield

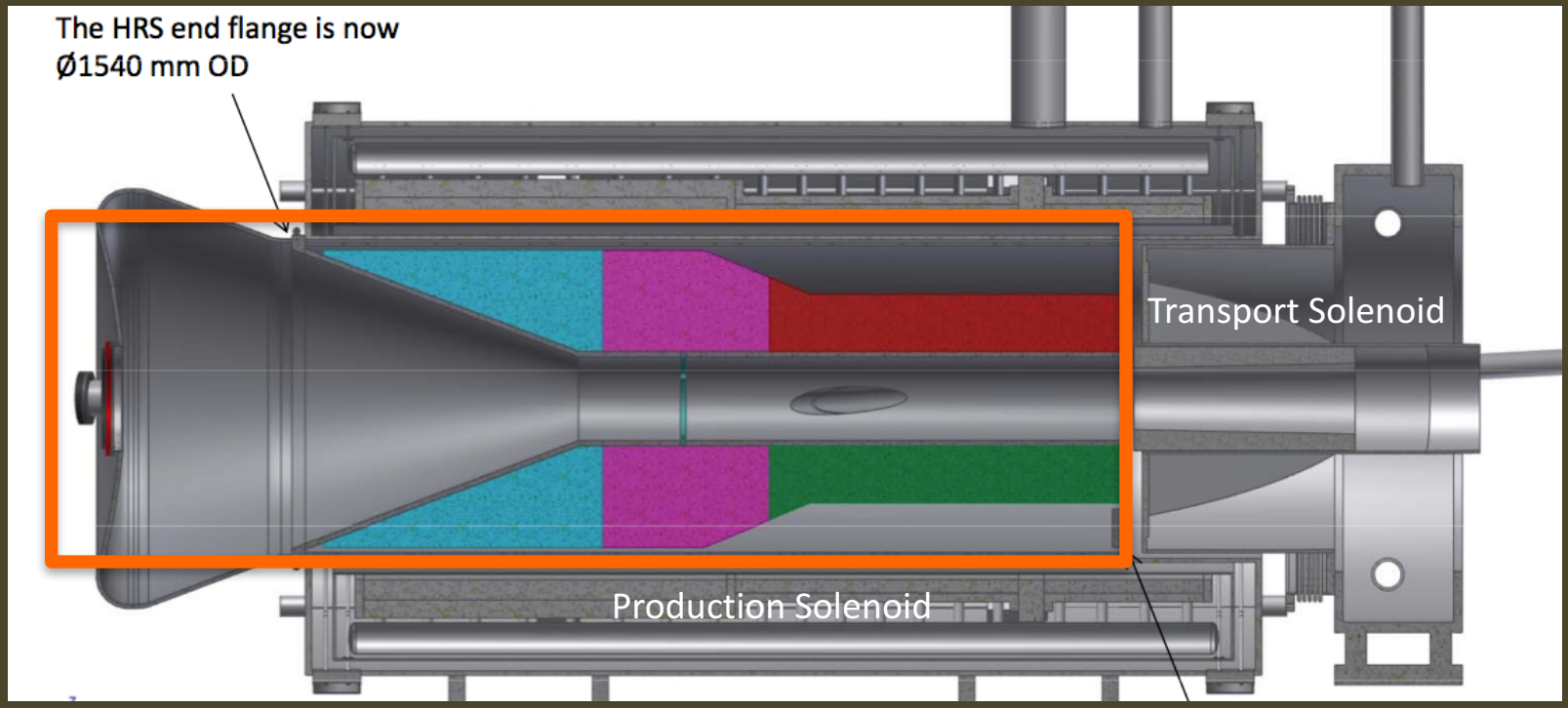

- Must protect production solenoid from heat and radiation deposits from proton beam

Muon momentum distribution

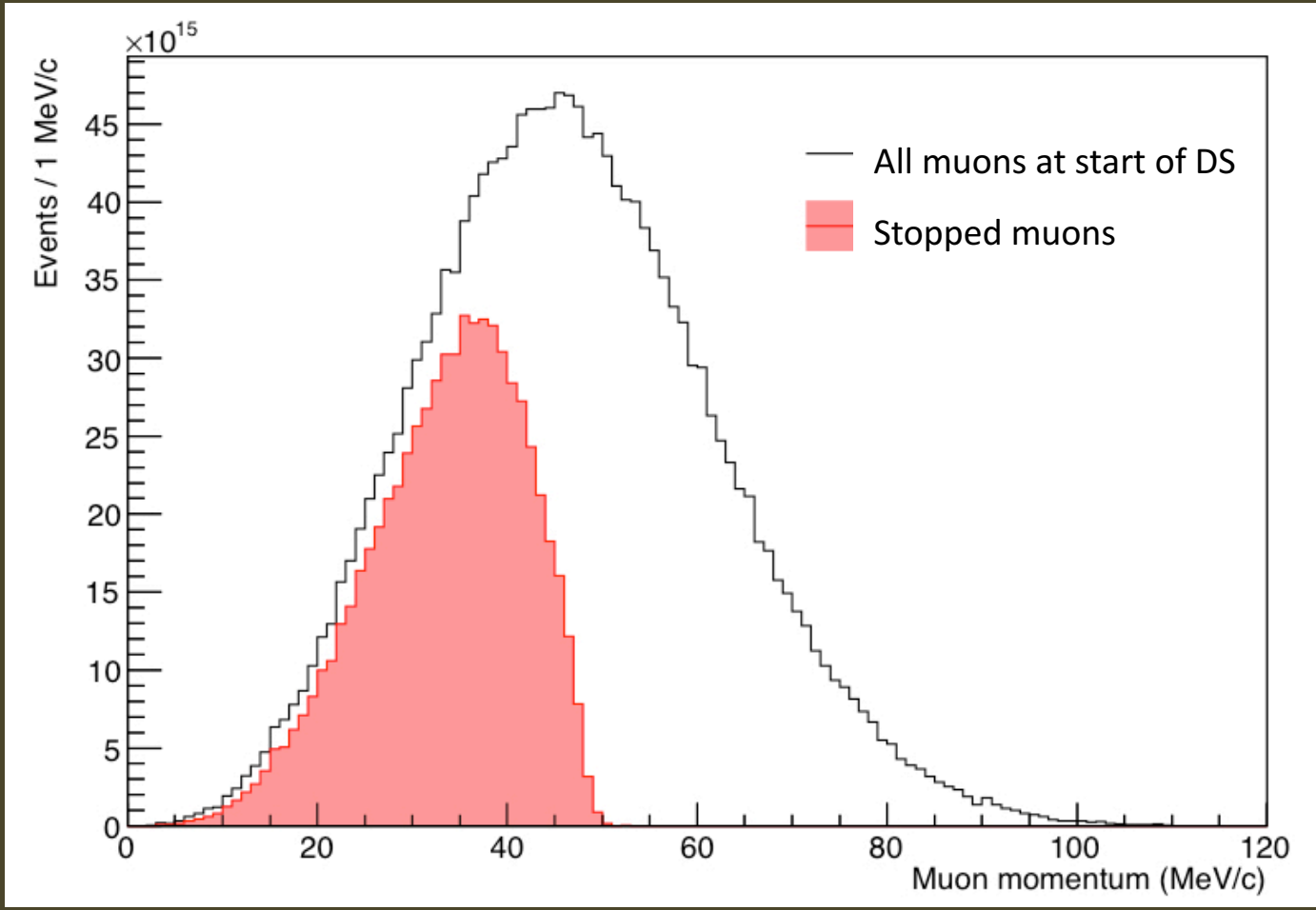

- The muons that stop are low momentum

Stopping Target Monitor

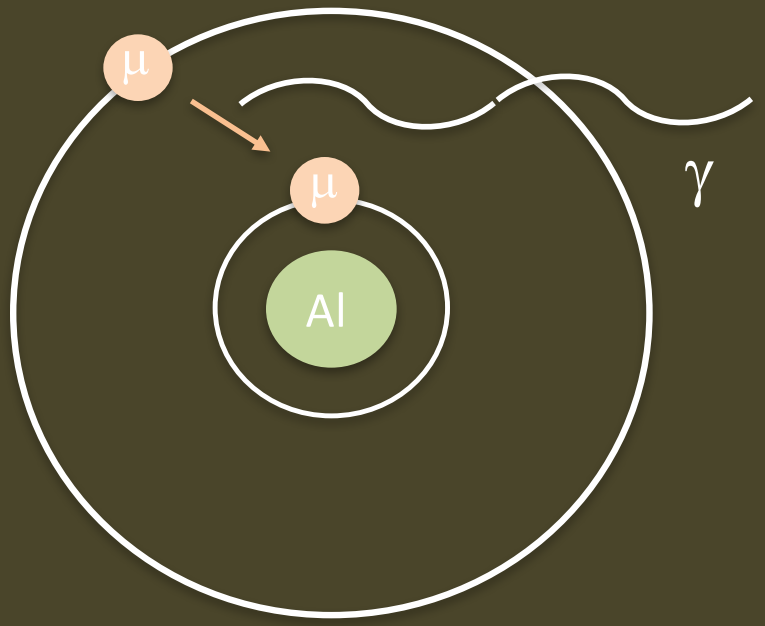

Get diagram of transitions
- for aluminum
- for Mg*

- When muon stops in aluminum it quickly (10^{-15} s) cascades to 1s ground state
- Emits photons at characteristic energies that can be used to monitor no. stopped muons

Stopping Target Monitor

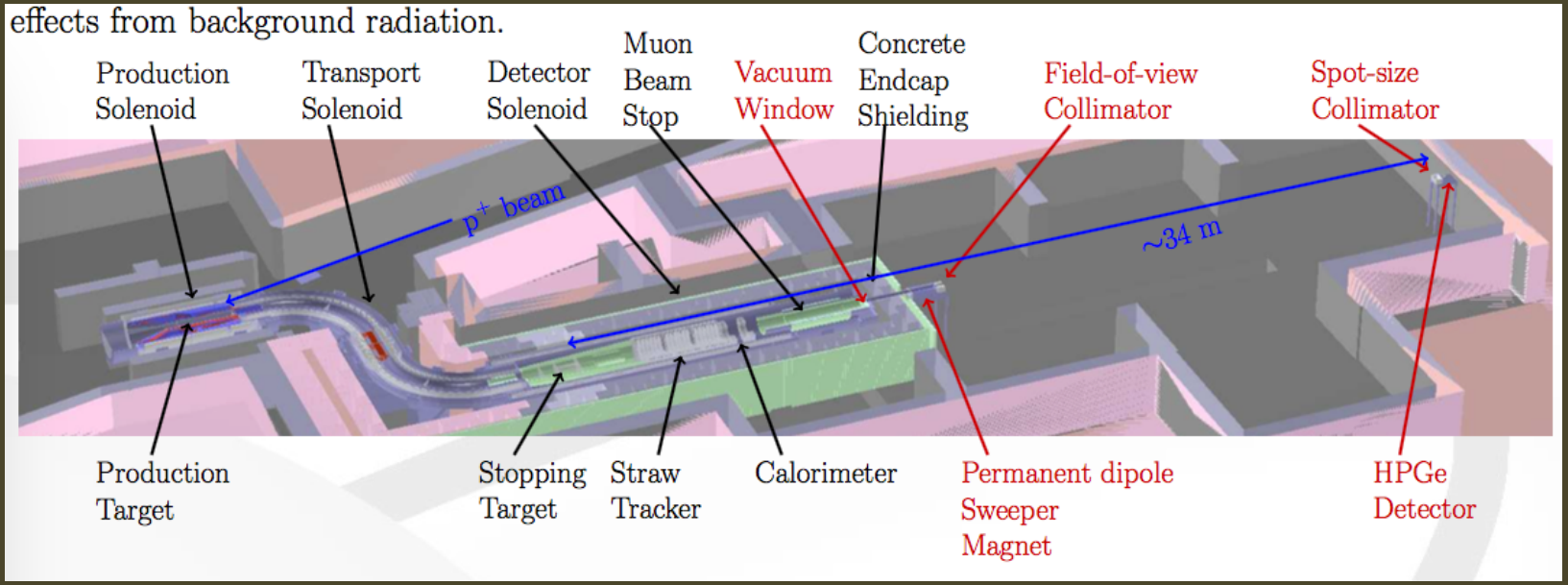

- Employ HPGe to monitor these photon lines

Stopping Target Monitor

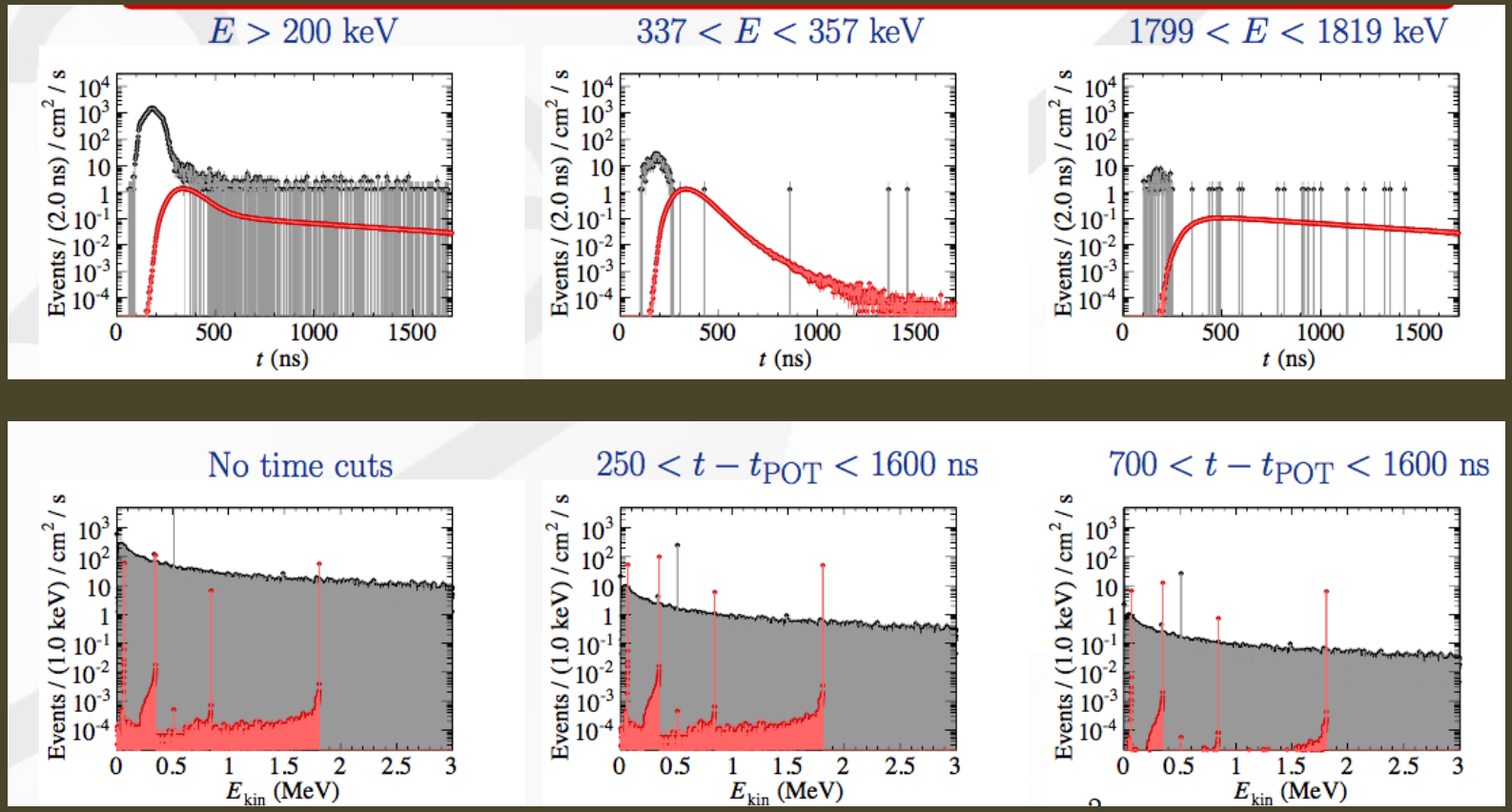

- Rates at STM vs time and energy

Understanding muon capture

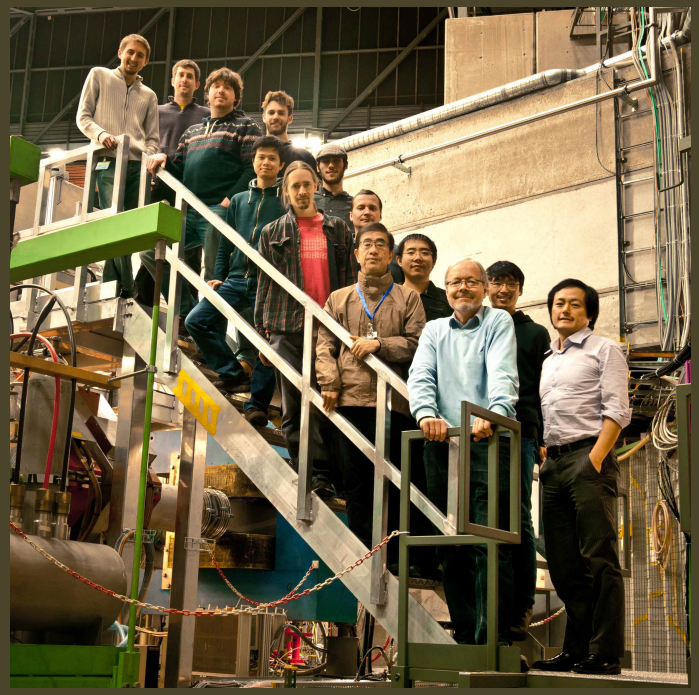

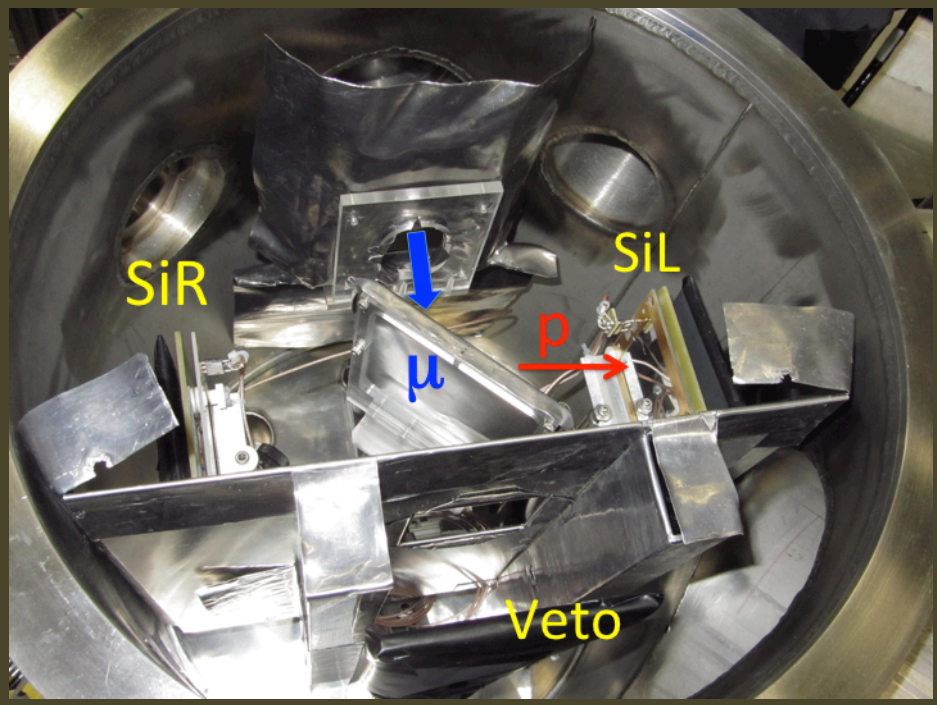

- AlCap – measurement of products of muon captures on aluminum
  - Joint Mu2e/COMET effort
  - Took data in 2013 & 2015

Test Beam – December 2013

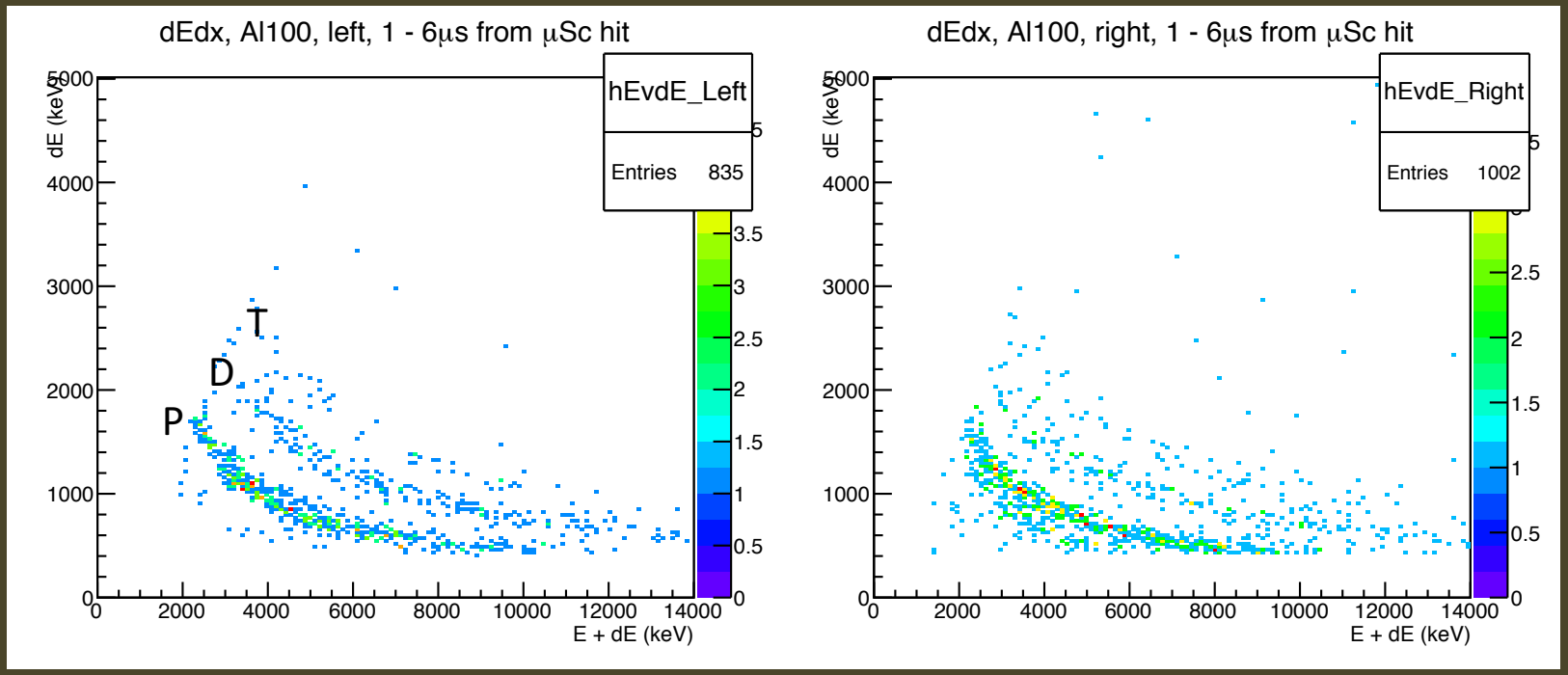

- Preliminary AlCap results
  - Analysis ongoing, but proton, deuteron lines clear

Beam Extinction

Table 4.31. Specifications of the three harmonics of the Extinction AC dipole.

Magnet	Frequency (kHz)	Length (cm)	Aperture		Peak B Field (Gauss)
			bend plane (cm)	non-bend (cm)	
A	300	300	7.8	1.2	120
B	3800	300	7.3	1.2	15

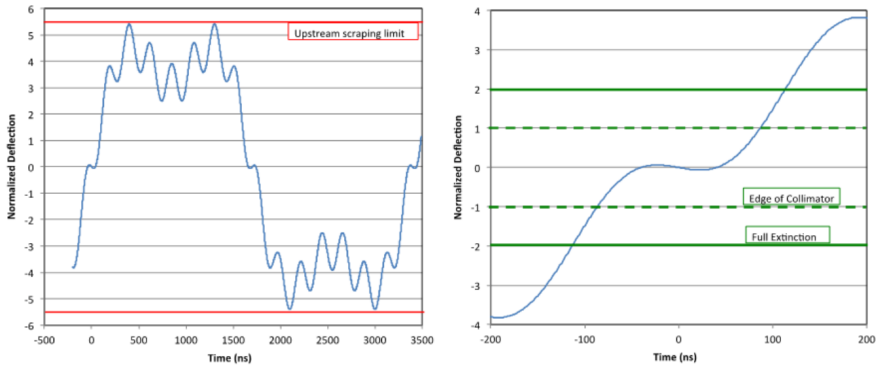

Figure 4.106. Final AC dipole waveform. On the left is the waveform over a complete cycle and on the right is the waveform over the transmission window.

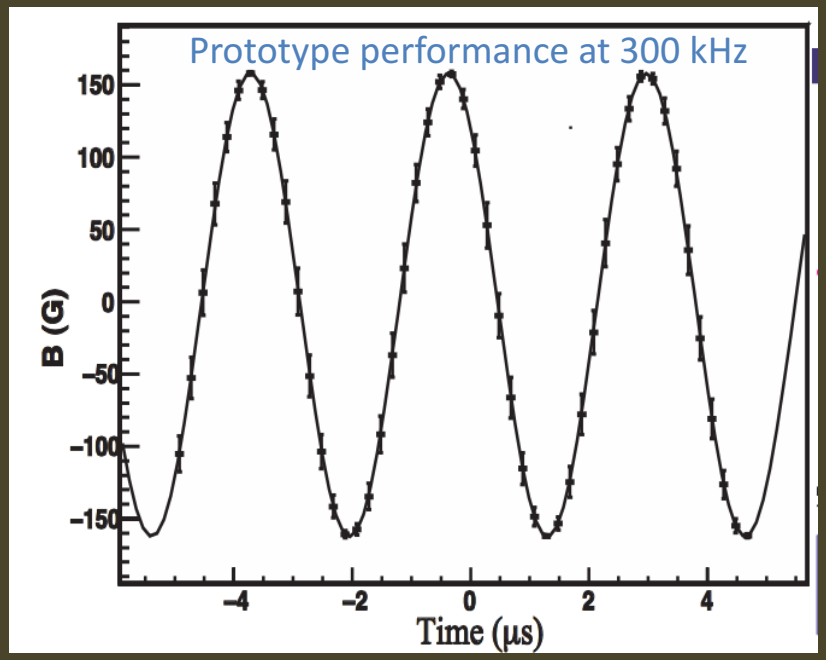

- Intrinsic extinction in Recycler Ring: 10^{-5}
- Additional extinction from AC Dipole: 10^{-6}-10^{-7}

Beam Extinction Monitor

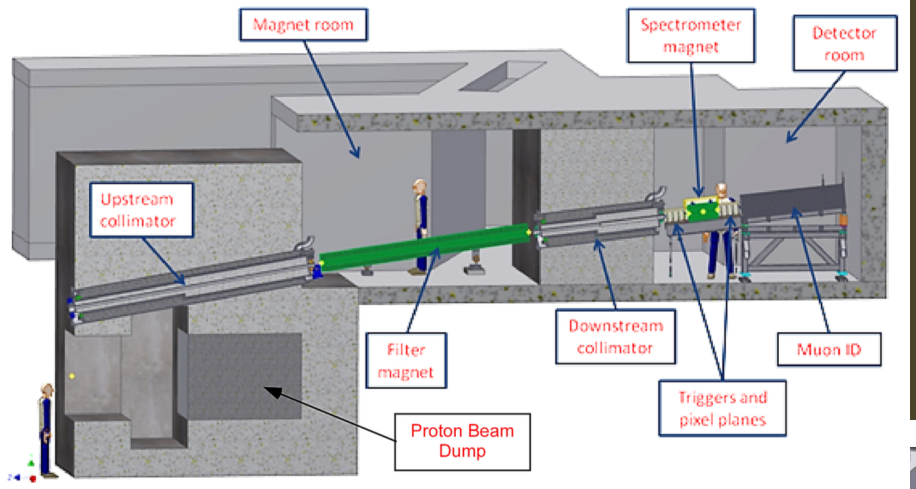

Figure 4.116. The components for the target extinction monitor

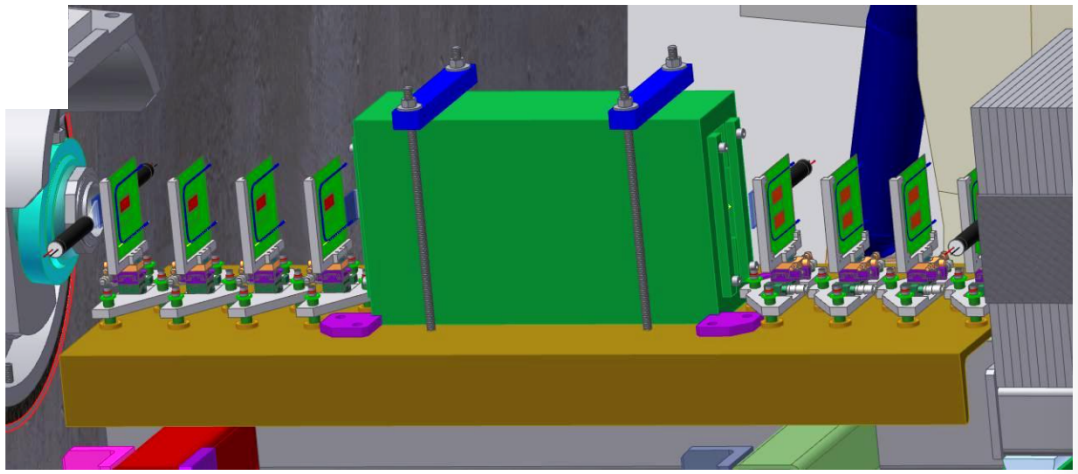

Figure 4.130. Triggers, pixels and spectrometer magnet on the channel table.

- Measure extinction at 10^{-10} to 10% in ~ 1h

Beam Extinction Monitor

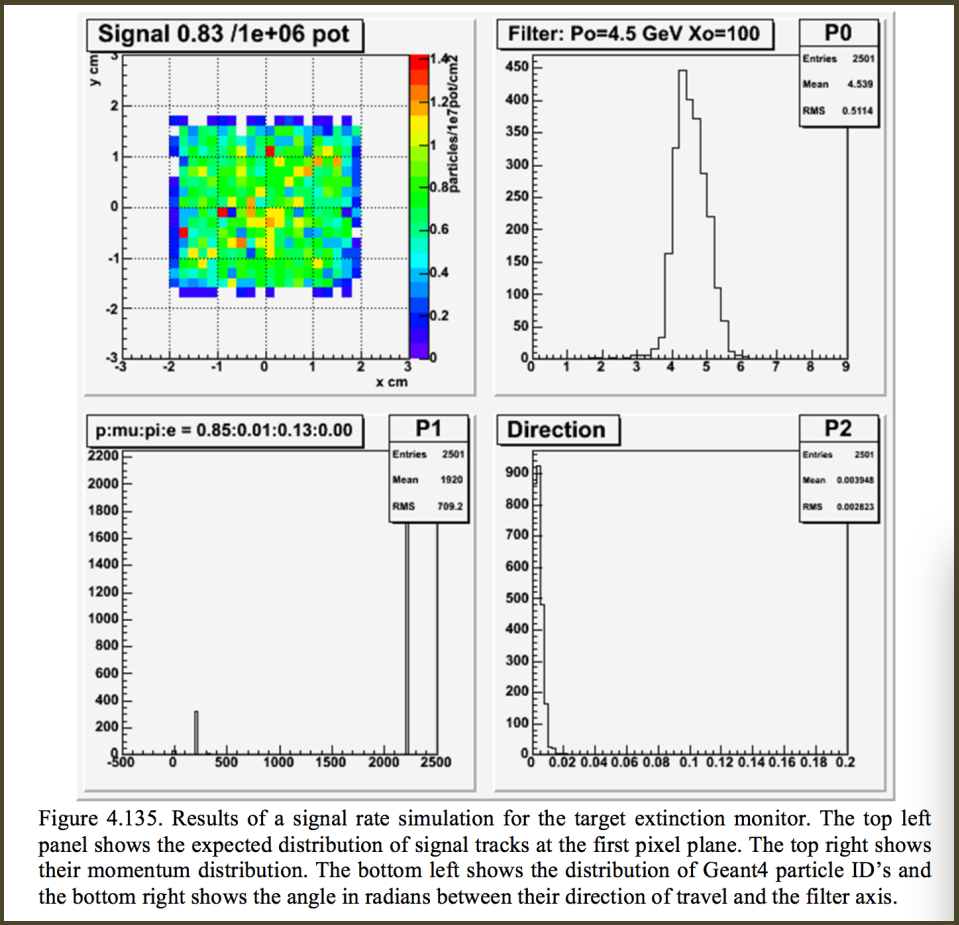

Figure 4.135. Results of a signal rate simulation for the target extinction monitor. The top left panel shows the expected distribution of signal tracks at the first pixel plane. The top right shows their momentum distribution. The bottom left shows the distribution of Geant4 particle ID's and the bottom right shows the angle in radians between their direction of travel and the filter axis.

- Measure extinction at 10^{-10} to 10% in ~ 1h

Mu2e Sensitivity

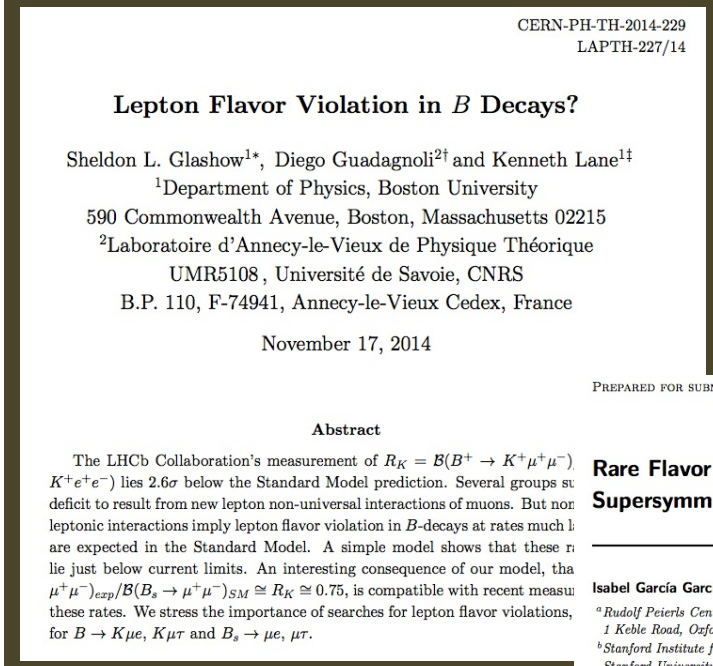

CERN-PH-TH-2014-229
LAPTH-227/14

Lepton Flavor Violation in B Decays?

Sheldon L. Glashow[1*], Diego Guadagnoli[2†] and Kenneth Lane[1‡]
[1]Department of Physics, Boston University
590 Commonwealth Avenue, Boston, Massachusetts 02215
[2]Laboratoire d'Annecy-le-Vieux de Physique Théorique
UMR5108, Université de Savoie, CNRS
B.P. 110, F-74941, Annecy-le-Vieux Cedex, France

November 17, 2014

Abstract

The LHCb Collaboration's measurement of $R_K = \mathcal{B}(B^+ \to K^+\mu^+\mu^-)$ $K^+e^+e^-)$ lies 2.6σ below the Standard Model prediction. Several groups su deficit to result from new lepton non-universal interactions of muons. But nor leptonic interactions imply lepton flavor violation in B-decays at rates much l are expected in the Standard Model. A simple model shows that these r lie just below current limits. An interesting consequence of our model, tha $\mu^+\mu^-)_{exp}/\mathcal{B}(B_s \to \mu^+\mu^-)_{SM} \cong R_K \cong 0.75$, is compatible with recent measu these rates. We stress the importance of searches for lepton flavor violations, for $B \to K\mu e$, $K\mu\tau$ and $B_s \to \mu e$, $\mu\tau$.

arXiv:1411.0565

arXiv:1409.5669

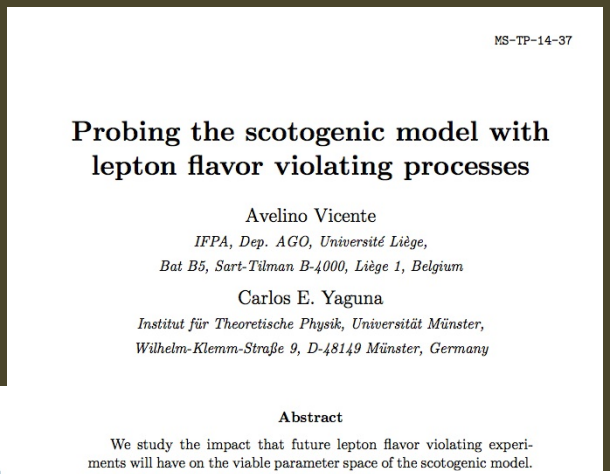

MS-TP-14-37

Probing the scotogenic model with lepton flavor violating processes

Avelino Vicente
IFPA, Dep. AGO, Université Liège,
Bat B5, Sart-Tilman B-4000, Liège 1, Belgium
Carlos E. Yaguna
Institut für Theoretische Physik, Universität Münster,
Wilhelm-Klemm-Straße 9, D-48149 Münster, Germany

Abstract

We study the impact that future lepton flavor violating experi- ments will have on the viable parameter space of the scotogenic model. Within this model, the dark matter particle is est singlet fermion and two cases are consider relic density is obtained: via self-annihilatio with the scalars. For each case, a scan over

arXiv:1411.6612

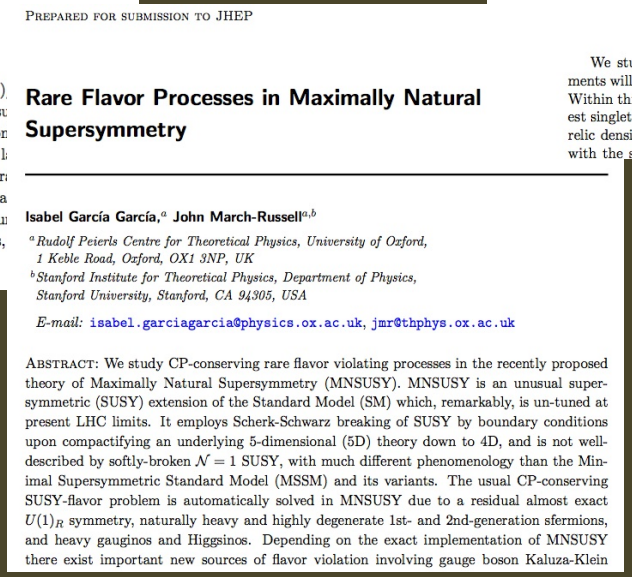

Prepared for submission to JHEP

Rare Flavor Processes in Maximally Natural Supersymmetry

Isabel García García,[a] **John March-Russell**[a,b]
[a]*Rudolf Peierls Centre for Theoretical Physics, University of Oxford, 1 Keble Road, Oxford, OX1 3NP, UK*
[b]*Stanford Institute for Theoretical Physics, Department of Physics, Stanford University, Stanford, CA 94305, USA*
E-mail: isabel.garciagarcia@physics.ox.ac.uk, jmr@thphys.ox.ac.uk

Abstract: We study CP-conserving rare flavor violating processes in the recently proposed theory of Maximally Natural Supersymmetry (MNSUSY). MNSUSY is an unusual super- symmetric (SUSY) extension of the Standard Model (SM) which, remarkably, is un-tuned at present LHC limits. It employs Scherk-Schwarz breaking of SUSY by boundary conditions upon compactifying an underlying 5-dimensional (5D) theory down to 4D, and is not well-described by softly-broken $\mathcal{N} = 1$ SUSY, with much different phenomenology than the Min- imal Supersymmetric Standard Model (MSSM) and its variants. The usual CP-conserving SUSY-flavor problem is automatically solved in MNSUSY due to a residual almost exact $U(1)_R$ symmetry, naturally heavy and highly degenerate 1st- and 2nd-generation sfermions, and heavy gauginos and Higgsinos. Depending on the exact implementation of MNSUSY there exist important new sources of flavor violation involving gauge boson Kaluza-Klein

arXiv:1412.2545

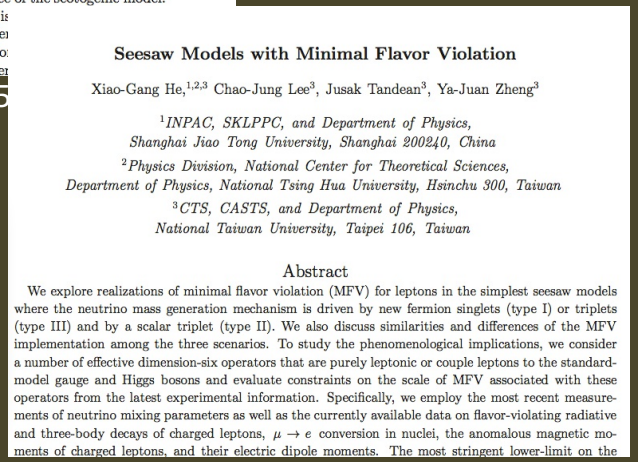

Seesaw Models with Minimal Flavor Violation

Xiao-Gang He,[1,2,3] Chao-Jung Lee[3], Jusak Tandean[3], Ya-Juan Zheng[3]
[1]*INPAC, SKLPPC, and Department of Physics, Shanghai Jiao Tong University, Shanghai 200240, China*
[2]*Physics Division, National Center for Theoretical Sciences, Department of Physics, National Tsing Hua University, Hsinchu 300, Taiwan*
[3]*CTS, CASTS, and Department of Physics, National Taiwan University, Taipei 106, Taiwan*

Abstract

We explore realizations of minimal flavor violation (MFV) for leptons in the simplest seesaw models where the neutrino mass generation mechanism is driven by new fermion singlets (type I) or triplets (type III) and by a scalar triplet (type II). We also discuss similarities and differences of the MFV implementation among the three scenarios. To study the phenomenological implications, we consider a number of effective dimension-six operators that are purely leptonic or couple leptons to the standard-model gauge and Higgs bosons and evaluate constraints on the scale of MFV associated with these operators from the latest experimental information. Specifically, we employ the most recent measure- ments of neutrino mixing parameters as well as the currently available data on flavor-violating radiative and three-body decays of charged leptons, $\mu \to e$ conversion in nuclei, the anomalous magnetic mo- ments of charged leptons, and their electric dipole moments. The most stringent lower-limit on the

- Persistent interest in Lepton Flavor Violation and in muon-to-electron conversion (ie. Mu2e)

As a function of Z

- Things change